Comparison of rock density determination methods used in South African platinum mines for resource planning purposes

By

Duncan James Jarman

Submitted in partial fulfilment of the requirements for the degree M.Sc. (Earth Science Practice and Management) in the Faculty of Natural and Agricultural Science

University of Pretoria

Pretoria

December 2011

Title of Treatise: Comparison of rock density determination methods used in South African platinum mines for resource planning purposes

Author: Duncan James Jarman

Supervisor: Dr James Roberts

Department: Department of Geology, Faculty of Natural and Agricultural Sciences, University of Pretoria

Degree: MSc in Earth Science Practice and Management

SUMMARY

Rock density is critical for determining the tonnage of an orebody and therefore impacts on the total resource of a deposit. Density is defined as the concentration of matter, and is expressed as mass per unit volume (g/cc; g/cm^3 or t/m^3). The density that is calculated will depend on the nature of the rock, and whether the volume calculated includes the open and/or closed pore volume of the rock. The pore volume will depend on the rock's internal and external characteristics.

This study looks at two methods commonly used to determine the rock density of samples taken from boreholes drilled for platinum mines on the North Eastern limb of the Bushveld Complex, South Africa. The first method is a gas pycnometer, which is almost exclusively used by laboratories. A Grabner Minidens air gas pycnometer was used. The second method is a hydrostatic immersion method, using water as the Archimedean fluid. An adapted Snowrex NH – 3 scale that can weigh a rock sample in air and in water was used.

The first part of the study investigates the possible differences between conducting rock density measurements on finely milled core in the Grabner Minidens air gas pycnometer or on solid halved core samples using a hydrostatic immersion method, and the implications thereof. The second part of the study, not only investigates the differences between conducting density measurements on solid core samples or on milled core samples, but also looks at how the type of method used and how location affects the density measurement obtained.

The location is important because changes in temperature and atmospheric pressure have been shown to produce small, but measurable changes in density. The density of pure water at 4 ℃ is approximately 1 g/cm^3, increases or decreases in temperature will marginally decrease the density of water. The density of pure water at room temperature (21 ℃) is 0.998 g/cm^3. Changes in atmospheric pressure have been shown to have a negligible effect on the density of most solids.

The diamond drill core samples were taken from boreholes targeting the platinum group element (PGE) rich Merensky reef (MR) and Upper Group 2 (UG2) chromitite layer of the Upper Critical Zone. Samples were taken from the hangingwall (HW), reef and footwall (FW) of the MR and UG2. These rocks are made up of closely interlocking minerals, typical of cumulates. There are generally no visible pore spaces apart from highly fractured and altered samples.

In part one of the study, 18,430 samples were used. The halved core samples were first measured using the hydrostatic immersion method at the exploration offices close to where the boreholes were drilled, referred to as the "Driekop" method. The samples were then sent to a laboratory in Johannesburg. Each sample was first milled to a fine powder (40 μm), and then a small portion of the milled sample (4 cm^3) measured using the Grabner Minidens air gas pycnometer, referred to as the "Grabner Milled" method. For quality control, 811 of the remaining halved core samples were re-measured using the hydrostatic immersion method.The Grabner Milled results were found to be consistently higher than the Driekop results, with a mean average relative difference (AVRD) of approximately 5 % for all

stratigraphic units. The difference observed can be accounted for, from the way in which the sample is prepared and the type of density that is measured. The Driekop method calculates the bulk density of the solid halved core sample, which includes all the open and closed pores of the rock. The Grabner Milled method calculates the true density of the finely milled sample, which through comminution, has excluded all open and closed pores that were in the rock. The quality control repeat measurements on the remaining halved core samples showed a good correlation with the original measurements, with a mean AVRD of only 0.33 %.

In part two of the study, 82 randomly selected samples were used. The density of each solid sample was first determined using the hydrostatic immersion method. The same hydrostatic immersion method used in part one was applied at the same location; therefore it is also referred to as the "Driekop" method. The same hydrostatic method was then conducted on the samples at the laboratory in Johannesburg, referred to as "Lab water solid". The gas pycnometer method was only conducted at the laboratory. The samples were first measured as a solid, referred to as "Grabner solid". The samples were then milled to 40 μm and re-measured in the Grabner Minidens, referred to as "Grabner Milled". The three solid methods results showed good correlation, with an average AVRD of only 0.01 % for the two hydrostatic immersion methods. On the other hand, there was a marked difference in results between the solid methods and the Grabner Milled method, the most significant difference being between the Grabner Milled and Grabner solid method (AVRD = 3.42 %).

The resource model parameters for a project within the study area were used to illustrate the effect of density on resource planning. The average density used in the resource calculation will depend on what density method is used. The AVRD between the two methods for the mining cut density was approximately 5 %. The resource calculation showed that the difference in tonnage and 4E ounces between the two methods was also approximately 5 %. Changes in density result in equal changes in tonnage and metal content (4E ounces).

Increases in dilution or overbreak from 10 to 30 cm above the optimal mining cut showed increases in tonnage and decreases in metal content. Due to similarities in rock composition between the HW, reef and FW of the MR, further dilution caused only a marginal decrease in density. The UG2 was found to be much more sensitive to dilution because of the distinct differences in rock composition between the reef, which is a chromitite layer and the HW and FW, which are both made up of plagioclase pyroxenite. Emphasis is commonly placed on the effect of dilution on grade; however this shows that the effect of density can be as important.

The hydrostatic method of density determination is a very practical way of determining rock density at a remote exploration site. The whole sample can be measured and it is not restricted by the size or shape of the sample. Modern gas pycnometers have a higher degree of accuracy and precision, but need to be operated in a laboratory controlled environment, and are only capable of measuring a small amount of sample. With the correct application of quality control, both are suitable methods of density determination. The selection will depend on what type of density is required, the nature of the rock and whether the method must include or exclude pore spaces in the rock.

ACKNOWLEDGEMENTS

DECLARATION OF ORIGINALITY

UNIVERSITY OF PRETORIA

Full names of student:………………………………………………………………………...

Student number: …………………………………………………………………………

Topic of work: ………………………………………………………………………….

Declaration

1. I understand what plagiarism is and am aware of the University's policy in this regard.

2. I declare that this dissertation is my own original work. Where other people's work has been used (either from a printed source, Internet or any other source), this has been properly acknowledged and referenced in accordance with departmental requirements.

3. I have not used work previously produced by another student or any other person to hand in as my own.

4. I have not allowed, and will not allow, anyone to copy my work with the intention of passing it off as his or her own work.

SIGNATURE ………………………………………………………………………….

TABLE OF CONTENTS

LIST OF FIGURES

LIST OF TABLES

LIST OF TABLES IN APPENDIX B

LIST OF TABLES IN APPENDIX C

LIST OF TABLES IN APPENDIX D

LIST OF ABBREVIATIONS

4E grade	Weighted average grade of Pt, Pd, Rh and Au in g/t
Au	Gold
AVRD	Average relative difference (refer to equation 8)
BQ	Diamond drill core size diameter equal to 36.10 mm
°C	Degrees Celsius
cm	Centimeters
Driekop	Water hydrostatic method of rock density determination, conducted on solid core samples at the exploration site
Driekop check	Water hydrostatic method of rock density determination, conducted on the remaining solid halved core samples at the exploration site in order to check the original results
g	Grams
g/cc or g/cm^3	Grams per cubic centimetre
g/t	Grams per ton
Ga	One billion years
GPM	Gapasha Project
Grabner Milled	Grabner Minidens air gas pycnometer method of rock density determination, conducted on milled/powdered core samples at the laboratory in Johannesburg
Grabner Solid	Grabner Minidens air gas pycnometer method of rock density determination, conducted on solid core samples at the laboratory in Johannesburg
KPa	Kilopascals
km	Kilometers
Lab water solid	Water hydrostatic method of rock density determination, conducted on solid core samples at the laboratory in Johannesburg
LPM	Lebowa Project
m	Meters
Ma	One million years
ml	Milliliters
mm	Millimeters
MR	Merensky reef
MRFW	Merensky reef footwall
MRHW	Merensky reef hangingwall
Oz	Ounce (31.1034831 grams)
Pd	Palladium
PGE	Platinum group elements
Pt	Platinum
Rh	Rhodium
t/m^3	Tons per cubic meter
THP	Twickenham Project
Tons	One thousand kilograms
UG2	Upper Group 2 chromitite layer
UG2FW	Upper Group 2 chromitite footwall
UG2HW	Upper Group 2 chromitite hangingwall
°	Degrees

LIST OF DEFINITIONS

Accuracy	Measure of closeness to the true value
Apparent or skeletal density	Mass divided by apparent volume
Apparent or skeletal volume	Solid volume plus closed pore volume, all open pore volume is excluded
Bulk density	Mass divided by bulk volume
Bulk volume	Solid volume plus all pore volume, open, closed and inter-particle, as with powders
Comminution	The process whereby rocks are reduced in size by crushing, grinding and milling
Density	The concentration of matter, that is mass per unit volume
Envelope volume	The volume of a particle around a tight fitting envelope
Grade	Metal or element content in g/t
Mining cut	The reef, together with the optimal thickness of hangingwall and footwall
Precision	Measure reproducibility or repeatability
Sampling cut	The sampled components of the hangingwall, reef and footwall
True or absolute density	Mass divided by true volume
True or absolute volume	The volume of only the solid; all open and closed pore volume is excluded

1. INTRODUCTION

The density of a rock sample or any material is the ratio of the mass of the rock/material to a given volume of the sample. It can be defined as the concentration of matter. Dense materials will have a high mass to volume ratio.

Density is calculated by taking the mass of the sample and dividing it by the sample's volume. Density is expressed as grams per cubic centimetre (g/cc or g/cm^3) or tons per cubic meter (t/m^3), which are numerically equivalent (Britt and Consolmagno, 1998; Britt et al., 2002; Capano, 2000; Geddis et al., 1996; Goldman and Buskirk, 1959; Weindorf and Wittie, 2003).

The mass of a rock sample can easily be determined using an analytical balance. Calculating the volume is more complicated. The volume of regular solid objects such as cubes or cylinders can be readily determined from physical measurements of the object. Irregular objects such as rock samples require indirect methods of volume determination, the results of which will depend on whether the method accounts for the pore volume within the rock (Geddis et al., 1996; Weindorf and Wittie, 2003).

A typical rock sample is made up of a collection of minerals. The rock may have cracks or pores that either connects to the surface exterior of the rock (open pores) or those that are isolated within it (closed pores). Closed pores may be in the form of cracks/structures within the rock, and/or within mineral grains, and/or along grain boundaries depending on the mineral assemblage or arrangement. Milled or ground rock samples will also have inter-particle spaces that will depend on the size and shape of the individual particles and how they are packed (Webb, 2001).

Mining and exploration companies routinely send rock samples to laboratories that determine the metal/mineral grade and density of the samples. These samples may be taken from underground and surface boreholes that intersect the target horizon or from underground excavations or surface exposures of the target horizon. The density of the sample is of utmost importance as it is used in resource planning to ultimately determine the tonnage of the orebody. The relative proportions of hangingwall, reef and footwall are used to determine the average density for the optimal mining cut of the deposit. The proportions of hangingwall, reef and footwall

may be constrained to geological zones or structural blocks, related to geotechnical constraints or orebody characteristics (grade, internal waste, etc). The dip area and density are used to calculate the expected tonnage of the resource, and then the average grade and tonnage are used to determine the expected metal/mineral content. Incorrect density determinations could potentially have a detrimental effect on the accuracy of resource calculation.

Within the guidelines of the SAMREC code (2007), concerning the reporting of tonnages and density data, it states that the density measurements must be representative of the material being reported and that the method used must adequately account for void spaces, moisture and differences between rock and alteration zones within the deposit.

Rock density is most often determined using hydrostatic immersion or by means of a gas pycnometer. Gas pycnometers are almost exclusively used by laboratories specializing in mineral analysis, whereas the hydrostatic immersion method may be applied anywhere.

With the hydrostatic method, the volume of the sample is calculated by comparing the weight of the sample in air to the weight of the sample immersed in a liquid of known density. The method makes use of Archimedes' principle i.e. a body immersed in a fluid is buoyed up by a force equal to the weight of the displaced fluid (Brit et al., 1987; Goldman and Buskirk, 1959; Turner et al., 1978; Weindorf and Wittie, 2003).

Gas pycnometers are commonly used to measure the volume of milled samples, powders and small solids. The volume is determined by calculating the pressure change resulting from the displacement of gas by a solid object (Archimedean principle) and solving for the ideal gas law. Modern devices are automated with built in analytical balances for determining the mass, then the volume and finally the density (Agnew et al., 2003; Chang, 1988; Geddis et al., 1996; Orr et al., 1991; Turner et al., 1978; Webb, 2001).

The largest supply of platinum in the world comes from the Merensky reef (MR) and Upper Group 2 (UG2) chromitite layer of the Bushveld Complex, South Africa. The MR and UG2 are located within the Upper Critical Zone of the Rustenburg Layered Suite. Comparative studies of the density method that should be

used for the MR and UG2, and the considerations that need to be taken before deciding which method to use, are limited.

This study will compare results obtained using the hydrostatic immersion and gas pycnometer methods to determine the density of the rocks that make up the MR and UG2 and their immediate hangingwall and footwall lithologies. The implications of using one method over the other and the considerations that need to taken will be investigated. The samples used in the study are taken from BQ sized diamond drill boreholes, drilled in the North Eastern limb of the Bushveld Complex, South Africa.

1.1. THE RESEARCH PROBLEM

1.1.1. Statement of the research problem

- o Is there a significant difference in results obtained when using a hydrostatic immersion or gas pycnometer method to determine rock density?

  - What are the differences between the two methods?

  - Are these differences significant and what are the implications thereof?

1.1.2. Delimitations

- o The comparison is limited to samples taken from split diamond drill core samples.

- o The samples were taken from boreholes drilled in the North Eastern limb of the Bushveld Complex, South Africa.

- o Only rocks of the MR and UG2 chromitite layer and their immediate hangingwall and footwall lithologies will be considered.

- o Only the density of the in situ rock required for resource planning will be analysed. It will not address the density of the rock during mining, metallurgical processing and recovery.

- o Resource planning in the context of this study will be limited to the influence of the rock density on the resource calculation.

1.2. RELEVANCE OF THE STUDY

The study was initiated from the need to have some form of in house density measurement that could be used to compare the results determined by the laboratory, as a quality control measure.

In the case of the gas pycnometer method that is currently in use, the core sample is milled to a fine powder (± 40 μm) and then only a small portion (± 4 cm^3) of the powder is used for the density measurement. Concerns had arisen as to whether the results determined using the gas pycnometer method were true representations of the density of the rock in its natural state. A hydrostatic immersion method was used for the comparison, as the density of the sample is determined using the entire core sample and it is a practical way of determining density at a field exploration site.

This study will show whether the hydrostatic immersion method and gas pycnometer method are comparable. It will also show whether the hydrostatic immersion method can be used as an in house quality control measure to compare density results received from the laboratory.

In terms of resource planning, the study will show what factors need to be considered before selecting the method of density determination. It will show how these factors may affect the density of the MR and UG2, and the possible impact on the resource calculation.

2. METHODS OF ROCK DENSITY DETERMINATION

Different methods of rock density determination depend on the type of volume to be measured. In this chapter, the different types of volume will be discussed, followed by descriptions of commonly used density determination methods.

2.1. DENSITY TERMINOLOGY

The introduction (chapter 1), highlighted the complexity of determining the volume of irregularly shaped rock samples. The volume calculated will depend on the structure and composition of the rock, and whether the volume determination method accounts for any open or closed pores within the rock.

There are a number of different terms for the type of volume measured (Geddis et al., 1996). Webb (2001) provides an excellent summary of the different types of volume, density and porosity definitions from the British Standards Institute (BSI, 1991) and American Society for Testing and Materials (ASTM, 1991). The volume defined is often dependant on the measurement method, operating conditions and whether the substance is one piece (solid monolith) or made up of a fine powder (collection of particles). The density is defined according to the type of volume that is measured (Webb, 2001).

Bulk volume is a measure of the solid volume plus all pore volume made up of open, closed and inter-particle as with powders. Envelope volume, which as the name implies, is the volume of a particle around a tight fitting envelope, taking into account any surface irregularities but including all open and closed pores (figure 1A). Bulk and envelope density are often used interchangeably, depending on whether the sample is powder or a solid monolith. Generally, bulk density is used to define the density of a collection of particles and envelope density is used to define a singular particle or solid monolith (figure 1A). Apparent or skeletal volume is a measure of the solid volume plus closed pore volume, all open pore volume is excluded (figure 1B). True or absolute volume is a measure of only the solid volume (figure 1C); all open and closed pore volume is excluded (ASTM D 2638, 1997; Britt and Consolmagno, 1998; Britt et al., 2002; Geddis, et al., 1996; Webb, 2001).

"Envelope" encompassing the particle

External or open pore within the envelope

A) Envelope or bulk volume (Solid plus open and closed pores)

B) Skeletal volume (Solid plus closed pores)

C) Absolute volume (Solid volume only)
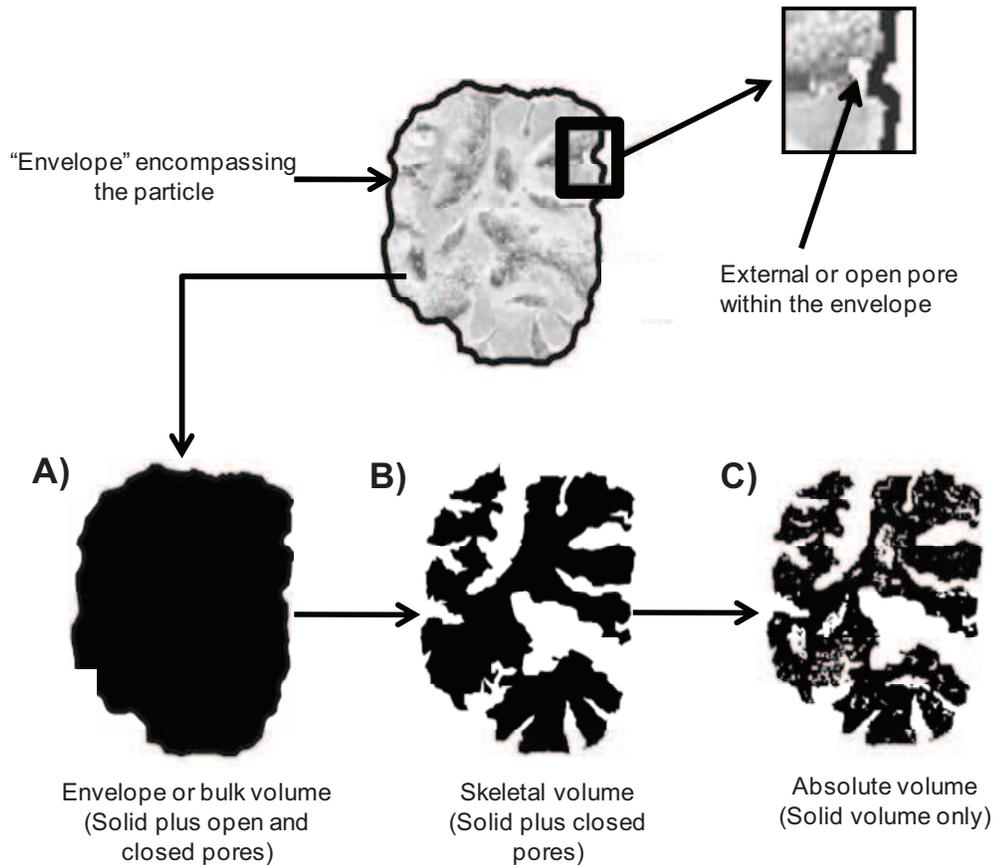
Figure 1. Schematic showing the different types of volume (After Webb, 2001).

The pore volume can be readily calculated by subtracting the true volume from the bulk volume of the rock. Similarly, the pore density is determined by subtracting the bulk density from the true density. The pore volume or pore density is often expressed as a percentage, by either dividing the pore volume with the bulk volume and multiplying the result by 100 or by dividing the pore density with the true density and multiplying by 100 (Britt and Consolmagno, 1998; Britt et al., 2002; Chang, 1988).

The composition, internal and external properties of the rock, together with the measurement method and conditions under which the measurement is conducted, will determine the volume obtained. The density is defined according to the type of volume measured, from figure 1: bulk density includes open and closed pores; envelope density includes open pores, closed pores and surface irregularities; skeletal density excludes open pores and includes closed pores; and true or absolute

density excludes all pores (ASTM D 2638; 1997; Britt and Consolmagno, 1998; Britt et al., 2002; Geddis, et al., 1996, Webb, 2001).

2.2. HYDROSTATIC IMMERSION

In this method the volume of the sample is calculated by comparing the weight of the sample in air to the weight of the sample immersed in a liquid of known density. Water is the most common reference liquid used; however, different reference liquid/material may be used depending on the application. For soils and compost with a density less than that of water, hexane (0.6 g/cc) may be used (Weindorf and Wittie, 2003). In order to determine the bulk density of asteroids without contaminating the sample using water, Britt and Consolmagno (1998) used 40 µm glass spheres as the Archimedean fluid.

Relative density can be defined as the ratio of the density (mass of a unit volume) of a substance to the density of a given reference material, usually water (Chunnett et al., 2006). The formula for relative density is as follows:

$$\text{Relative Density} = \frac{\text{Density}_{sample}}{\text{Density}_{water}} = \frac{\dfrac{\text{Weight}_{sample}}{\text{Volume}_{sample}}}{\dfrac{\text{Weight}_{water}}{\text{Volume}_{water}}} = \frac{\text{Weight}_{sample}}{\text{Weight}_{water}} \qquad (1)$$

Therefore using Archimedes' principle (weight of water is equal to the buoyancy force), the equation becomes (Chunnett et al., 2006):

$$\text{Relative Density} = \frac{\text{Weight}_{sample}}{\text{Buoyancy force}} \qquad (2)$$

Buoyancy force is equal to the difference of the weight of the sample in air and the weight of the sample in water. Therefore in order to obtain the relative density of the sample, the sample needs to be weighed in air and then in water (Chunnett et al., 2006):

$$\text{Relative Density} = \frac{\text{Weight}_{\text{sample (air)}}}{\text{Weight}_{\text{sample (air)}} - \text{Weight}_{\text{sample (water)}}} \quad (3)$$

The actual density of the sample is then determined by multiplying the relative density by the density of water (Chunnett et al., 2006). The density of pure water at approximately 4 ℃ is 1 g/cm^3. The density of water decreases with higher and lower temperatures (table 1).

Table 1. The effect of temperature on the density of pure water (After Snelling, 2010).

Temperature °C	Density (g/cc)	Temperature °C	Density (g/cc)
0 (Solid)	0.915	15	0.999099
0 (Liquid)	0.999841	16	0.998943
1	0.9999	17	0.998774
2	0.999941	18	0.998595
3	0.999965	19	0.998405
4	0.999973	20	0.998203
5	0.999965	21	0.997992
6	0.999941	22	0.99777
7	0.999902	23	0.997538
8	0.999849	24	0.997296
9	0.999781	25	0.997044
10	0.9997	26	0.996783
11	0.999605	27	0.996512
12	0.999498	28	0.996232
13	0.999377	29	0.995944
14	0.999244	30	0.995646

It is evident from table 1 that the effect of temperature on the density of water is very small. However, changes in temperature can produce measurable changes in density, which will depend on the application. The effect of changes in atmospheric pressure has a negligible effect (Capano, 2000). Changes in pressure and temperature have a much larger effect on gases than on solids and liquids. Contamination or alteration of the sample by immersing it in the reference fluid must also be considered when using this method.

The type of density measured using this method will depend on the ability of the water to infiltrate through any open pores/fractures within the samples structure (Geddis et al., 1996). This will obviously depend on the permeability of the sample,

mineral arrangement, composition and structure. Apart from highly permeable, porous or fractured samples, infiltration will be limited given the close interlocking nature of the mineral grains. In most cases the bulk or envelope density is measured.

It is possible to coat the sample in wax or resin of known density to ensure that the open and closed pore volume is included in the volume measurement. The sample is weighed and then dipped in molten wax, and once dried, weighed again. Care must be taken to ensure any bubbles within the wax are pressed out before it dries. The difference between the weight of the sample in wax and the weight of the sample before coating gives the weight of the wax. The volume of the wax coating is determined by dividing the volume of the sample by the density of the wax (Chang, 1988; Regimand, 2001; Webb, 2001). Regimand (2001) describes using preformed resilient bags and vacuum sealing the bag around the sample, as an alternative to wax coating. One of the issues with using wax in highly porous samples is that wax may penetrate into the pore spaces, and it is also often difficult to remove (Regimand, 2001).

Following the hydrostatic immersion method described above, the volume of the coated sample is determined by the difference of the weight of coated sample in air and the weight of the coated sample in water. The volume of the uncoated sample is determined by subtracting the volume of the coated sample and the volume of the wax coating. The bulk or envelope density of the sample can now be readily calculated by dividing the mass of the uncoated sample by the volume of the uncoated sample (Chang, 1988; Regimand, 2001; Webb, 2001).

2.3. GRADUATED FLASK

Using this method, the volume of the sample is determined by placing the sample in a water filled graduated flask and reading off how much water is displaced. The flask is usually calibrated in millilitres, where 1 ml = 1 cm^3. The mass of the sample is measured using a balance and density can be readily calculated.

As with the hydrostatic method, the density determined will depend on the ability of the water to infiltrate through any open pores/fractures within the core samples structure (Geddis et al., 1996). This will obviously depend on the permeability of the sample, mineral arrangement, composition and structure.

2.4. PYCNOMETER BOTTLES

Pycnometer is derived from the Greek word meaning dense. A pycnometer is a bottle with a known volume. The bottle is commonly made up of glass, with a tight sealing stopper that has a capillary tube through it in order for bubbles to escape (figure 2). This device is used to determine the density of milled or powdered samples, or small solids, and is also widely used for determining the density of soils or compost. As with the previous two methods where the reference liquid is water, the same constraints apply. These constraints are the permeability, mineral arrangement, composition and structure of the sample. The ability of the water to enter small pores may also be restricted by surface tension (Geddis et al., 1996).

In this case, the weight of the pycnometer filled only with water is established. The dry, pre-weighed sample is then added to the pycnometer and the rest is filled with water. The density of the sample can be calculated from the known density of the water; the weight of the pycnometer filled only with the water; the weight of the pycnometer containing both sample and water; and the weight of the sample (Geddis et al., 1996).

Figure 2. Pycnometer bottle.

2.5. GAS PYCNOMETERS

Gas pycnometers determine the volume by calculating the pressure change resulting from the displacement of gas by a solid object (Archimedean principle) and solving for the ideal gas law (equation 4). There are a number of different designs, and these machines are used in a wide variety of applications.

Dry air or helium are the gases most commonly used. The gas used will depend on the size of the gas molecules, size of the pores within the sample or how the gas reacts with the surface of the sample. Helium is often preferred over air as it can readily diffuse into smaller pores given its smaller molecular size (Agnew et al., 2003; Chang, 1988; Geddis et al., 1996; Orr et al., 1991; Turner et al., 1978; Webb, 2001). Figure 3 shows two examples of modern gas pycnometers available on the market.
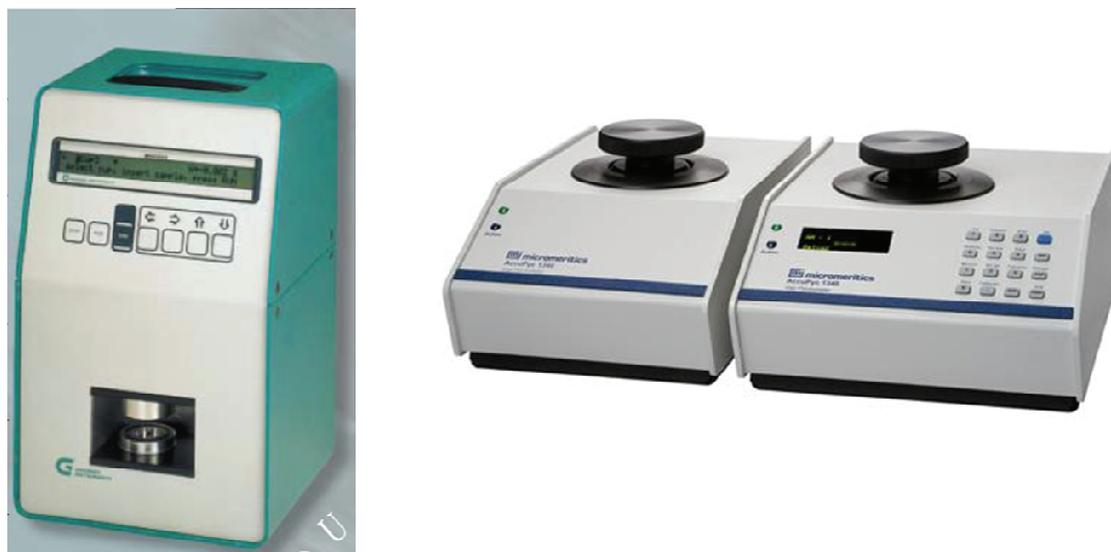
Figure 3. Example of modern gas pycnometers.

> **Note:** On the left is the Grabner Minidens air gas pycnometer and on the right is the Micromeritics Acupyc II helium gas pycnometer.

The measurement process is explained using figure 4 and the equations below (equation 4 to 7). The unknown sample volume (V_x) is placed into the chamber of known volume (V_s). The chamber is sealed and the pressure recorded (P_s). The reference chamber of known volume V_R is then charged to pressure (P_R), at a pressure higher than that of the sample chamber (figure 4). By applying the ideal gas law, the sample volume can be determined. The calculation for this initial state is given in equation 4 (Agnew et al., 2003; Chang, 1988; Geddis et al., 1996; Turner et al., 1978; Webb, 2001).
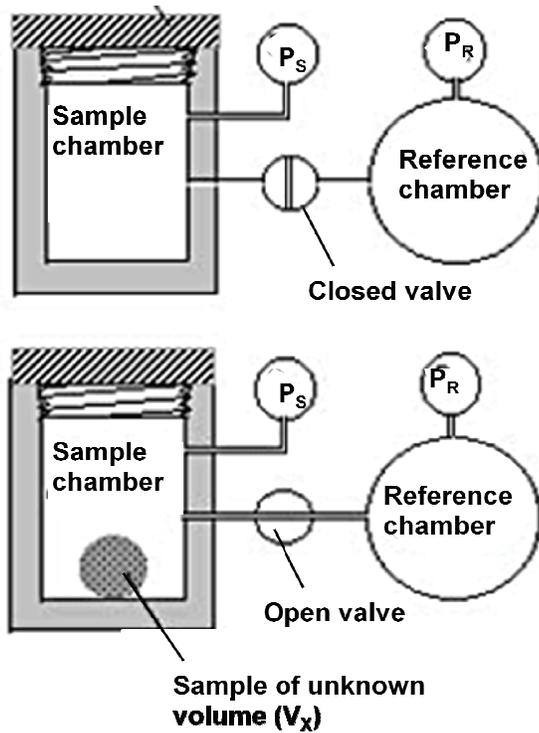
Figure 4. Illustration showing how a gas pycnometer functions (After Webb, 2001).

The valve separating the sample chamber from the reference chamber is then opened, allowing the pressure in the system (P_{SYS}) to equilibrate (equation 5). By substitution the unknown sample volume can be determined (equation 6 to 7); (Agnew et al., 2003; Chang, 1988; Geddis et al., 1996; Turner et al., 1978; Webb, 2001).

$$P_S(V_S - V_X) + P_R V_R \quad = \quad nRT \tag{4}$$

Where **T** is temperature and **n** the number of gas molecules which remains constant throughout the experiment; **R** is the gas constant

$$P_{Sys}(V_S + V_R - V_X) \quad = \quad nRT \tag{5}$$

$$P_S((V_S - V_X) + P_R V_R \quad = \quad P_{Sys}(V_S + V_R - V_X) \tag{6}$$

$$V_X \quad = \quad \frac{(P_{SYS}V_S + P_{SYS}V_R - P_S V_S - P_R V_R)}{(P_{SYS} - P_S)} \tag{7}$$

Modern gas pycnometers are capable of determining the skeletal or very close to the true density of a sample with a high degree of accuracy and precision. These automated devices also have built in analytical balances for determining the mass and are able to compute the density of each, which can then be downloaded to a computer.

In order to achieve a high degree of accuracy and precision, the sample and gas used must be free of moisture. Volatiles that may contribute their partial pressure and thus cause error must also be removed (Agnew et al., 2003; Chang, 1988; Geddis et al., 1996; Turner et al., 1978; Webb, 2001). Gas pycnometers are also relatively expensive, and are sensitive to external variables such as changes in ambient temperature, and therefore need to be operated in a controlled environment.

Gas pycnometers can be used to determine the density of larger monolithic substances, but there is limited information on the use of gas pycnometers to determine the bulk or envelope density of larger solid rock/core samples. Modern automated gas pycnometers can only take a very small amount of sample. However, in principle, the method described above can be applied to determine the bulk or envelope density of a solid core or rock sample.

3. REGIONAL GEOLOGICAL SETTING

The Bushveld Complex is situated in the northern part of South Africa, within the provinces of the North-West, Limpopo and Mpumalanga. Figure 5 is a simplified geological map of the Bushveld Complex, showing the location of the study area in the North Eastern limb, highlighted by the red polygon.
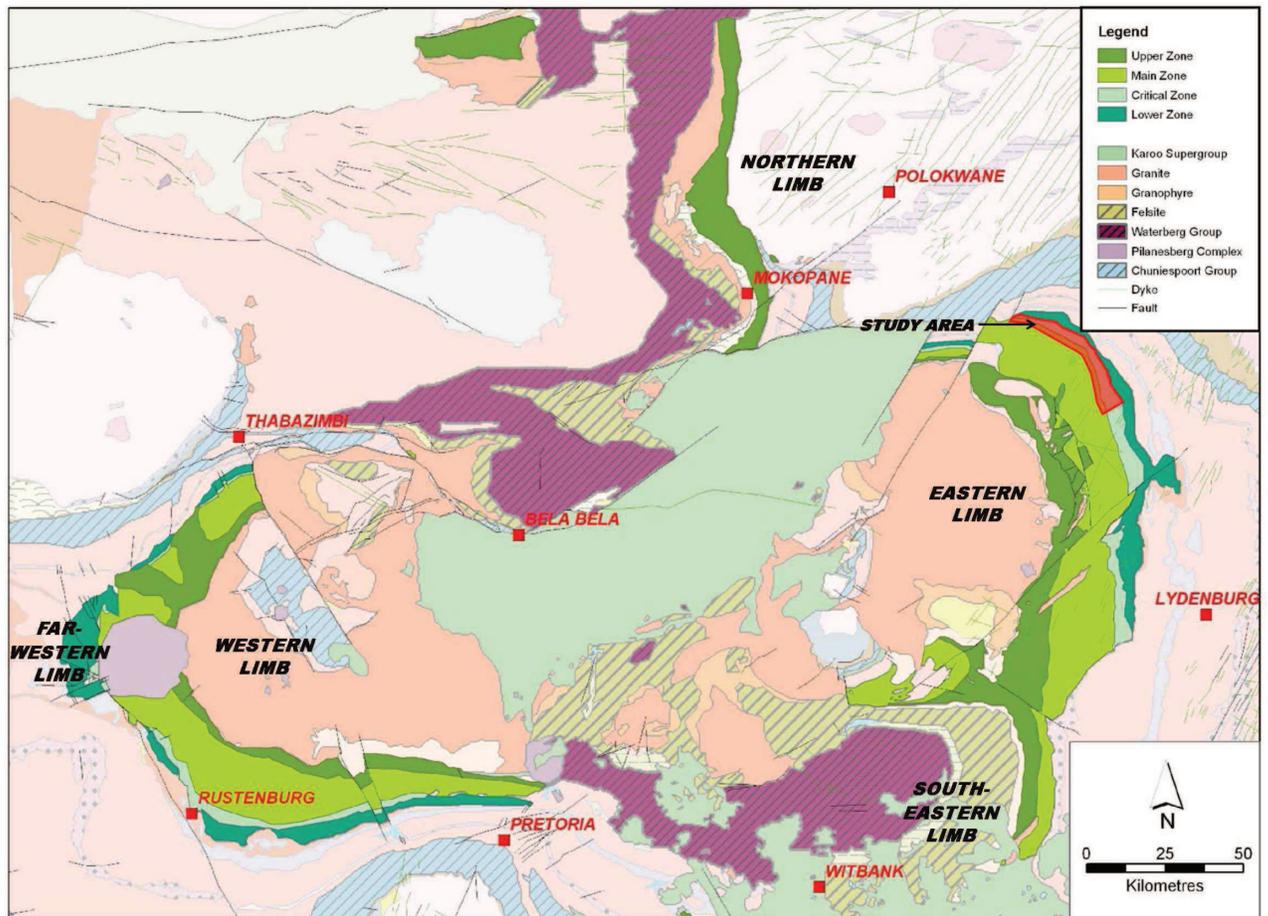
Figure 5. Simplified geological map of the Bushveld Complex, showing the study area in red (After Brown, 2005a).

The Rustenburg Layered Suite is the worlds largest layered mafic to ultramafic intrusion, at its extremities stretching approximately 450 km from east to west and 350 km north to south (Naldrett et al., 2009). It outcrops over an area of approximately 65 000 km^2, with thicknesses of about 7 to 8 km (Eales, 2001; Cawthorn and Webb, 2001; SACS, 1980; Seabrook, 2004).

The Rustenburg Layered Suite was emplaced into the Transvaal sequence of the Kaapvaal craton, beneath the acid volcanics of the Rooiberg Group (Cawthorn and Walraven, 1998). The Rustenburg Layered Suite has been dated to have intruded into the Transvaal basin at 2.054 Ga (Von Gruenewaldt et al., 1985; Scoates and Friedman, 2008).

The Rustenburg Layered Suite may be divided into five compartments or limbs. The five limbs are the Western Bushveld, Eastern Bushveld, South-Eastern Bushveld, Northern Bushveld and Far-Western Bushveld, as shown in figure 5 (Cawthorn and Walraven, 1998; Eales, 2001; Naldrett et al., 2009; Seabrook, 2004). The Western and Eastern limbs dip inwards beneath the central granite and granophyres suites, averaging 10° - 20°. The Northe rn limb dips independently in a westerly direction (Eales, 2001).

The Rustenburg Layered Suite of the Bushveld Complex is divided into five zones based on the main rock types and geochemistry (Barnes and Maier, 2002; Cawthorn and Walraven, 1998; SACS, 1980). They are from the bottom, the Marginal Zone which is only locally developed above the underlying Transvaal Supergroup; Lower Zone; Critical Zone; Main Zone; and Upper Zone.

A generalized lithostratigraphic column of the Rustenburg Layered Suite in the Eastern Bushveld is given in figure 6. Figure 6 shows the average thickness of each zone and subzone in the Rustenburg Layered Suite of the Eastern Bushveld, together with the major rock types that make up each zone.
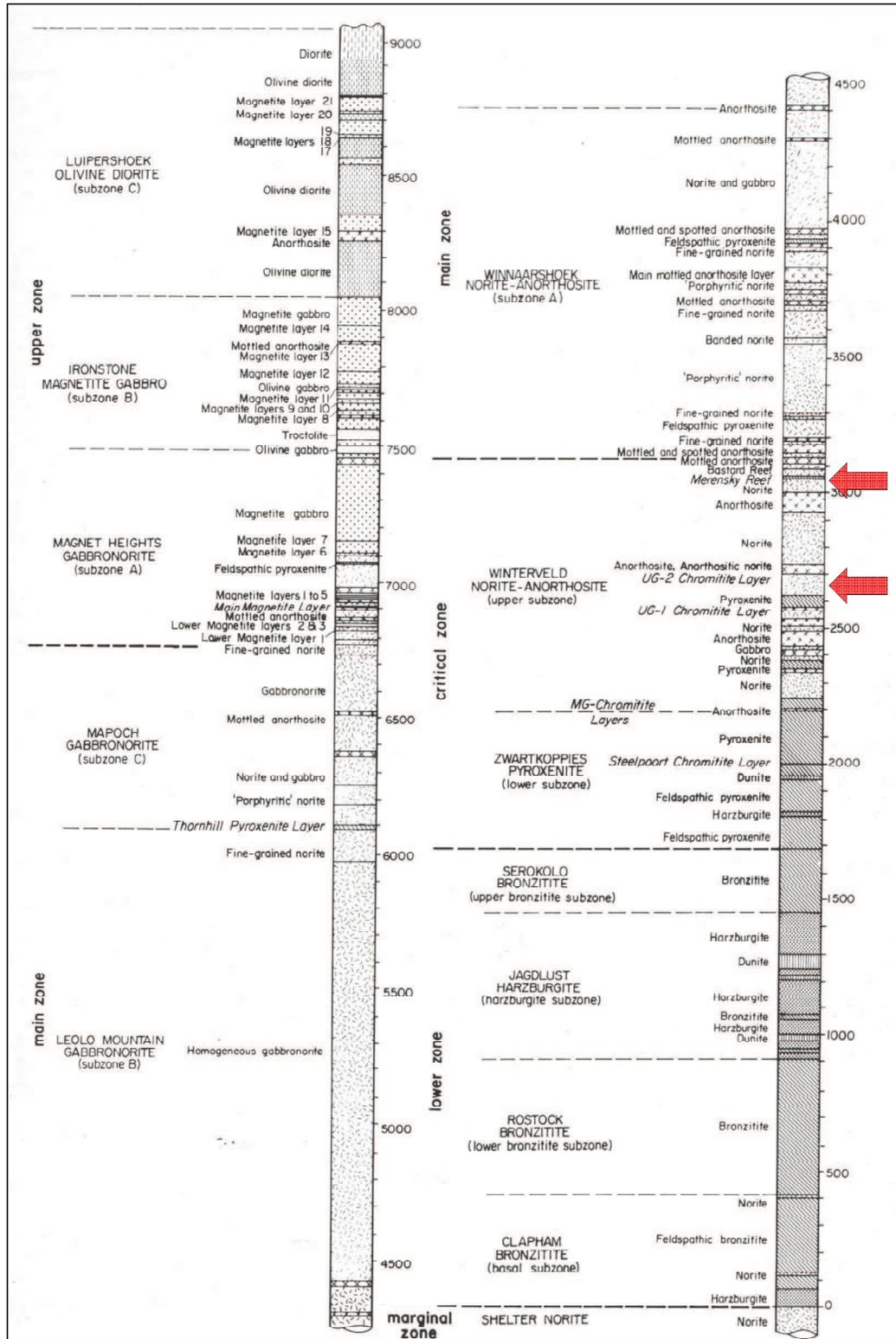
Figure 6. Lithostratigraphic column of the Rustenburg Layered Suite of the Eastern Bushveld (Von Gruenewaldt et al., 1985).

Note: The positions of the MR and UG2 is indicated by the red arrows.

Economic concentrations of PGE are found in three very different layers: the MR and UG2 of the Upper Critical Zone (red arrows in figure 6, and figure 7), which are found in both the Eastern and Western limbs, and the third layer, the Platreef, which is located in the Northern limb. The Platreef is considerably thicker than the MR (figure 7); (Cawthorn et al., 2002).
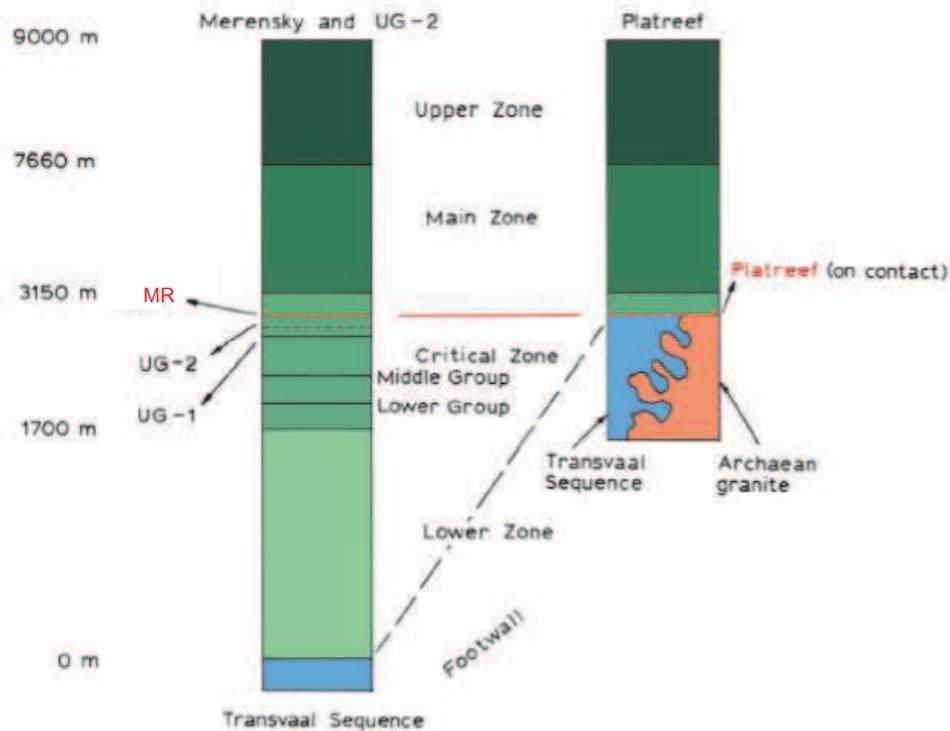
Figure 7. Simplified stratigraphic column of the Rustenburg Layered Suite (After Kinloch and Schouwstra, 2000).

> **Note:** The column on the left shows the positions of the Merensky Reef and Upper Group 2 chromitite layer found in the Western and Eastern limbs, in relation to the column on the right showing the Platreef of the Northern limb.

These zones show remarkable stratigraphic and petrological similarities between the Western and Eastern limbs. The average thickness and correlations between the Western and Eastern limb are given in figure 8 (Cawthorn and Walraven, 1998).
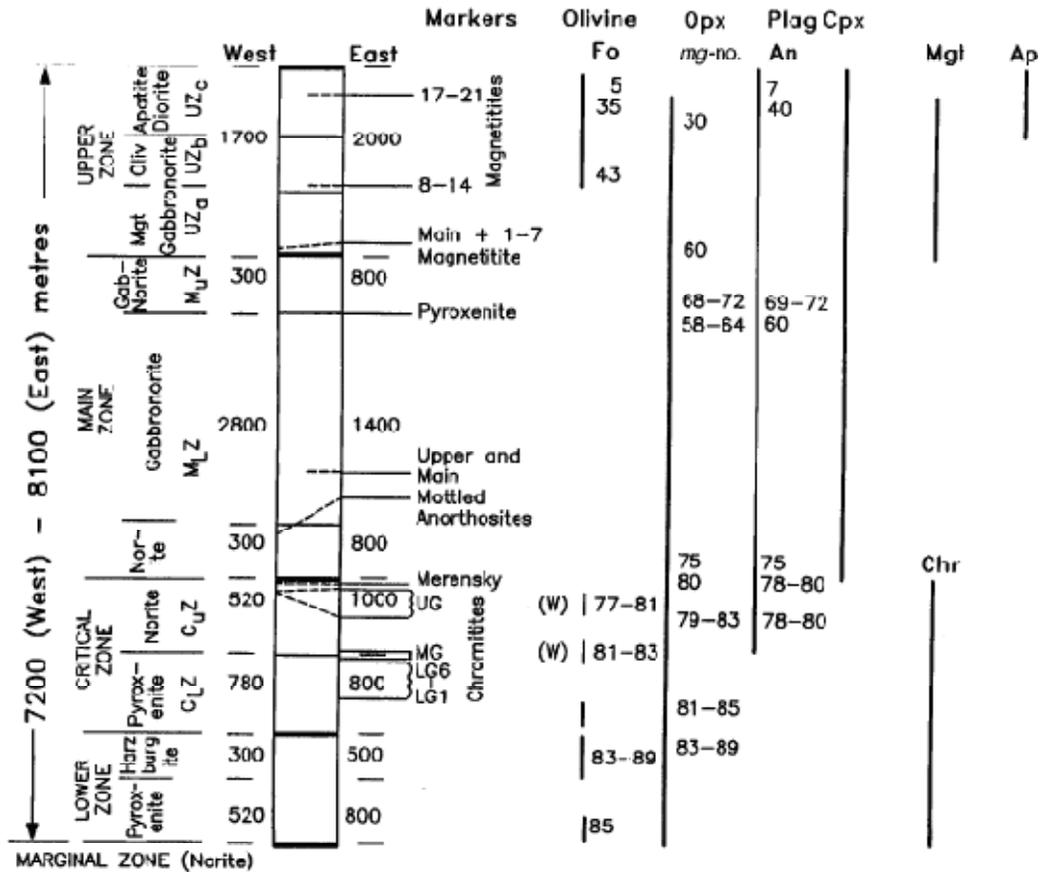
Figure 8. Simplified stratigraphic column of the Western and Eastern limbs of the Rustenburg Layered Suite (Cawthorn and Walraven, 1998).

Note: Correlations between the two limbs are shown. Solid lines indicate marker horizons found in both limbs. Dashed lines indicate that they occur on only one limb. The major changes in mineral composition that define the zones are also shown.

Using these similarities, together with the analysis of gravity, seismics and resistivity data, Cawthorn and Webb (2001) and Webb et al. (2004) have put forward a model that supports the connectivity between the Western and Eastern limbs.

The floor rocks of the Bushveld Complex are generally made up of the clastic and chemical sedimentary rocks, consisting mainly of quartzite, argillite, dolomite and banded iron formation, with only the Northern limb showing transgression though the Transvaal sequence into the Archean granites (figure 7); (Cawthorn and Walraven, 1998; Clarke et al., 2005; Naldrett et al., 2009; Von Gruenewaldt et al., 1985).

4. GEOLOGY OF THE STUDY AREA

4.1. MR AND UG2

The samples related to this study were taken from the MR, UG2 and their immediate hangingwall and footwall lithologies. Samples are taken to represent a typical mining cut and cover the extent of the visible mineralization within the reef. Samples seldom extend more than 60 cm into the hangingwall and footwall. A basic stratigraphic column of the MR, UG2 and the rocks that make up the hangingwall and footwall lithologies is given in figure 9. Figures 10 and 11 are underground pictures of the MR and UG2 mining cuts.

From the south to the north of the study area, the average middling between the MR and UG2 decreases from ± 400 m to 350 m, and the dip increases from 12° to 24° respectively (Langwieder, 2005).

Normal Merensky reef is defined as the mineralized medium crystalline (± 1 - 2 mm) poikilitic plagioclase orthopyroxenite layer at or near the base of the Merensky differentiated unit. It is made up of cumulate orthopyroxene (80 - 90 %) and intercumulus plagioclase. It shows both poikilitic and porphyritic textures, and commonly contains large (10 - 20 mm) clinopyroxene oikocrysts. It is usually more than 0.5 m wide and not more than 2 m wide. It is usually bound at the top and bottom by a thin chromitite layer, 2 mm to 30 mm thick. In certain areas the MR may have up to four thin chromitite layers that are locally discontinuous. In some cases the top and bottom chromitite layers are completely absent (Brown, 2004a, 2005a, 2005b; Lee and Butcher, 1990; Mathez et al., 1997; Mitchell and Scoon, 2007; Schwellnus et al., 1976).

The MR is overlain by a medium crystalline plagioclase orthopyroxenite layer, similar to the MR, between 0.4 m to 0.7 m thick which then grades into norite. The MR is underlain by a pegmatoidal (up to 20 mm) plagioclase orthopyroxenite that varies in thickness but is typically between 0.2 m to 1.5 m wide, which is then followed by a medium crystalline plagioclase orthopyroxenite which may extend up to 10 m below the MR, which then typically grades into a medium crystalline gabbronorite (Brown, 2004a, 2005a, 2005b). Gabbronorite layers may directly underlie the pegmatoidal plagioclase orthopyroxenite or be inter-layered within the

medium crystalline plagioclase orthopyroxenite (Brown, 2004a, 2005a, 2005b; Brown and Lee, 1987; Lee and Butcher, 1990; Mathez et al., 1997; Schwellnus et al., 1976).
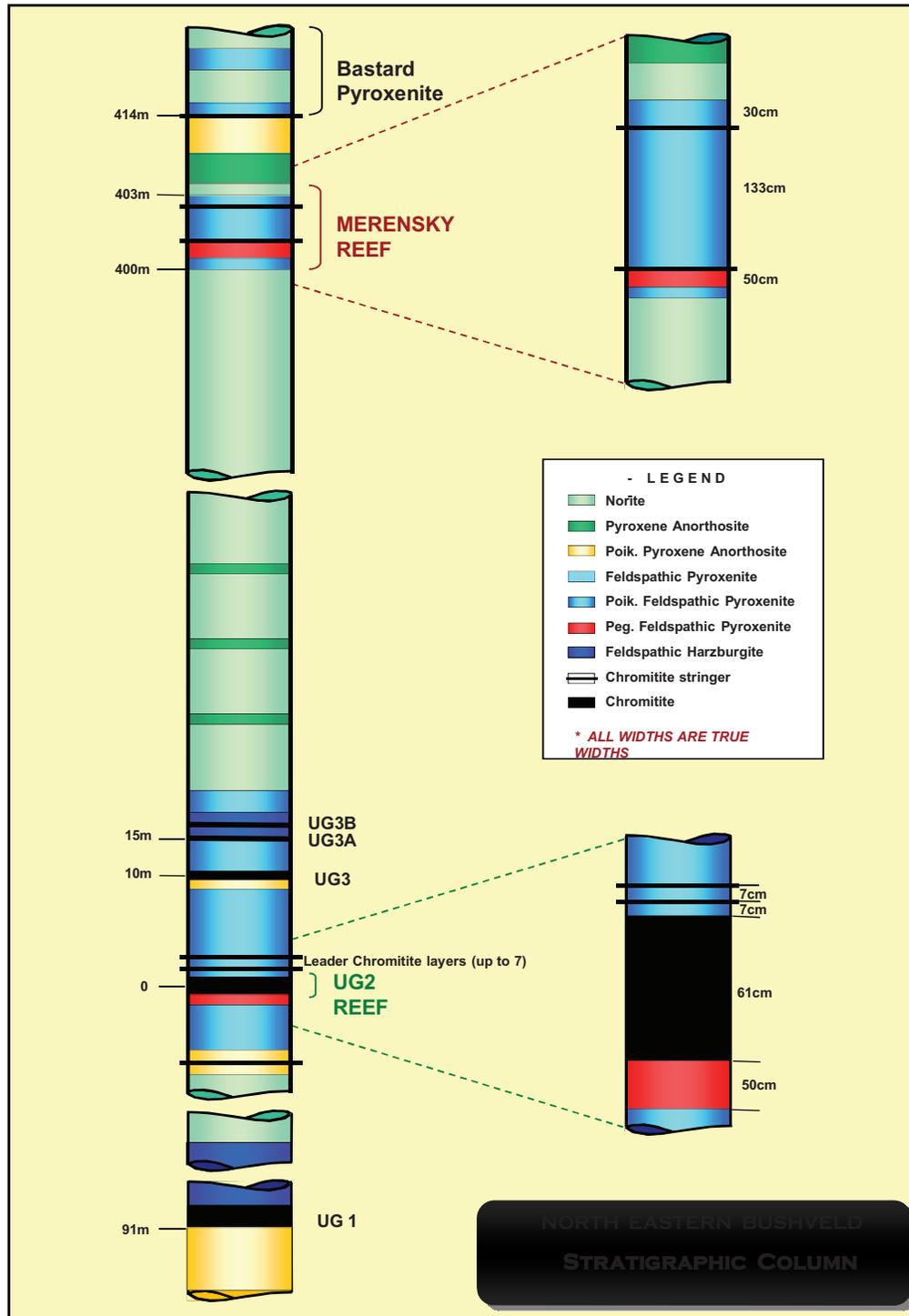
Figure 9. Stratigraphic column of the MR and UG2 reefs in the North Eastern limb of the Bushveld Complex.

Hangingwall medium crystalline plagioclase pyroxenite

Top contact chromitite layer

Reef medium crystalline plagioclase pyroxenite

Bottom contact chromitite layer (not as clear in photo)

Footwall pegmatoidal plagioclase pyroxenite
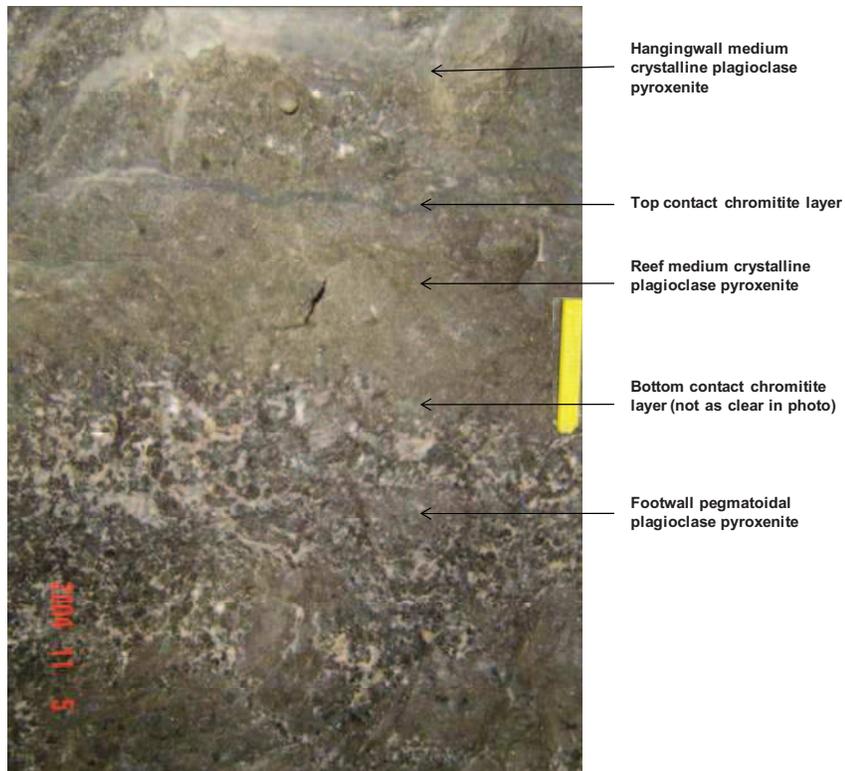
Figure 10. Underground picture of the MR mining cut (after Brown, 2005a).

Leader chromitite layer

Hangingwall medium crystalline plagioclase pyroxenite

UG2 chromitite reef

Footwall pegmatoidal plagioclase pyroxenite
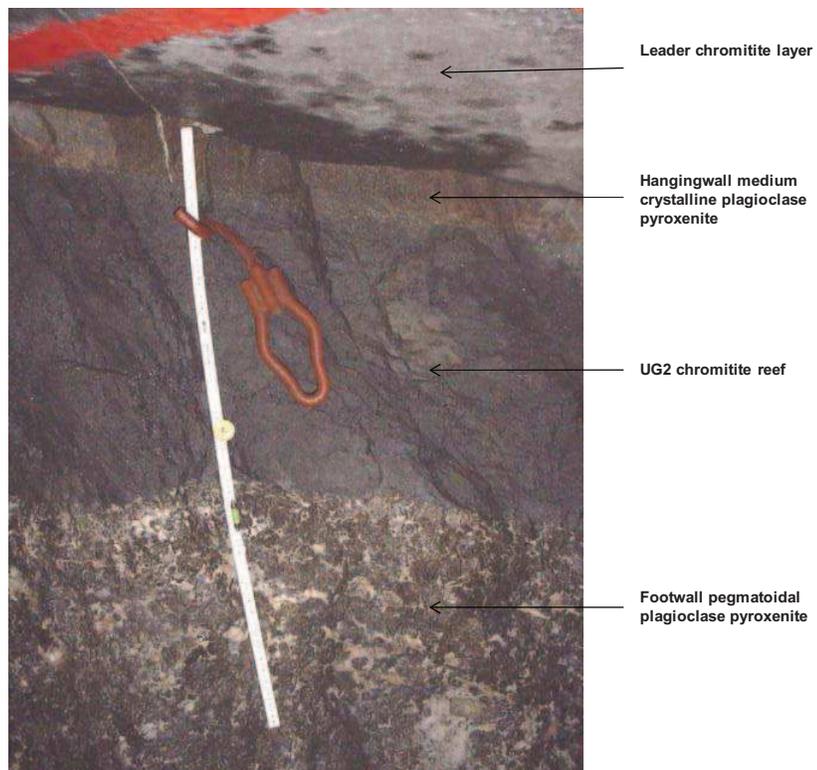
Figure 11. Underground picture of the UG2 mining cut (after Brown, 2005a).

The plagioclase pyroxenite of the MR hosts variable accumulations of chromite, base and precious metal sulphides. This mineralization may extend to the immediate hangingwall and footwall lithologies. Base metal sulphides, chalcopyrite, pentlandite, pyrrhotite and pyrite occur as anhedral crystals sharing interstitial space with plagioclase, within a silicate cumulus framework of orthopyroxene and minor clinopyroxene. Base metal sulphides are also found associated with the chromitite layers, and commonly exhibit high grades or value zones over these layers, especially the top chromitite layer of the MR. PGE mineralization is found contained within the base metal sulphides in solid solution and as distinct platinum group metals that are often spatially associated with base metal sulphides and chromitite. The platinum group metals are mainly made up of PGE sulphides, arsenides, sulpharsenides, bismuthides, tellurides, antimonides, bismuthotellurides and alloys. Solid solution PGE base metal sulphides and platinum group metals may also be found as totally enclosed crystals within the cumulus orthopyroxene or within the cleavage planes of cumulus orthopyroxene crystals due to remobilization (Brown, 2004a, 2005a, 2005b; Brown and Lee, 1987; Lee and Butcher, 1990; Mathez et al., 1997; Schwellnus et al., 1976).

The UG2 is a chromitite layer developed close to the base of the differentiated UG2 unit. The UG2 occurs as a chromite cumulate (75 – 90 %) that is either made up of pure chromite or as a dense cumulate framework of chromite together with fine crystalline interstitial plagioclase and/or orthopyroxene. Interstitial silicates are rarely visible to the naked eye. Interstitial sulphides are also sometimes found within the cumulate chromite and are often visible to the naked eye in the UG2 of the Eastern limb. The UG2 has a fairly consistent average width of 0.6 m, but can range from about 0.2 m to 1.5 m (Brown, 2004a, 2005a, 2005b; Cameron, 1982; Gain, 1985; Mabuza, 2006; Mondal and Mathez, 2007).

The UG2 is overlain by a medium crystalline plagioclase orthopyroxenite. A number of chromitite layers are found within this hangingwall unit. They are variable in width averaging only 5 mm to 10 mm. They are found at varying distances and distributions above the UG2, ranging from a 10 mm to 700 mm. They are generally poorly mineralized. The UG2 is underlain by a pegmatoidal plagioclase pyroxenite which is in turn underlain by a medium crystalline plagioclase pyroxenite marking the base of the UG2 unit. In some instances the UG2 is underlain by norite or anorthosite (Brown, 2004a, 2005a, 2005b; Cameron, 1982; Gain, 1985; Mabuza, 2006; Mondal and Mathez, 2007).

Economic PGE and base metal sulphide concentrations are usually found exclusively within the UG2 chromitite layer. The pegmatoidal plagioclase pyroxenite may contain chromitite as blebs, thin irregular discontinuous layers and/or disseminations. This is often associated with lower concentrations of PGE mineralization. No PGE mineralization extends into the immediate hangingwall unit of the UG2. As with the MR, the PGE mineralization is found as solid solution PGE within the base metal sulphides, as discrete platinum group metals, associated with base metal sulphides. Base metal sulphides and platinum group metals are also found totally or partly encompassed within the individual chromite crystals (Brown, 2004a, 2005a, 2005b).

The most common rock density determination methods have been discussed in Chapter 2. The chapter highlighted the importance of understanding the internal and external structure of the rock being measured. The rock types that make up the MR, UG2 and their immediate hangingwall and footwall are made up of interlocking tightly fitting mineral grains typical of cumulates. There are typically no visible pore spaces on the core samples. However, there may be a small percentage of closed pores or fractures within the internal structure of the rock, for example along the individual mineral grain boundaries. Alteration zones within the orebody as well as zones with intense jointing/fracturing may also affect the density of the rock sample. The method used together with the nature of the rock sample will determine the type of density that is measured.

4.2. STRUCTURE

The study area is characterized by three major fault/lineament/joint directions. They are North-northeast – South-southwest, which is the most prominent; East – West, and North-northwest – South-southeast. They are generally steeply dipping, ranging from 70° to 90°. The aeromagnetic survey of the project area in figure 12 clearly highlights the prominent dyke/structural features and their trend direction.

The study area is fairly uncomplicated in terms of faulting. Displacement is generally small, averaging ≤ 1 m. Where faulting does occur, they consist of dextral and sinistral strike-slip faults, normal and reverse dip-slip faults, as well as faults of both components. There are only two major faults within the study area, one near the southern border of the project area with a displacement of 20 m and one near the northern border of the project area with a displacement of 100 m.
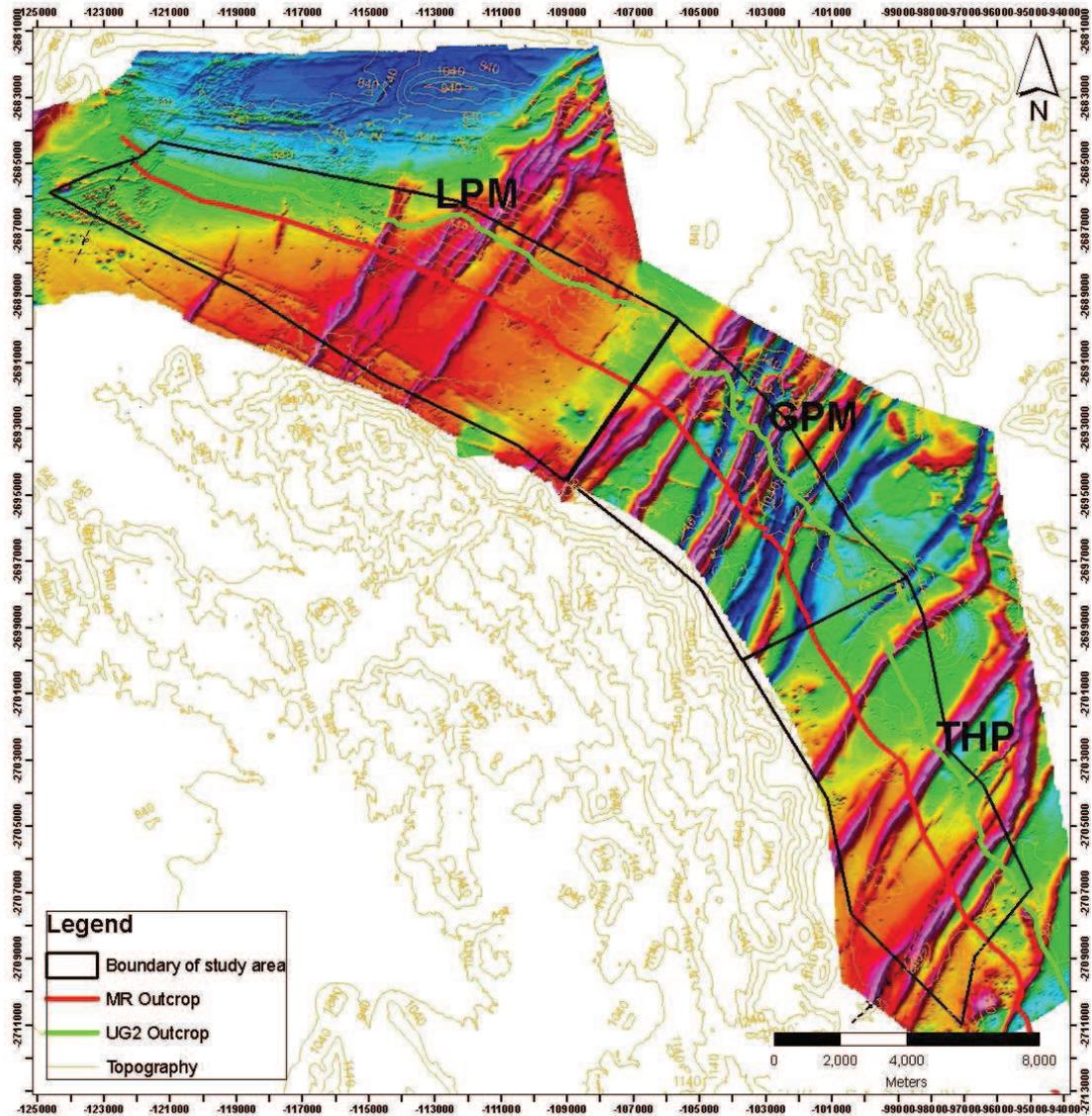
Figure 12. Aeromagnetic survey of the study area, highlighting structural features and directional trend.

A number of dykes occur over the study area. They trend North-northeast – South-southwest, with dips that range from 62° to 89° (figure 13). They are comprised of fine crystalline dolerite and are post Karoo in age, younger than 300 ma (Brown, 2004a). They vary greatly in width from a couple of centimetres to over 30 m, occurring as a single entity or as a dyke swarm. Jointing, alteration and minor faulting is commonly associated with the dykes, but field observations have indicated that this is not excessive. It is generally accepted that an area of 10 m on either side of the dyke will be affected.
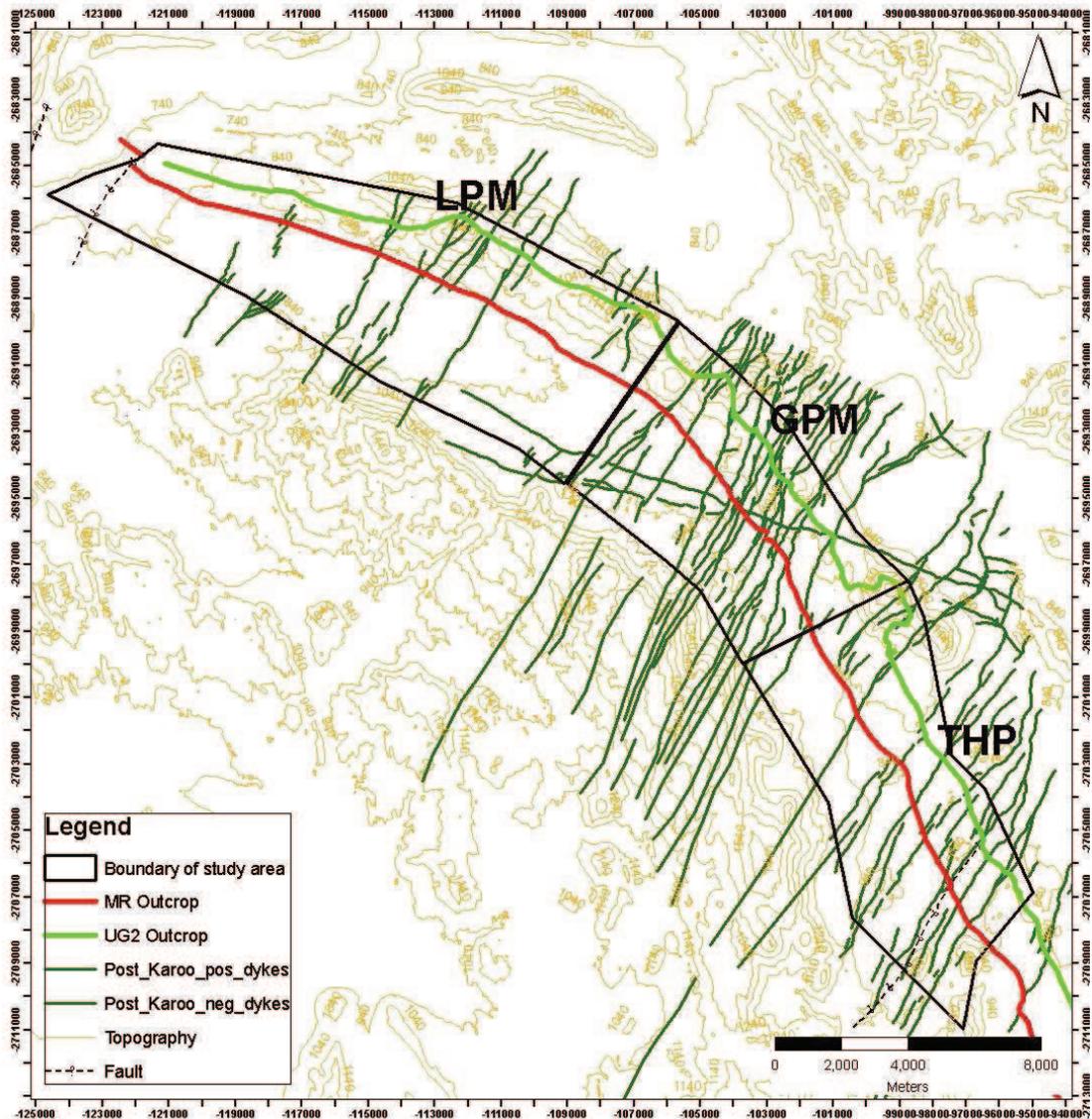
Figure 13. Distribution of dykes across the study area.

The "Footwall 3 shear", is a prominent shear associated with a low-angle thrust fault that occurs 7 – 15 m below the UG2. Apart from this, there is limited evidence of shearing. Several strike parallel lineaments have been indicated from the geophysical survey that may be interpreted as shear zones. It is more likely that they are strike parallel fault/fracture zones which are layer parallel.

Randomly occurring late stage discordant pegmatites are present within the study area. They can be felsic, intermediate, mafic or ultramafic. White sub-vertical felsic veins are common and they seldom exceed 100 mm. Occasionally, irregular

shaped, pegmatitic masses occur, but they are seldom more than 2 m across (Brown, 2004b; Brown and Lee, 1987).

The MR and UG2 are occasionally disrupted by potholes, where the reef discordantly plunges from its normal stratigraphic elevation into a magmatically created depression. The potholes are usually circular to ovoid in shape. They vary greatly in size from a few metres to hundreds of metres across. They are the result of post-crystallisation thermochemical erosion and defluidisation of the cooling footwall stratigraphy caused by the injection of superheated, convecting magma above. These processes created depressions in the transient magma chamber floor into which the MR and UG2 reefs have respectively crystallised. The depth of the potholes are highly variable and depend on a number of factors, in particular, the efficiency of thermochemical erosion and the composition of the footwall lithologies, Potholes may be disruptive, where the degree of reef disruption makes it un-minable, often being highly irregular or completely absent. Potholes may also be non disruptive, in which case normal reef may be developed along a flat base, making it mineable (Brown, 2004a, 2004b, 2005a, 2005b; Brown and Lee, 1987; Mathez et al., 1997). Figure 14 shows the distribution of MR and UG2 potholes within the study area.
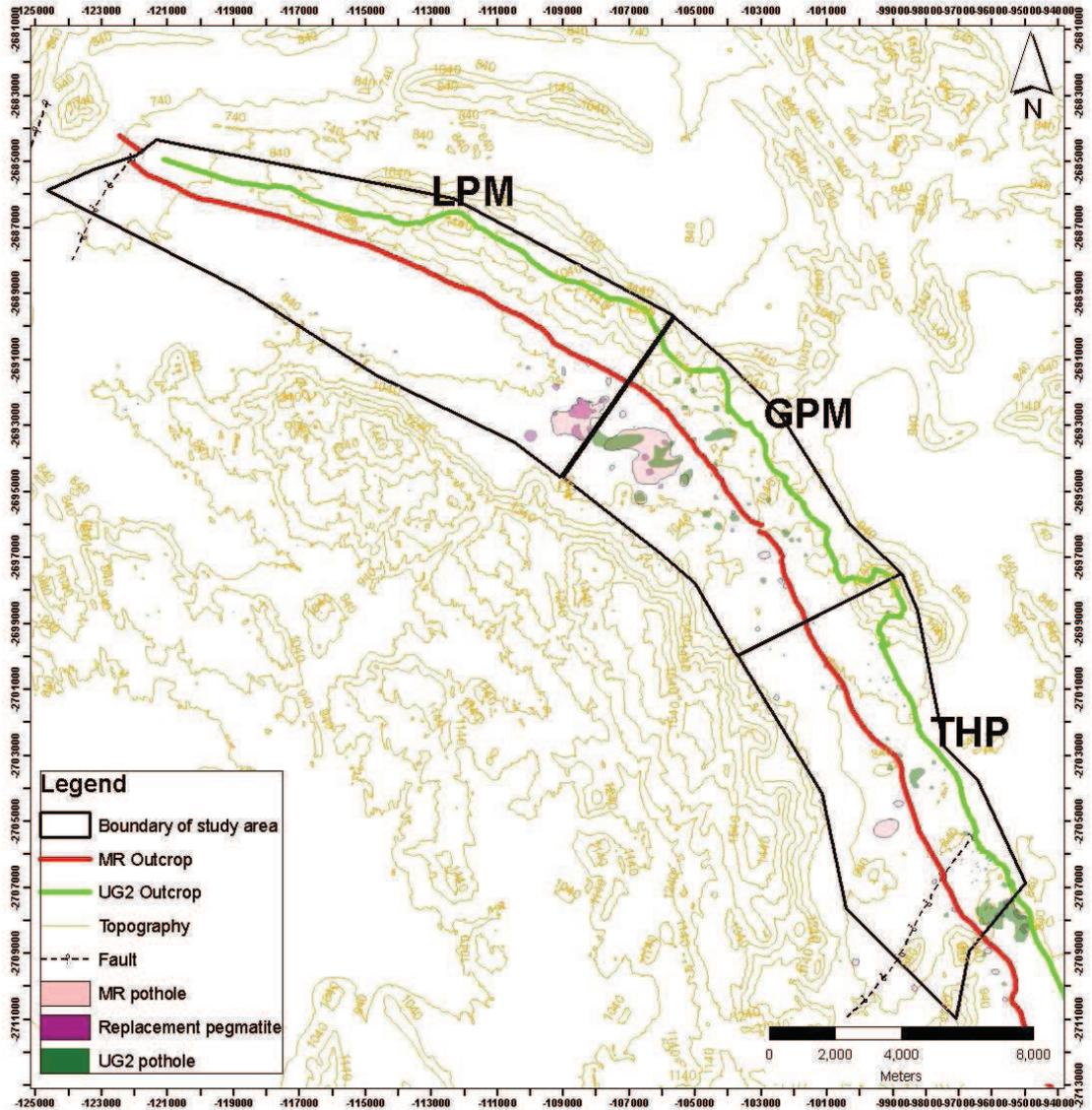
Figure 14. Distribution of potholes and replacement pegmatites across the study area.

Replacement pegmatites are often found spatially associated with potholes (figure 14). They are however formed much later than the potholes. They are the result of upward and lateral fluid driven late hydromagmatic post cumulus events like infiltration metasomatic replacement that may occur along old defluidisation channels, crystal pile weaknesses and newly evolving structural discontinuities (Brown, 2004b, 2005a, 2005b; Brown and Lee, 1987).

5. PART ONE: COMPARISON OF THE HYDROSTATIC AND GAS PYCNOMETER METHODS

5.1. PART ONE: RESEARCH METHODOLOGY

Over a period of three years the density of all exploration core samples were first measured on site using a hydrostatic method and then sent to a laboratory in Johannesburg where the density was determined from the milled core using a gas pycnometer. The first part of the study will compare these results.

5.1.1. Water hydrostatic method

The measurements were conducted at the North Eastern limb projects exploration coreyard, known as Driekop. It is situated near to where the boreholes were drilled, approximately 30 km North of Burgersfort, South Africa.

A Snowrex Clover NHV – 3 scale was used for the site measurements (figure 15). It is an electronic digital scale with a capacity of 3 kg and readability of 0.1 g intervals. Results of the hydrostatic method conducted at the exploration offices based near Burgersfort will be referred to as "Driekop".
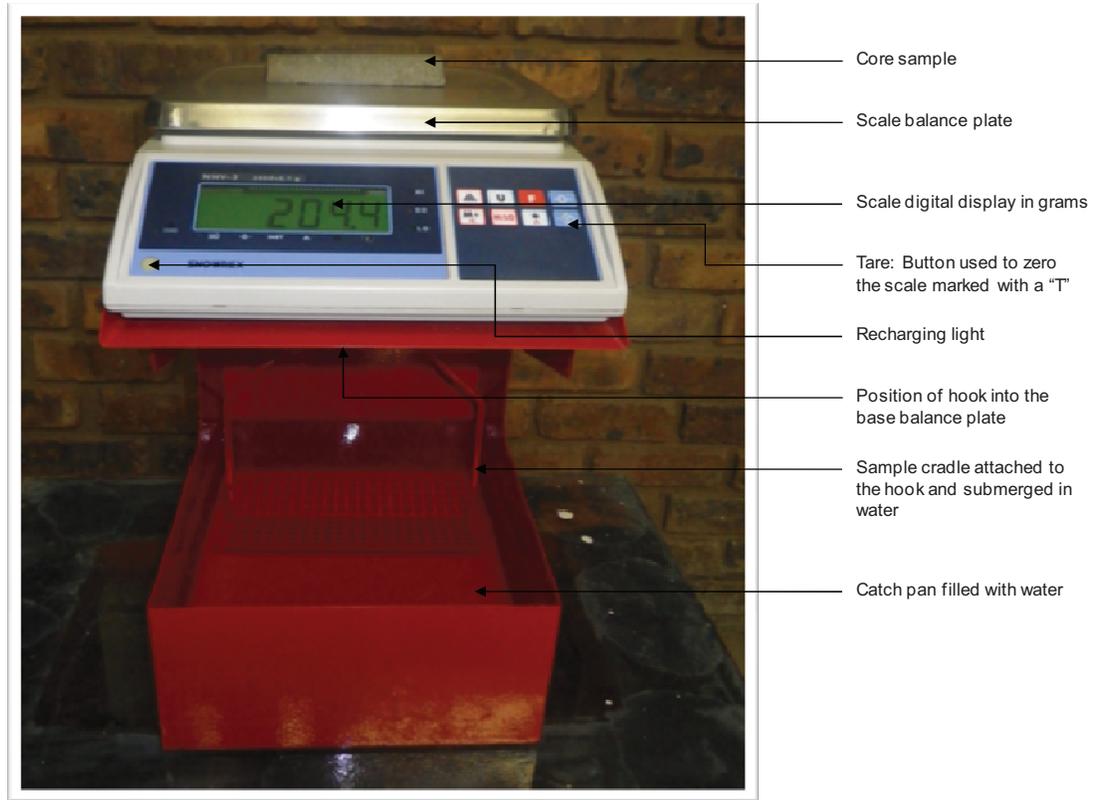
Figure 15. Snowrex Clover NHV – 3 Scale.

The measurements were not conducted in a laboratory environment; however care was taken to ensure that procedure was consistent and conducted in a controlled manner, devoid of any external influences. The guidelines from the Snowrex operation manual were strictly followed to ensure that the scale was set up properly and correctly calibrated (Snowrex precision instruments, 2008).

The full standard measurement procedure that was followed is included in Appendix A.

In order to determine the density of the sample, it must be weighed in air and then in water, as described in Chapter 2.2. By using equation 3 in Chapter 2.2, the density is then easily calculated. These results were tabulated in an Excel spreadsheet.

5.1.2. Gas pycnometer

These measurements were taken at a laboratory based in Johannesburg. They were conducted on milled or powdered core samples using a Grabner Minidens air gas pycnometer (figure 3). For reference purposes, these measurements will be referred to as "Grabner Milled" in the results section.

An annotated cross-section of the Grabner Minidens is given in figure 16. The Minidens has a mass measurement range up to 35 g. It is capable of measuring densities in the range of 0.500 to 8.000 g/cm^3 with an accuracy of approximately 0.003 g/cm^3. The principle of how a gas pycnometer calculates the volume of a sample is explained in Chapter 2.5.

1 ... Balance
2 ... Sample chamber
3 ... Sample cup
4 ... Balance body
5 ... Upper lid of measuring chamber
6 ... Precision piston drive
7 ... Pressure transducer
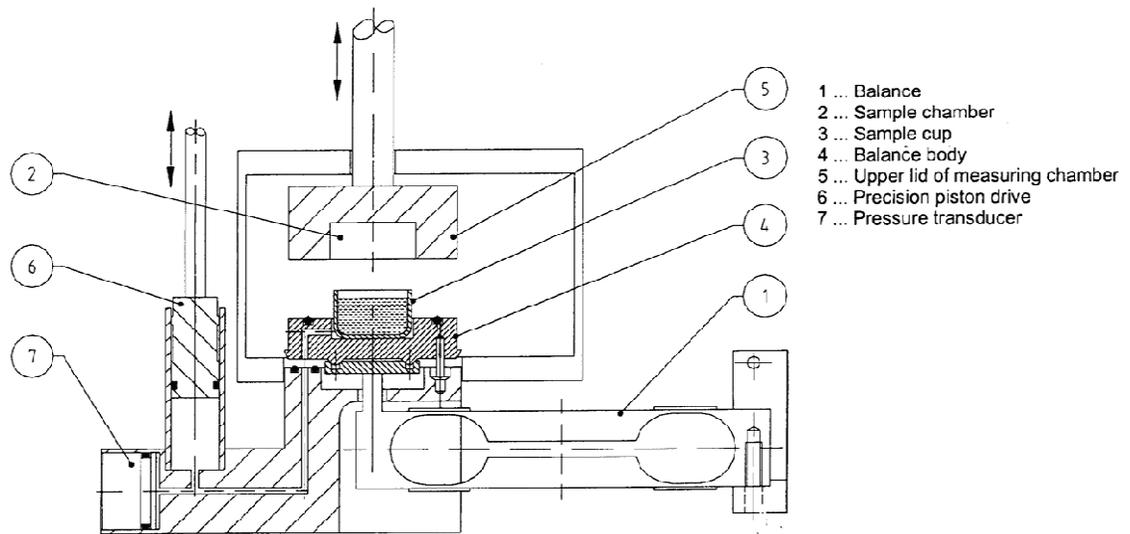
Figure 16. Cross-section of the Grabner Minidens air pycnometer (Grabner, 2008).

The samples are first milled to a particle size of approximately 40 μm. About 4 cm^3 of the milled sample is used for the density measurement. After filling the small aluminium sample cup with the milled sample, the cup is placed on to the balance top plate inside the tester, the lid is closed and the measurement is started. From here the process is fully automated. The mass of the sample is determined with the built in analytical balance. Volume is calculated as follows: Air pressure inside the measuring chamber is increased or decreased with the precision piston drive for approximately 20 kPa and then decreased or increased again until the original

barometric pressure is reached. From the expansion and compression curve the volume of the sample is determined. The measurement procedure is repeated twice and the results compared. If the two values correlate the average is taken. A third value is determined if the two values do not correlate. An error message will be displayed if they still do not correlate. The temperature of the laboratory in which the Grabner Minidens is operated is regulated to 21 ℃. The density of a sample can be automatically corrected to a preset temperature using the measured temperature and the programmed expansion coefficient (Grabner, 2008).

For quality control purposes, two materials of known density, crushed quartz and an aluminium block, were measured at the beginning and end of each batch of samples, usually every forty to fifty samples. Ten percent of the samples were sent to another laboratory for comparison, and another ten percent of the milled samples were split and measured again as duplicates. The ten percent check was also conducted using a gas pycnometer. The average percentage difference in 2008 was found to be less than one percent (Van Der Neut, 2008).

5.1.3. Comparison of results

18,430 samples were available for the comparison. Each sample was measured using the two methods described in section 2.2 and 2.5, namely Driekop for the hydrostatic method on solid core and Grabner Milled for the gas pycnometer method on milled/powdered core.

The boreholes were drilled over three exploration projects on the North Eastern limb, namely Lebowa (LPM), Gapasha (GPM) and Twickenham (THP). In order to check for variation of results between the three projects, the results were split into the three projects, referred to as LPM, GPM and THP in the results section. Figure 17 shows the distribution of boreholes over the three projects. A total of 285 boreholes were used, 121 for LPM, 66 for GPM, and 98 for THP. The total does not include deflections.
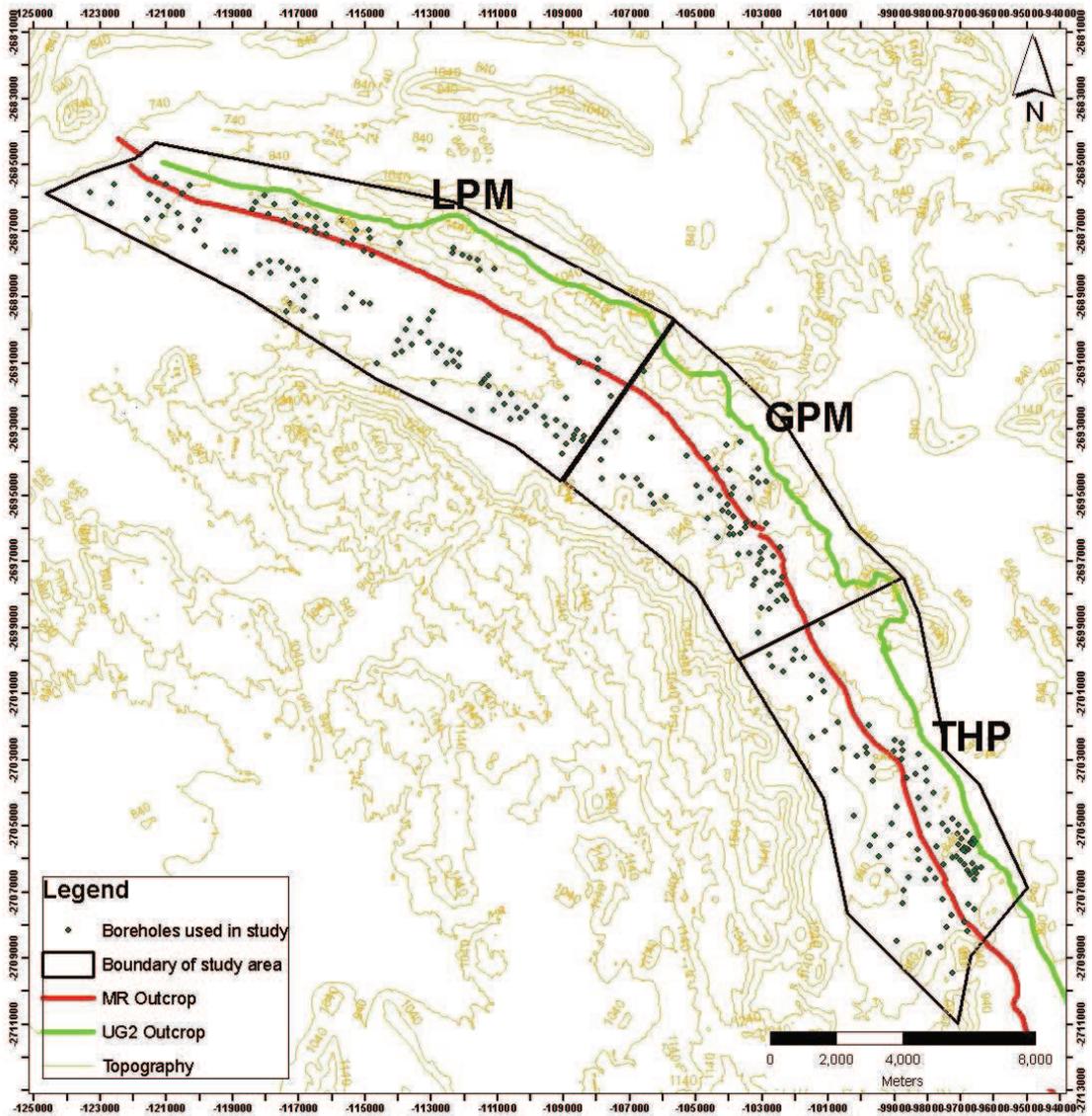
Figure 17. Distribution of boreholes across the three projects on the North Eastern limb of the Bushveld Complex, LPM, GPM and THP.

The average relative difference (AVRD) between the two results for each sample was calculated. The formula for the AVRD between two samples is given in equation eight below.

Result 1 (Grabner Milled)	Result 2 (Driekop)
X	Y

$$AVRD = ((X - Y)/((X + Y)/2)) * 100 \qquad (8)$$

The AVRD is written as a percentage. An AVRD of zero will indicate the densities of the two methods are equal. A positive value indicates the Grabner Milled density is higher, whereas a negative value indicates the Driekop density is higher. The descriptive statistics of the Grabner Milled and Driekop datasets, together their AVRD results were then calculated. Samples with an AVRD that was greater than or less than three standard deviations away from the mean AVRD for all the samples were considered outliers and removed from the database. In total 328 samples (1.8 %) were removed. The total number of samples for each project, together with the number of outliers and number of samples available for the comparison from each project are given in table 2.

Table 2. Breakdown of the number of samples from each project.

Project	Original dataset (no. samples)	Outliers (no. samples)	Dataset available for comparison (no. samples)
LPM	8,924	148	8,776
GPM	3,626	74	3,552
THP	5,880	106	5,774
Total	18,430	328	18,102

The descriptive statistics of the original dataset; the outlier parameters; the list of outliers removed; the list of the data without outliers used in the comparison; and the descriptive statistics of data without outliers used in the comparison, for each project are tabulated in Appendix B. Tables B1 to B7 for LPM; tables B8 to B14 for GPM; and tables B15 to B21 for THP.

For the descriptive statistics of the original dataset refer to tables B1 (LPM), B8 (GPM); and B15 (THP). For the outlier parameters refer to tables B2 (LPM), B9 (GPM); and B16 (THP). For the list of outliers removed refer to tables B3 (LPM), B10 (GPM); and B17 (THP). For the list of the data without outliers used in the comparison refer to tables B4 (LPM), B11 (GPM); and B18 (THP). For descriptive statistics of the data without outliers used in the comparison refer to tables B5 (LPM), B12 (GPM); and B19 (THP).

A scatter graph of the original data showing the outliers was produced for each project.

The samples were then split into the stratigraphic units that make up the Merensky and Upper Group 2 chromitite sampling cut: Merensky hangingwall (MRHW); Merensky reef (MR); Merensky footwall (MRFW) and Upper Group 2 chromitite hangingwall (UG2HW); Upper Group 2 chromitite layer (UG2) and Upper Group 2 chromitite footwall (UG2FW). Figure 9 shows the localized stratigraphy and the rocks that comprise the MR and UG2 reefs.

The density results of the Grabner Milled and Driekop methods for each stratigraphic unit were displayed as histograms in order to show the distribution of results for each method and how they compare. The AVRD of each sample were also displayed as frequency histograms within their respective stratigraphic units, showing the percentage difference between the Grabner Milled and Driekop results. The data used in the percentage difference frequency histograms is tabulated in Appendix B. Tables B6 (MR) and B7 (UG2) for LPM; tables B13 (MR) and B14 (UG2) for GPM; and tables B20 (MR) and B21 (UG2) for THP.

5.1.4. Quality control

When sampling the diamond drill core, the core is split into two halves. One half of the sample was retained at the exploration site; the other half was sent to the laboratory for analysis. 811 of these sampled halves that remained on site were randomly selected and measured again using the hydrostatic method described in Chapter 2.2, referred to as "Driekop Check" in the results. These results were compared to the original Driekop and Grabner Milled results. Certified weights (50 g; 100 g; 500 g; and 1000 g) were used at the beginning of each sample batch to be measured to ensure that the scale was correctly calibrated.

The average relative difference (AVRD) between the results for each sample was calculated.

The descriptive statistics of the three datasets and the AVRD of each were then calculated. Samples with an AVRD that was greater than or less than three standard deviations away from the mean AVRD of each dataset were considered outliers and removed from the database. In total 27 samples (3.4 %) were removed.

The descriptive statistics of the original dataset (table B22); the outlier parameters (table B23); the list of outliers removed (table B24); the list of the data without outliers used in the comparison (table B25); and the descriptive statistics of data without outliers used in the comparison (table B26) are tabulated in Appendix B.

Scatter graphs comparing the results of each dataset were produced. The AVRD between each sample was displayed as frequency histograms. The data used in the percentage difference frequency histograms is tabulated in Appendix B, table B27.

5.2. PART ONE: RESULTS

5.2.1. Comparison of the hydrostatic and gas pycnometer methods

The scatter plots for the three projects (LPM, GPM and THP) are displayed in figures 18, 19, and 20 respectively. The Grabner Milled results are shown on the y axis and the Driekop results on the x axis for each sample. The sample points in blue indicate the points used in the comparison, while the outliers are highlighted in pink. These outliers fall more than three standard deviations above or below the mean AVRD for the dataset.

The red diagonal line in each graph indicates the one-to-one line. Sample points plotting along this line have equal values for the Grabner Milled and Driekop methods. Points plotting above the red line will have higher Grabner Milled values and lower Driekop values. On the other hand, points plotting below the red line will have higher Driekop values and lower Grabner Milled values.
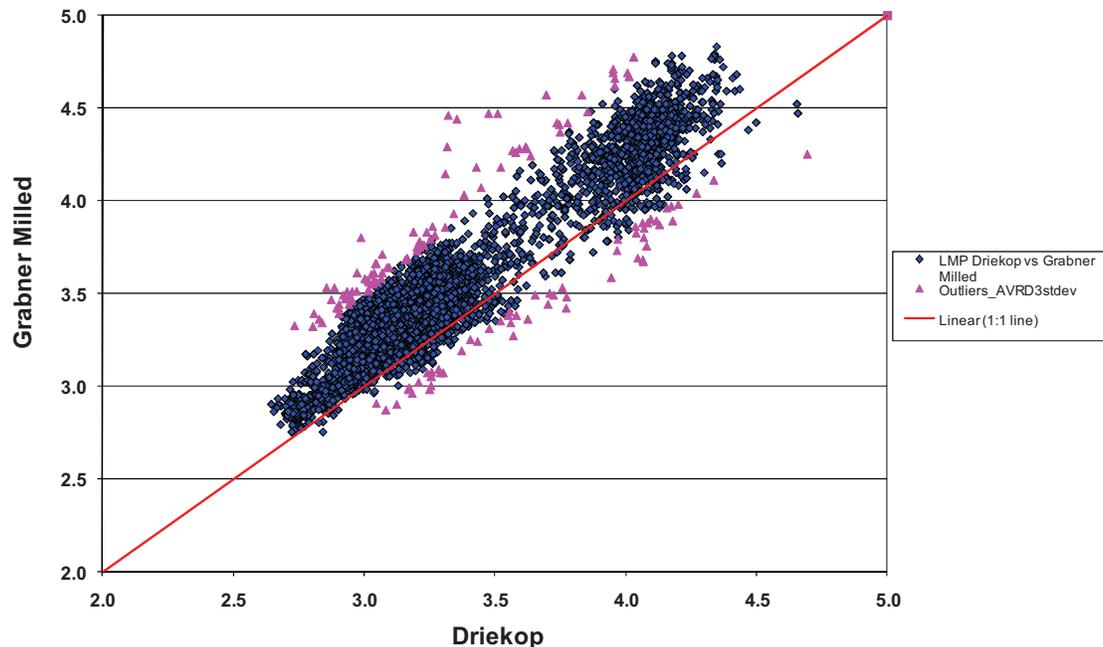
Figure 18. LPM project scatter plot of the Grabner Milled values over the Driekop values.

> **Notes** The mean AVRD indicates that the Grabner Milled results are 5.28 % higher than the Driekop results.
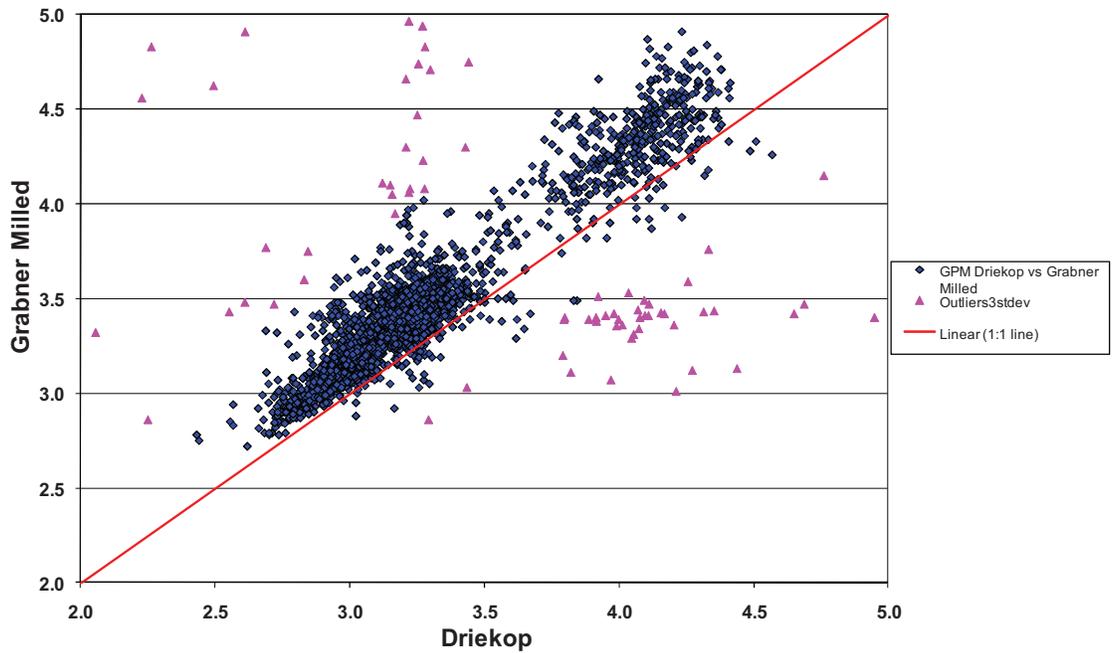
Figure 19. GPM project scatter plot of the Grabner Milled values over the Driekop values.

Notes The mean AVRD indicates that the Grabner Milled results are 5.55 % higher than the Driekop results.
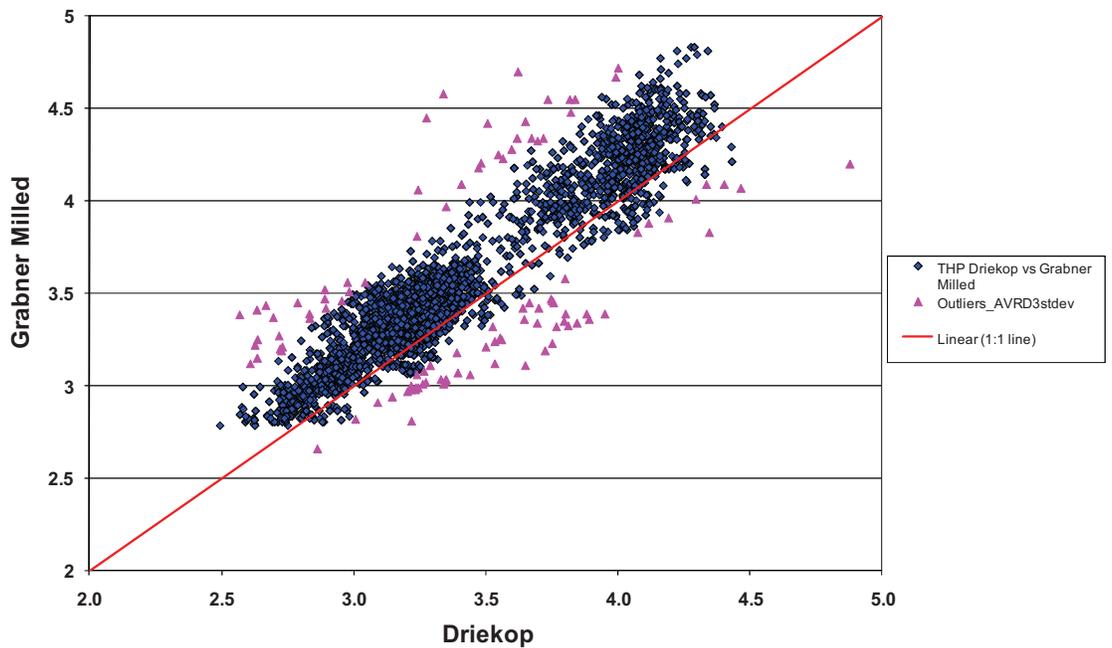
Figure 20. THP project scatter plot of the Grabner Milled values over the Driekop values.

Notes The mean AVRD indicates that the Grabner Milled results are 4.92 % higher than the Driekop results.

For all three projects, the majority of the sample points plot above the red line, indicating that the Grabner Milled values are higher than the Driekop values. It is also evident that the outliers for the GPM project have a much wider spread in comparison to the LPM and THP projects. The spread of outliers may be attributed to mixed or mislabelled samples or errors in recording the results. The remaining halves of all the samples are available at the exploration core yard. In order to check the outlier values, the remaining sample halves would have to be re-measured. However, the percentage of outliers in comparison to the size of the entire dataset for each project is relatively small, only 1.8 % (table 2). This is not envisaged to have any effect on the integrity of the data.

The descriptive statistics for the three projects with outliers removed are tabulated in Appendix B (table B5 for LPM; table B12 for GPM; and table B19 for THP). The mean AVRD for the LPM, GPM and THP project is 5.28 %, 5.55 %, and 4.92 % respectively, a positive AVRD indicating that on average the Grabner Milled results are higher. The wide range of densities is attributed to the variations in the lithologies that make up the MR and UG2 sampling cut (figure 9). The scatter plots in all three projects show two distinct populations that are the result of these variations in rock composition, as shown in figure 21, for LPM below.
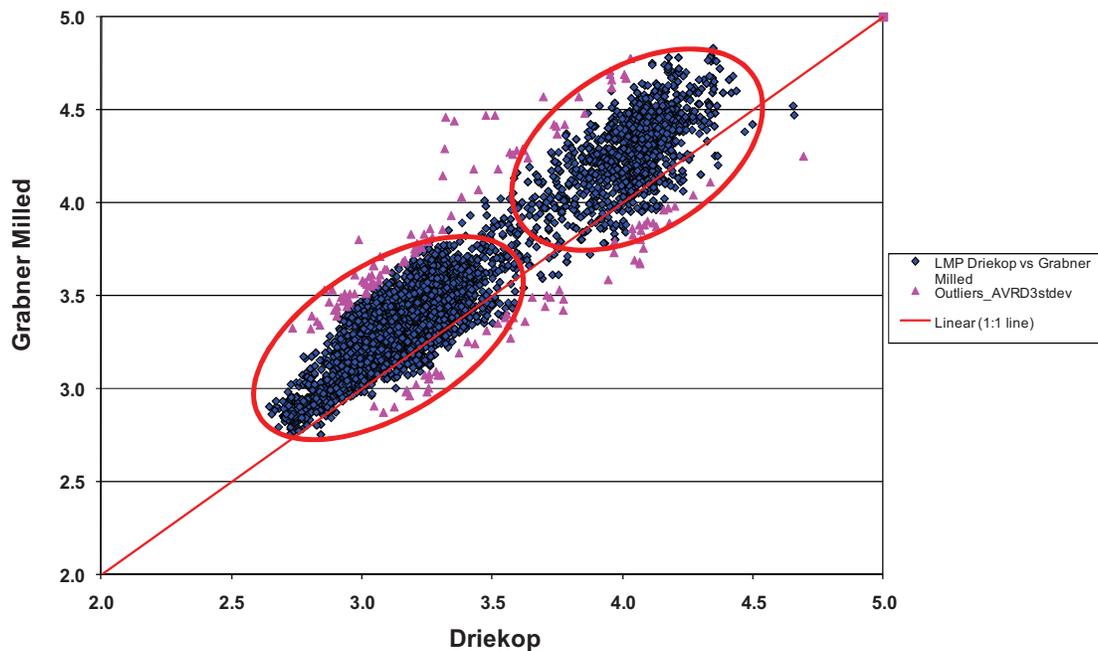
Figure 21. LPM project scatter plot of the Grabner Milled values over the Driekop values.

Notes The scatter plot shows two distinct populations, indicated by the red circles.

Histograms of the density values and summary statistics that make up the MR sampling cut for each project are given in figures 22, 23 and 24. There are three graphs in each figure, comprising of the hangingwall, reef and footwall. In the graphs the pink line represents the Driekop data and the blue line the Grabner Milled data. The density with the highest frequency is shown in each graph for both sets of data. The summary statistics table shows the mean density for the Grabner Milled and Driekop methods; the AVRD between the two methods; the standard deviation; range; and the number of samples for each stratigraphic unit.

MR Hangingwall at LPM
(Density histogram; labels: 3.3g/cc, 37.03%; 3.4g/cc, 28.67%; 3.1g/cc, 20.70%; 3.2g/cc, 21.28%; 3.2g/cc, 16.81%; 3.3g/cc, 15.16%)

MR Reef at LPM
(Density histogram; labels: 3.3g/cc, 64.90%; 3.5g/cc, 34.94%; Legend: Grabner milled, Driekop)

MR Footwall at LPM
(Density histogram; labels: 3.3g/cc, 35.23%; 3.4g/cc, 29.85%)
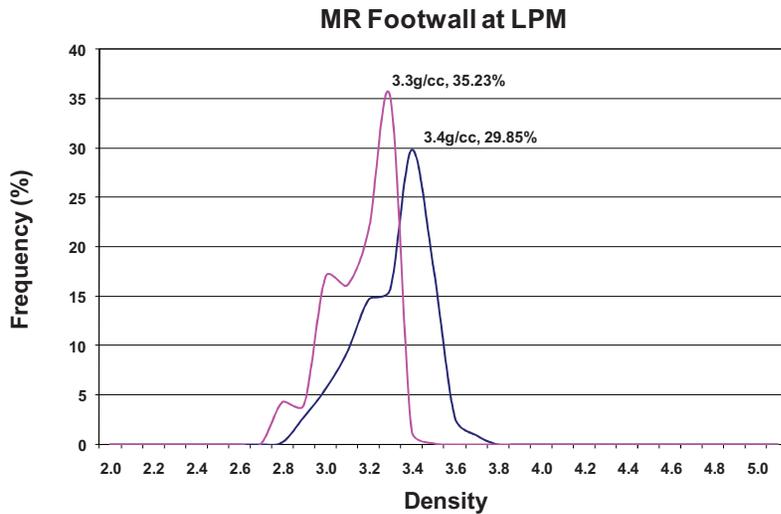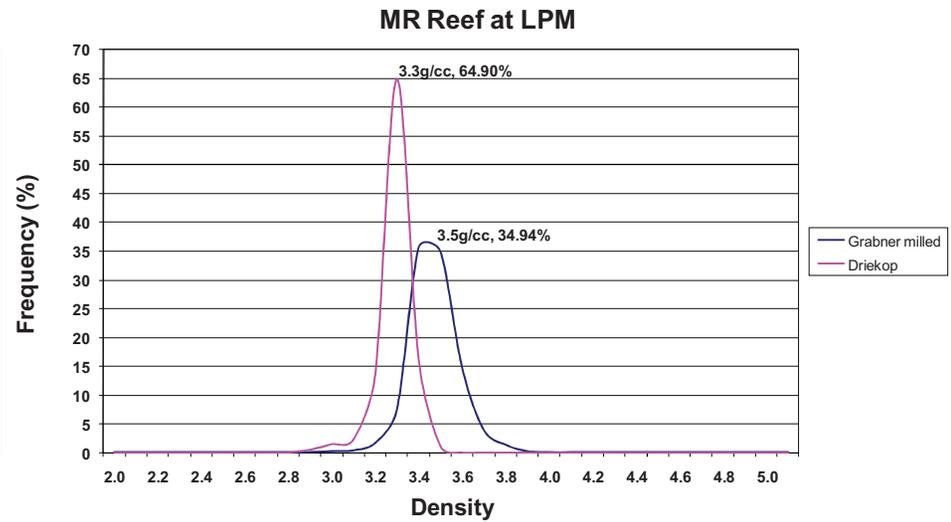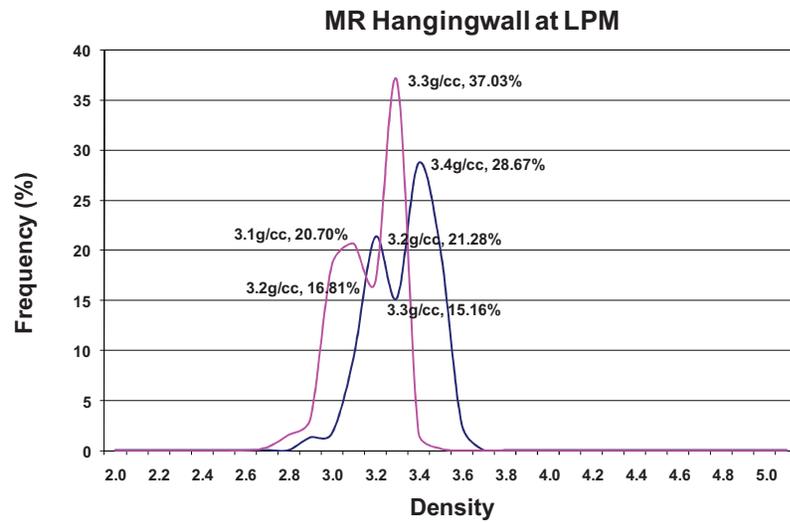
	Grabner Milled MRHW	Driekop MRHW	AVRD MRHW
Mean	3.28	3.12	5.18
Standard Deviation	0.15	0.13	2.39
Minimum	2.83	2.67	-3.38
Maximum	3.60	3.49	14.78
Count	1029	1029	1029
	Grabner Milled MR	Driekop MR	AVRD MR
Mean	3.42	3.24	5.44
Standard Deviation	0.11	0.08	2.85
Minimum	3.00	2.81	-4.45
Maximum	3.85	3.46	15.03
Count	624	624	624
	Grabner Milled MRFW	Driekop MRFW	AVRD MRFW
Mean	3.27	3.11	5.16
Standard Deviation	0.17	0.14	2.71
Minimum	2.75	2.68	-4.23
Maximum	3.66	3.48	14.92
Count	2248	2248	2248

Figure 22. LPM project – MR sampling cut density histograms and summary statistics.

Note: The Driekop histograms are in pink and the Grabner Milled histograms are in blue.

Figure 23. GPM project – MR sampling cut density histograms and summary statistics.

Note: The Driekop histograms are in pink and the Grabner Milled histograms are in blue.

MR Hangingwall at THP

MR Reef at THP

MR Footwall at THP
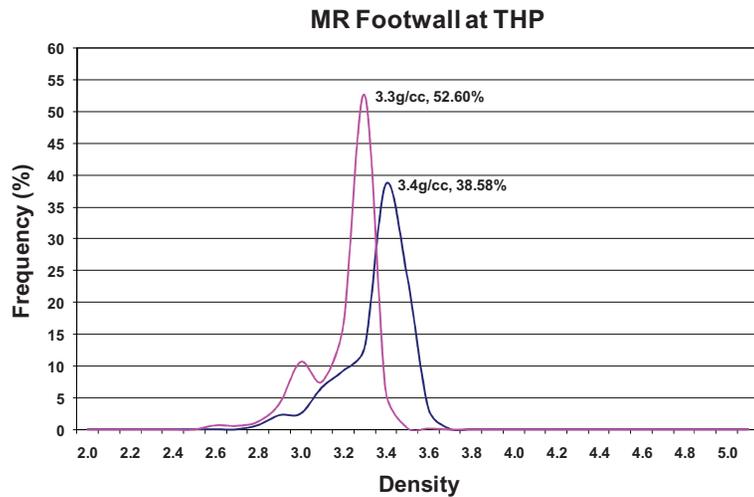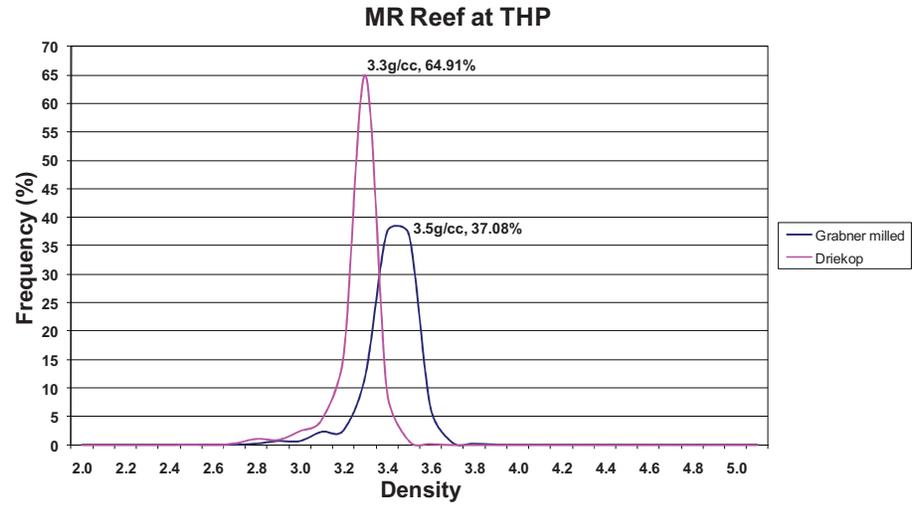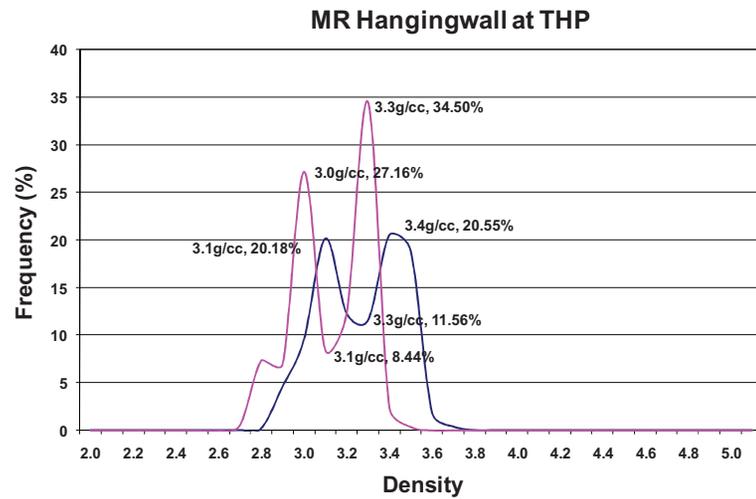
	Grabner Milled MRHW	Driekop MRHW	AVRD MRHW
Mean	3.22	3.07	4.65
Standard Deviation	0.19	0.17	2.47
Minimum	2.80	2.63	-4.92
Maximum	3.63	3.43	13.59
Count	545	545	545
	Grabner Milled MR	Driekop MR	AVRD MR
Mean	3.38	3.22	4.87
Standard Deviation	0.11	0.10	2.68
Minimum	2.78	2.49	-4.76
Maximum	3.73	3.53	14.72
Count	1103	1103	1103
	Grabner Milled MRFW	Driekop MRFW	AVRD MRFW
Mean	3.31	3.16	4.67
Standard Deviation	0.15	0.14	2.69
Minimum	2.78	2.57	-4.79
Maximum	3.64	3.51	15.32
Count	1213	1213	1213

Figure 24. THP project – MR sampling cut density histograms and summary statistics.

Note: The Driekop histograms are in pink and the Grabner Milled histograms are in blue.

The histogram profile of the Grabner Milled and Driekop values are similar, but the Grabner Milled values show higher densities (figures 22, 23 and 24). The density with the highest frequency for both methods is shown adjacent to the corresponding peak in the histograms. Both methods show similar peak profiles, but the Grabner Milled values peak at a higher density.

Generally, the MR sampling cut histograms look comparable between the stratigraphic units (figures 22, 23 and 24). All the MR histograms look similar. The MRHW histograms show a distinct double peak. The double peak is also present in the GPM MRFW. The LPM and THP MRFW display a much weaker, less pronounced double peak. The two peaks found in these histograms indicate two distinct variations in rock composition. The lower peak may be indicative of non mineralized pyroxenite, and the upper peak mineralized pyroxenite. For each project, this higher peak looks very similar to the MR histogram.

For each project, the mean density and mean AVRD for each stratigraphic unit is shown in the statistics tables in figures 22, 23 and 24. If one looks at each project and compares the mean densities for each stratigraphic unit, it is apparent that there is only a small difference or range in density between the respective stratigraphic units for each project. The THP project shows a consistently lower mean AVRD for each stratigraphic unit in comparison to the LPM and GPM projects. Between the three projects the mean density and mean AVRD range for each stratigraphic unit is:

- MRHW: Grabner Milled = 3.22 to 3.28 g/cc; Driekop = 3.07 to 3.12 g/cc; AVRD 4.65 to 5.23 % higher Grabner Milled results.

- MR: Grabner Milled = 3.38 to 3.43 g/cc; Driekop = 3.22 to 3.24 g/cc; AVRD 4.87 to 5.54 % higher Grabner Milled results.

- MRFW: Grabner Milled = 3.26 to 3.31 g/cc; Driekop = 3.10 to 3.16 g/cc; AVRD 4.67 to 5.16 % higher Grabner Milled results.

The histograms of the density values and summary statistics that make up the UG2 sampling cut for each project are given in figures 25, 26 and 27 below.

UG2 Hangingwall at LPM — 3.3g/cc, 69.96%; 3.5g/cc, 54.18%

UG2 Reef at LPM — 4.1g/cc, 25.45%; 4.5g/cc, 15.74% (Grabner milled, Driekop)

UG2 Footwall at LPM — 3.3g/cc, 52.06%; 3.4g/cc, 35.52%

	Grabner Milled UG2HW	Driekop UG2HW	UG2HW AVRD
Mean	3.42	3.25	5.09
Standard Deviation	0.11	0.09	2.49
Minimum	2.75	2.71	-4.08
Maximum	4.55	4.26	14.67
Count	932	932	932
	Grabner Milled UG2	Driekop UG2	UG2 AVRD
Mean	4.19	3.95	5.70
Standard Deviation	0.31	0.28	3.73
Minimum	2.85	2.74	-4.41
Maximum	4.83	4.66	15.03
Count	1277	1277	1277
	Grabner Milled UG2FW	Driekop UG2FW	UG2FW AVRD
Mean	3.40	3.22	5.24
Standard Deviation	0.15	0.12	2.76
Minimum	2.75	2.65	-4.43
Maximum	4.35	4.13	14.99
Count	2666	2666	2666

Figure 25. LPM project – UG2 sampling cut density histograms and summary statistics.

Note: The Driekop histograms are in pink and the Grabner Milled histograms are in blue.

UG2 Hangingwall at GPM

3.3g/cc, 49.83%
3.5g/cc, 45.30%

UG2 Reef at GPM

4.2g/cc, 18.05%
4.5g/cc, 15.91%

— Grabner milled
— Driekop

UG2 Footwall at GPM

3.3g/cc, 41.03%
3.4g/cc, 29.815%
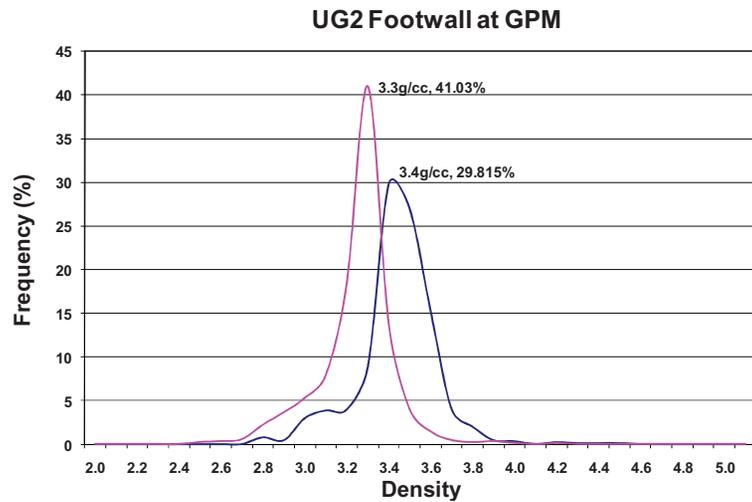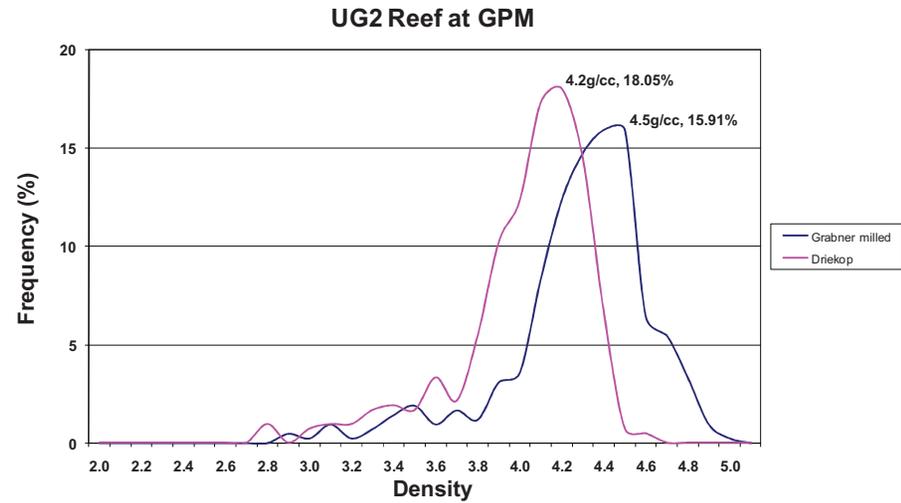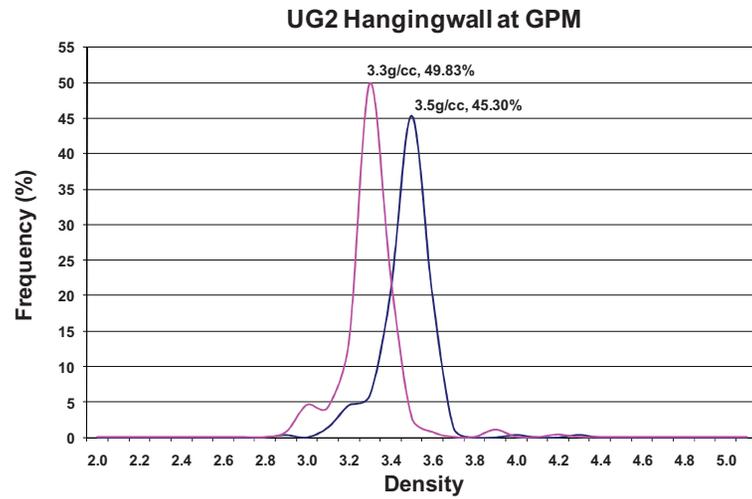
	Grabner Milled UG2HW	Driekop UG2HW	AVRD UG2HW
Mean	3.43	3.25	5.16
Standard Deviation	0.13	0.13	3.23
Minimum	2.87	2.80	-9.67
Maximum	4.23	4.13	14.98
Count	287	287	287
	Grabner Milled UG2	Driekop UG2	AVRD UG2
Mean	4.23	3.97	6.30
Standard Deviation	0.35	0.32	4.16
Minimum	2.84	2.73	-7.44
Maximum	4.91	4.57	17.89
Count	421	421	421
	Grabner Milled UG2FW	Driekop UG2FW	AVRD UG2FW
Mean	3.39	3.20	5.94
Standard Deviation	0.19	0.17	3.21
Minimum	2.72	2.43	-8.82
Maximum	4.48	4.12	21.33
Count	909	909	909

Figure 26. GPM project – UG2 sampling cut density histograms and summary statistics,

Note: The Driekop histograms are in pink and the Grabner Milled histograms are in blue.

UG2 Hangingwall at THP

UG2 Reef at THP

UG2 Footwall at THP
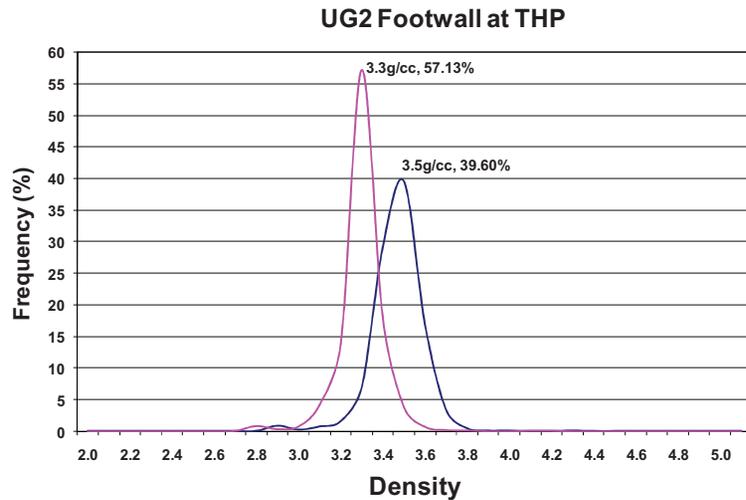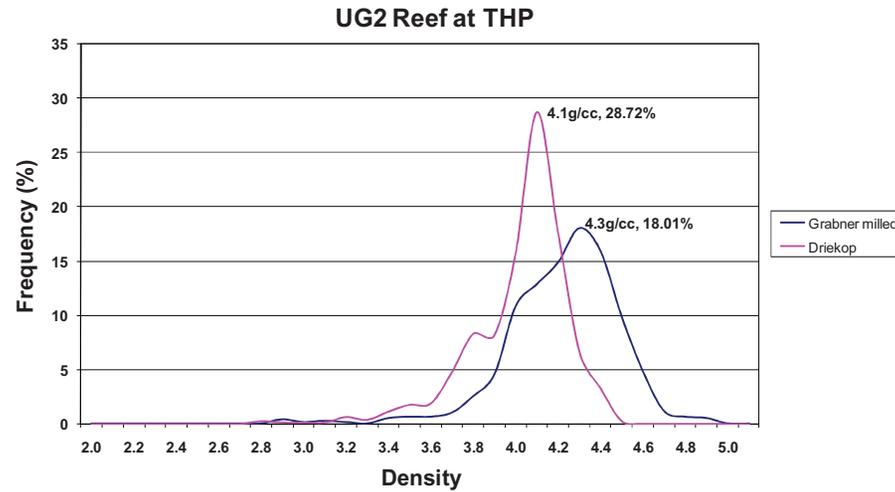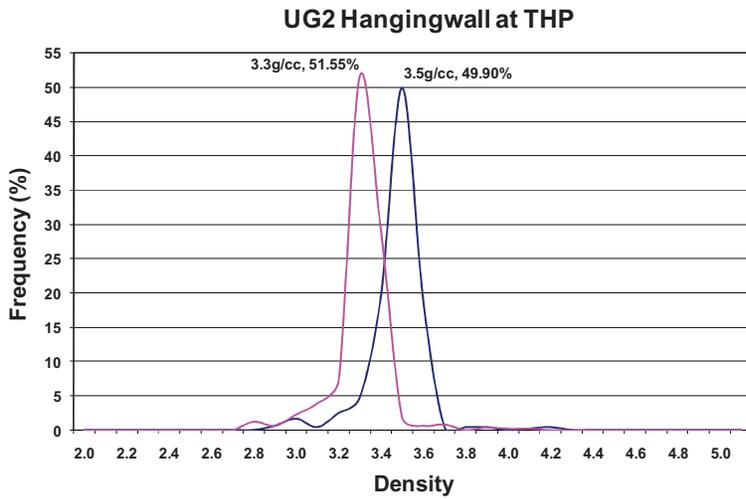
	Grabner Milled UG2HW	Driekop UG2HW	AVRD UG2HW
Mean	3.43	3.26	4.99
Standard Deviation	0.13	0.13	2.95
Minimum	2.82	2.74	-5.47
Maximum	4.20	4.09	15.26
Count	485	485	485
	Grabner Milled UG2	Driekop UG2	AVRD UG2
Mean	4.18	3.97	5.05
Standard Deviation	0.26	0.23	4.11
Minimum	2.82	2.71	-5.50
Maximum	4.83	4.43	15.09
Count	794	794	794
	Grabner Milled UG2FW	Driekop UG2FW	AVRD UG2FW
Mean	3.42	3.25	5.22
Standard Deviation	0.12	0.11	2.69
Minimum	2.82	2.64	-5.22
Maximum	4.21	4.13	15.01
Count	1409	1409	1409

Figure 27. THP project – UG2 sampling cut density histograms and summary statistics.

Note: The Driekop histograms are in pink and the Grabner Milled histograms are in blue.

The UG2 sampling cuts show the same trends as found for the MR. The density histograms for each method show similar profiles, but the Grabner Milled density values are higher. The Grabner Milled data peaks at a higher density than the Driekop data (figures 26, 27 and 28).

The UG2HW and UG2FW histograms for all the projects look comparable. Despite the UG2HW being made up of a medium grained plagioclase pyroxenite and the UG2FW of a pegmatoidal plagioclase pyroxenite they show similar densities. The UG2HW and UG2FW have tight histograms indicating a narrow range above and below the density with the highest frequency (figures 26, 27 and 28).

In comparison the UG2 histograms show a much wider distribution with much broader histograms. The UG2 may often be locally bifurcated with anorthosite or pyroxenite waste bands in between the chromitite, evident from the low minimum density range value. For the LPM and THP projects, the UG2 Grabner Milled histograms have a broader peak in comparison to the UG2 Driekop histograms which are narrower. For the GPM project the UG2 Grabner Milled and Driekop histograms show similar shaped profiles (figures 26, 27 and 28).

Between the three projects the mean density and mean AVRD range for each stratigraphic unit is:

- UG2HW: Grabner Milled = 3.42 to 3.43 g/cc; Driekop = 3.25 to 3.26 g/cc; AVRD 4.99 to 5.16 % higher Grabner Milled results.

- UG2: Grabner Milled = 4.18 to 4.23 g/cc; Driekop = 3.95 to 3.97 g/cc; AVRD 5.05 to 6.30 % higher Grabner Milled results.

- UG2FW: Grabner Milled = 3.39 to 3.42 g/cc; Driekop = 3.20 to 3.25 g/cc; AVRD 5.22 to 5.94 % higher Grabner Milled results.

There is only a small mean density difference between the respective stratigraphic units for each project. The three projects show some variation in the AVRD for each stratigraphic unit. The LPM and GPM projects show a higher mean AVRD for the UG2 (statistics table in figures 25 and 26). The GPM also shows a higher mean AVRD for the UG2FW.

The AVRD histograms of the MR sampling cuts for each project are given in figures 28, 29, and 30 below. The MR histogram is in red, MRHW in pink and MRFW

in blue. Adjacent to each high peak is the density and frequency at that point. The values are coloured according to the histogram the values represent.
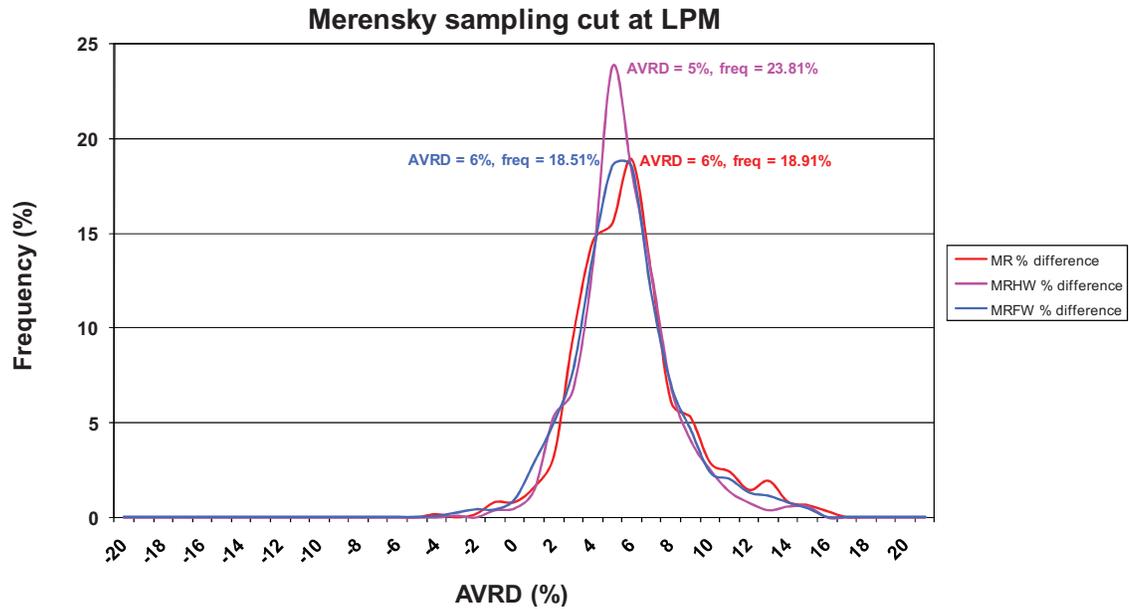
Figure 28. LPM project – MR sampling cut AVRD histograms.

    Notes MRHW histogram is in pink; MR histogram is in red and MRFW histogram is in blue.
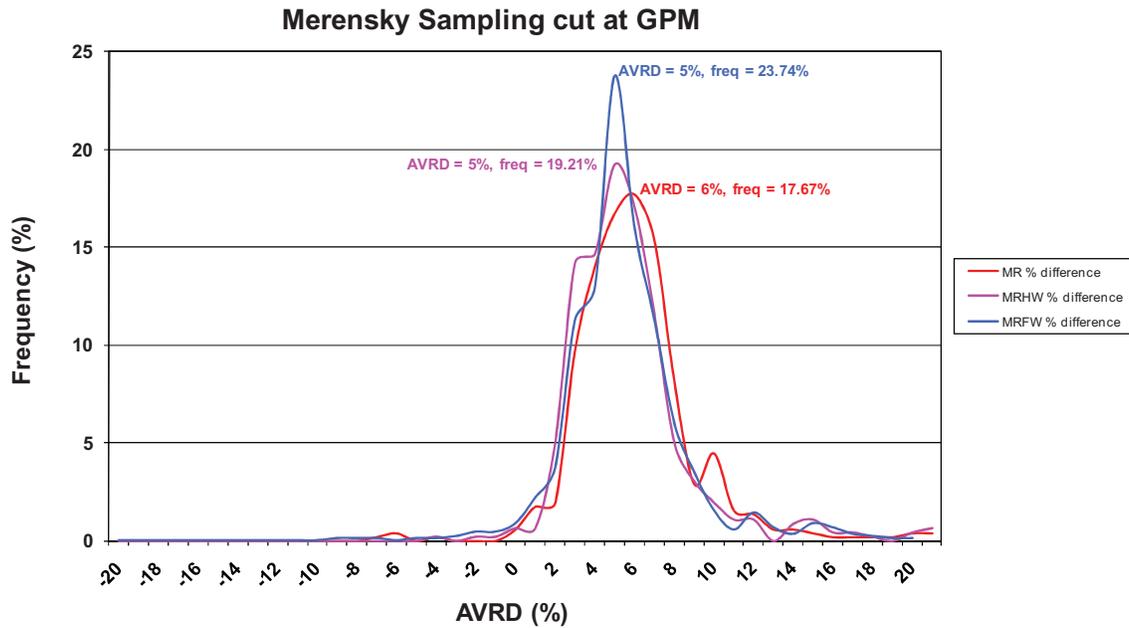
Figure 29. GPM project – MR sampling cut AVRD histograms.

    Notes MRHW histogram is in pink; MR histogram is in red and MRFW histogram is in blue.

Merensky sampling cut at THP
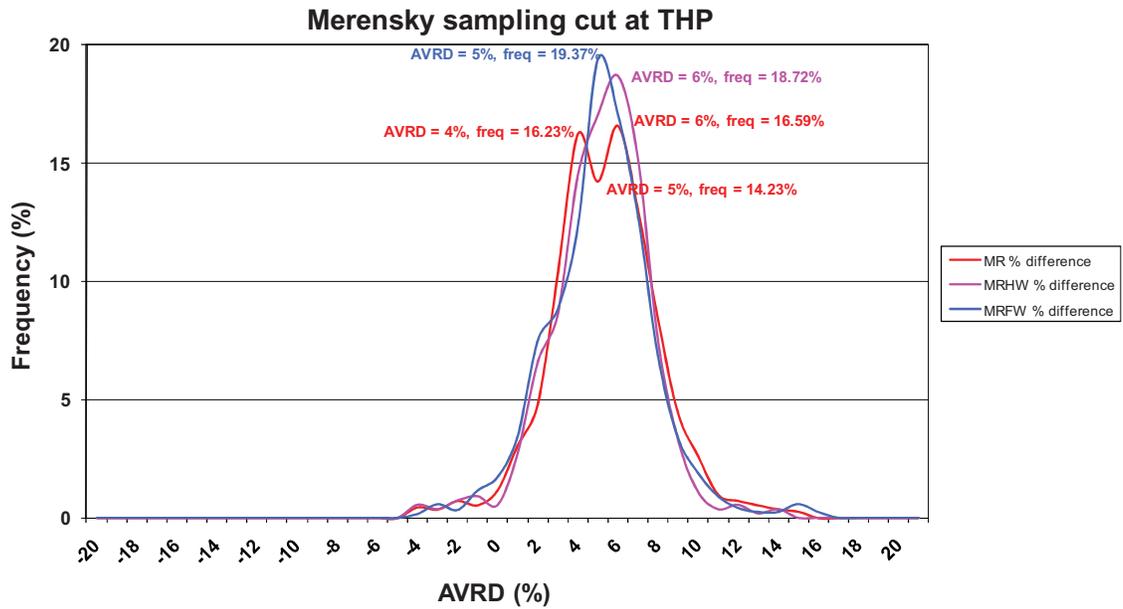
Figure 30. THP project – MR sampling cut AVRD histograms.

> **Notes** MRHW histogram is in pink; MR histogram is in red and MRFW histogram is in blue.

The MR AVRD histograms also clearly show that Grabner Milled density values are consistently higher. The majority of the samples have a positive AVRD of between 4 to 6 %. There is some variation in the AVRD out of this range, however the frequency associated with these points is very low (<5 %). The profiles of the hangingwall, reef and footwall AVRD histograms for each project look similar.

The AVRD histograms of the UG2 sampling cuts for each project are given in figures 31, 32, and 33 below. The UG2 histogram is in red, UG2HW in pink and UG2FW in blue.
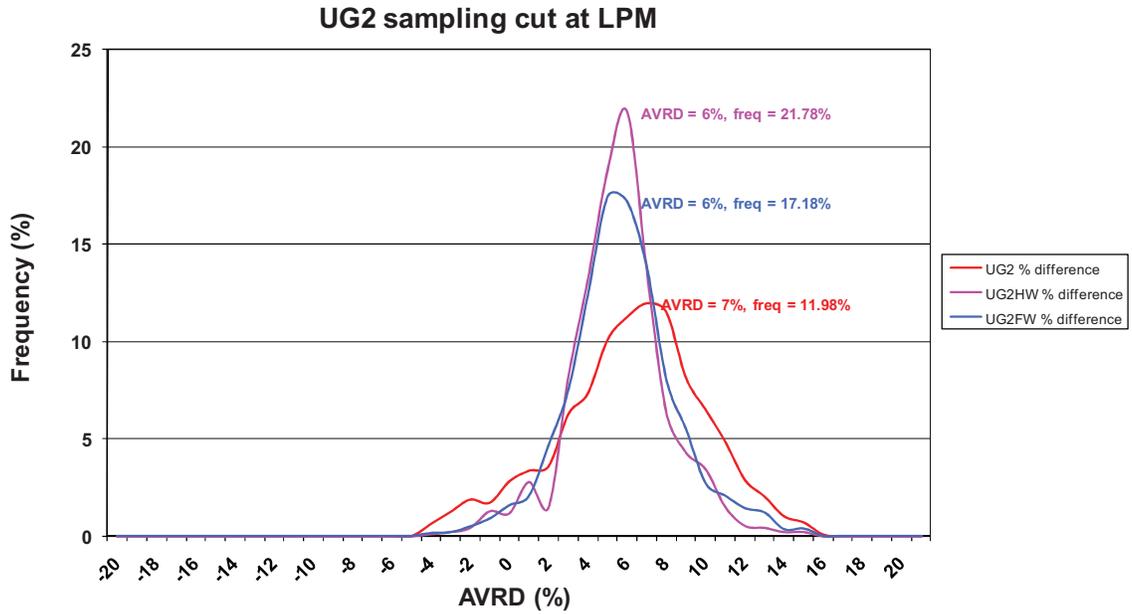
Figure 31. LPM project – UG2 sampling cut AVRD histograms.

> **Note:** UG2HW histogram is in pink; UG2 histogram is in red and UG2FW histogram is in blue.
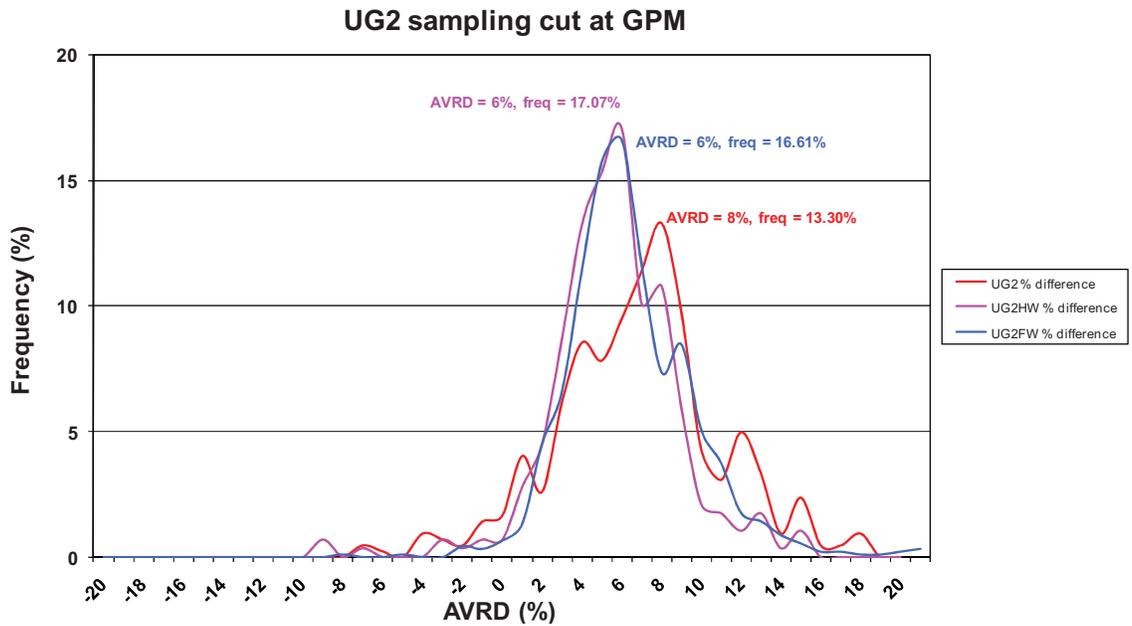
Figure 32. GPM project – UG2 sampling cut AVRD histograms.

> **Note:** UG2HW histogram is in pink; UG2 histogram is in red and UG2FW histogram is in blue.
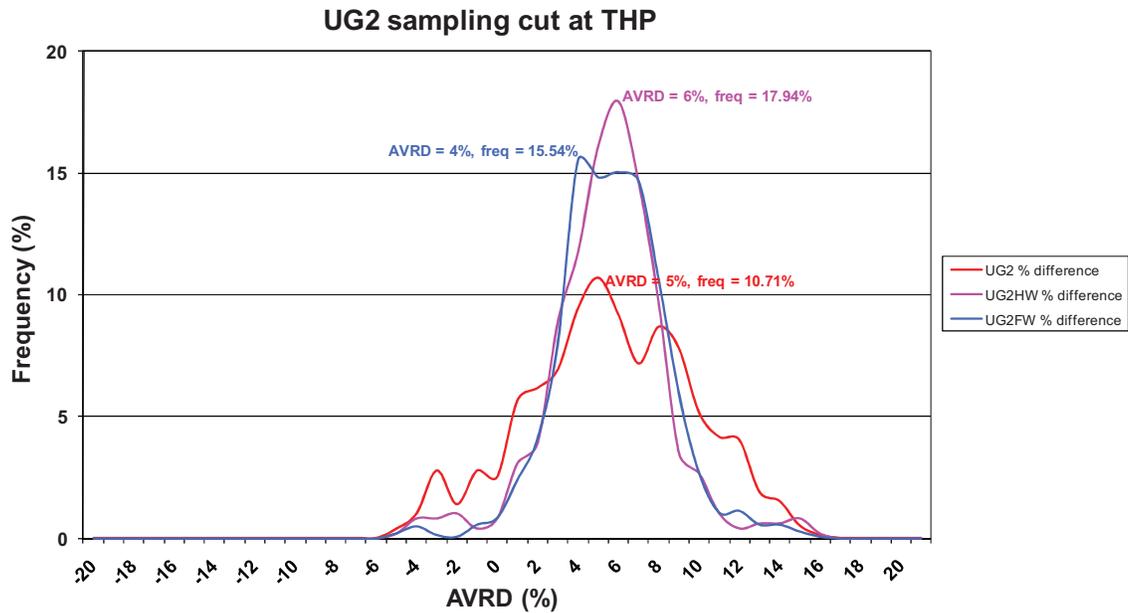
Figure 33. THP project – UG2 sampling cut AVRD histograms.

> **Note:** UG2HW histogram is in pink; UG2 histogram is in red and UG2FW histogram is in blue.

The UG2 AVRD sampling cut histograms also shows that the Grabner Milled values are higher, with the highest frequency of samples having an AVRD of between 4 to 8 %.

In general the UG2HW and UG2FW profiles for the three projects look similar. The GPM UG2HW and UG2FW do also show another peak at about eight percent. The THP UGFW has a flatter peak, with similar frequencies of about 15 %, between AVRDs of 4 to 8 %.

All three UG2 AVRD histograms have a broad distribution. The LPM UG2 AVRD histogram is smooth and normal; whereas the GPM and THP UG2 AVRD histograms show much more variation.

5.2.2. Quality control

The Driekop check samples that were re-measured were found to have densities very close to the Driekop original values.

Scatter plots of the Driekop original values over the Driekop check values, the Grabner Milled values over the Driekop check values, and the Grabner Milled values over Driekop original values are given in figures 34, 35 and 36 below.

In each scatter plot there is a red and black diagonal line. The black line represents the one-to-one linear trend line. Data points falling along this line have exactly the same value for two results being plotted and compared. The red line represents the linear trend line of the dataset.
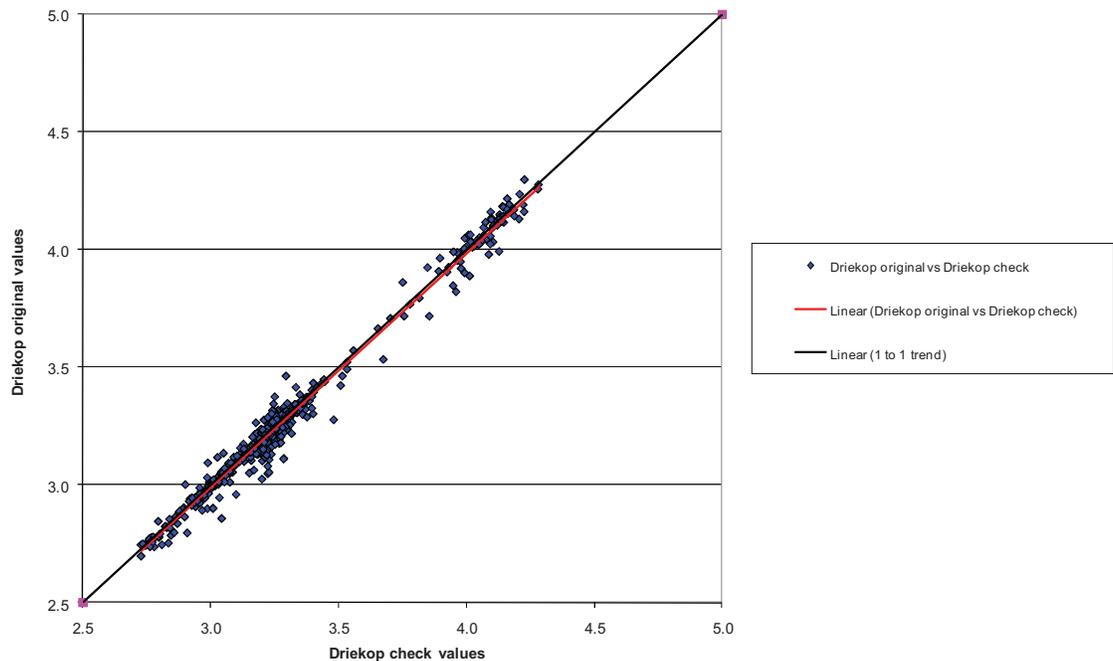
Figure 34. Scatter plot of the Driekop original values over the Driekop check values.

> **Notes** The mean AVRD indicates that the Driekop check values are 0.33 % higher than the Driekop original values.

The Driekop original values plot very closely to the Driekop check values (figure 34). The red dataset trend line sits on top of the black one-to-one trend line. This indicates a strong correlation between the original values and the Driekop check values. The mean AVRD is only 0.33 % (figure 34).
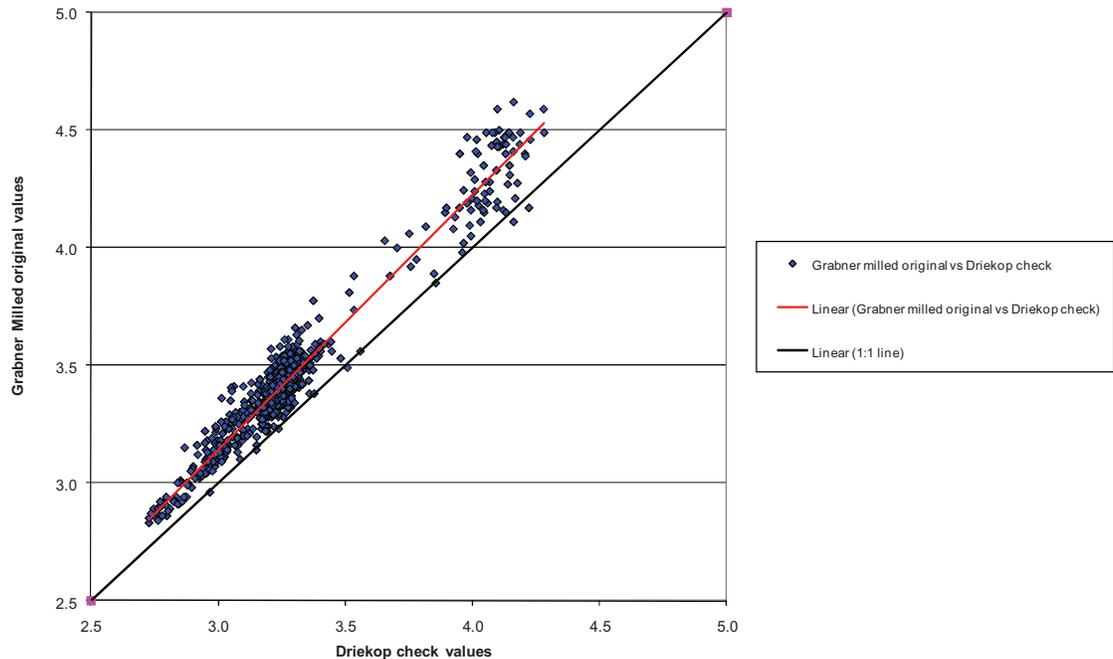
Figure 35. Scatter plot of the Grabner Milled original values over the Driekop check values.

> **Notes** The mean AVRD indicates that the Grabner Milled original values are 4.85 % higher than the Driekop check values.

The scatter plot of the Grabner Milled original values over the Driekop check values shows that the Grabner Milled values are generally higher (figure 35). The majority of the data points are above the black one-to-one trend line. This is further emphasized by the dataset red trend line, which sits approximately parallel to, but well above, the one-to-one trend line. The mean AVRD is 4.85 %, indicating that the Grabner Milled original values are higher (figure 35).
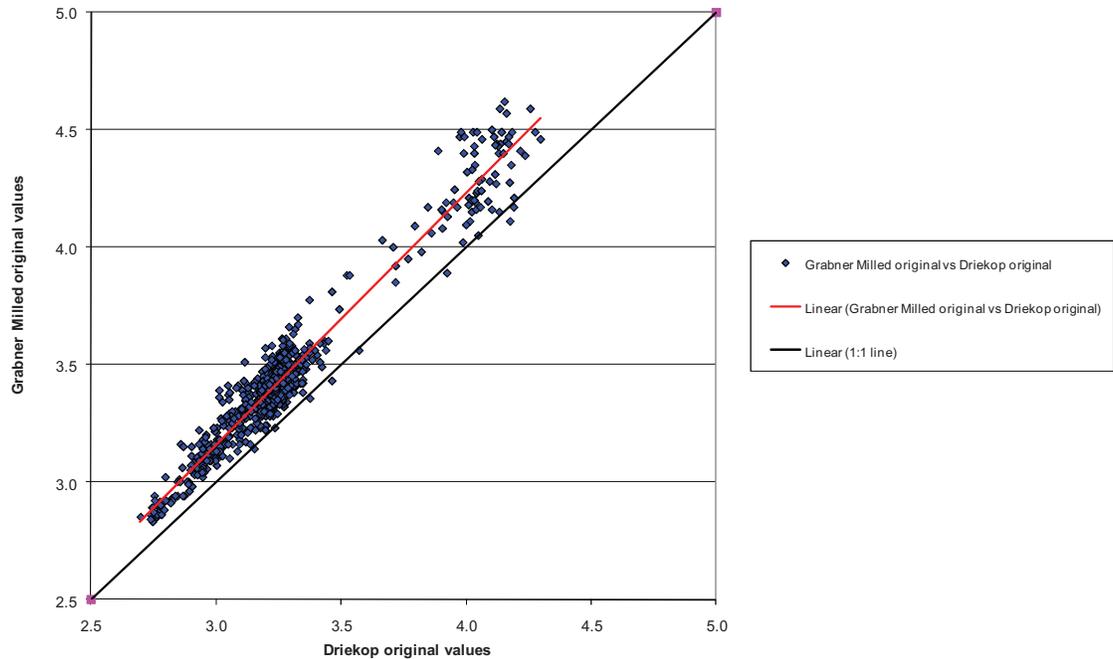
Figure 36. Scatter plot of the Grabner Milled original values over the Driekop original values.

> **Notes** The mean AVRD indicates that the Grabner Milled original values are 5.18 % higher than the Driekop original values.

The scatter plot of the Grabner Milled original values over the Driekop original values (figure 36) show similar results to the scatter plot of the Grabner Milled original values over the Driekop check values (figure 35).

The majority of the data points lie above the one-to-one trend line, as does the linear dataset trend line. The mean AVRD is 5.18%, indicating that the Grabner Milled values are higher. This mean AVRD is marginally higher than the mean AVRD of the Grabner Milled original values over the Driekop check values.

The AVRD between samples of the three datasets are shown in the frequency histogram below (figure 37). The AVRD between the Driekop check values and the Driekop original values are shown in dark blue; the AVRD between the Grabner Milled values and Driekop check values are shown in pink; and the AVRD between the Grabner Milled values and the Driekop original values are shown in light blue.
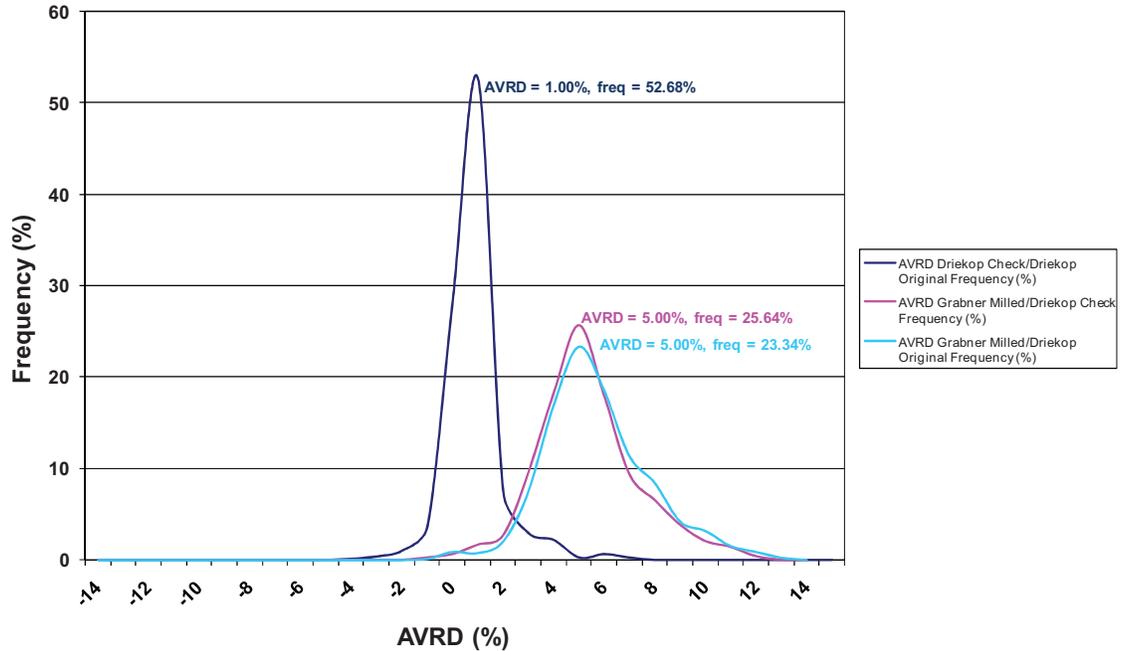
Figure 37. Quality control AVRD histograms.

> **Notes:** The AVRD histogram between the Driekop check values and the Driekop original values is in dark blue; the AVRD between the Grabner Milled values and Driekop check values is in pink; and the AVRD between the Grabner Milled values and the Driekop original values is in light blue.

The AVRD frequency histogram in figure 37 shows that there is a strong correlation between the Driekop original values and the Driekop check values. Approximately 53 % of the data has an AVRD of 1 %, with about 28 % showing an AVRD of zero.

Both the Driekop original and Driekop check values show a similar relationship to the Grabner Milled results (figure 37). Both AVRD histograms show a peak AVRD of 5 % at the highest frequency, indicating that the Grabner Milled results are generally higher than the Driekop original values and the Driekop check values.

5.3. PART ONE: DISCUSSION

5.3.1. Comparison of the hydrostatic and gas pycnometer methods

The results of part one showed that the Grabner Milled density method produces a higher average density than the Driekop method.

The scatter plot of the two methods, for all three projects (figures 18 − 20), clearly showed that per sample, the Grabner Milled value is generally higher than the Driekop value. Outliers in the scatter plots were easily identified, highlighting the need for repeating sample measurements for quality control.

The density distribution histograms of the various stratigraphic units for all three projects also showed that the Grabner Milled method produces higher density results (figures 22 − 27). Both methods produced similar, relatively normal shaped histograms for each stratigraphic unit; however the main difference was that the Grabner Milled method produced a higher range of densities and a higher peak density value.

The mean density of both methods and the AVRD between them for each project is summarized in table 3 below.

Table 3. The mean density and AVRD of the Grabner Milled and Driekop methods for each stratigraphic unit.

Stratigraphic unit	LPM			GPM			THP		
	Grabner Milled (g/cc)	Driekop (g/cc)	AVRD (%)	Grabner Milled (g/cc)	Driekop (g/cc)	AVRD (%)	Grabner Milled (g/cc)	Driekop (g/cc)	AVRD (%)
MRHW	3.28	3.12	5.18	3.25	3.08	5.23	3.22	3.07	4.65
MR	3.42	3.24	5.44	3.43	3.24	5.54	3.38	3.22	4.87
MRFW	3.27	3.11	5.16	3.26	3.10	5.04	3.31	3.16	4.67
UG2HW	3.42	3.25	5.09	3.43	3.25	5.16	3.43	3.26	4.99
UG2	4.19	3.95	5.70	4.23	3.97	6.30	4.18	3.97	5.05
UG2FW	3.40	3.22	5.24	3.39	3.20	5.94	3.42	3.25	5.22

The peaks in the density distribution histograms correspond to the major rock type being measured. The MR is a mineralized medium crystalline plagioclase pyroxenite and therefore has a higher mean density than the MRHW and MRFW, which are a medium crystalline plagioclase pyroxenite and a pegmatoidal plagioclase pyroxenite, respectively. Mineralization does however sometimes extend into the immediate hangingwall and footwall of the MR. Evidence for this is supported by the double peak found in the MRHW and MRFW histograms. There is a lower peak which may correspond to un-mineralized pyroxenite and a higher peak that may correspond to mineralized pyroxenite. The lower peak is not as pronounced in the LPM and THP MRFW.

As expected, the UG2 chromitite layer shows a much higher mean density than the UG2HW and UG2FW, which are also made up of a medium crystalline plagioclase pyroxenite and a pegmatoidal plagioclase pyroxenite, respectively. The UG2HW and UG2FW have higher mean densities than the MRHW and MRFW even though they have similar rock types. With the UG2, the PGE mineralization is almost exclusively contained within the UG2 chromitite layer. No PGE mineralization extends into the immediate hangingwall of the UG2. Mineralization may extend into the immediate footwall of the UG2 at lower PGE grades, where it is associated with chromitite blebs, disseminations, and laterally discontinuous thin chromitite layers. Thin chromitite layers are also found in the UG2HW pyroxenite. The chromitite in the UG2HW and UG2FW may attribute to the higher mean densities in the UG2HW and UG2FW, as compared to the MRHW and MRFW.

The mean density of each corresponding stratigraphic unit does vary slightly between the three projects (table 3). This variation or range was apparent in both methods (table 4).

Table 4. The mean density range of the Grabner Milled and Driekop methods for each stratigraphic unit.

Stratigraphic unit	Range Grabner Milled (g/cc)	Range Driekop (g/cc)
MRHW	0.06	0.05
MR	0.05	0.02
MRFW	0.05	0.06
UG2HW	0.01	0.01
UG2	0.05	0.02
UG2FW	0.03	0.05

The range in the MRHW, MRFW, and UG2HW does correlate well between the two methods (table 4). The Driekop method shows a slightly narrower range for the MR and UG2. The Grabner Method has a lower average MR density for the THP project in comparison to the LPM and GPM projects which obtained similar mean densities. For the UG2, the Grabner Milled method obtained a higher mean density for the GPM project compared to the other two projects which obtained similar mean densities. The Grabner Milled method showed less variation for the UG2FW. The Driekop method showed a higher mean UG2FW density for the THP project in comparison to the other two projects which showed similar mean densities.

The slight variation between the corresponding stratigraphic units may be due to subtle differences in rock composition and structure. To truly see if the variation corresponds with any geological features or zones, hangingwall, reef and footwall density composites will have to be made for each borehole and projected onto the geological map.

The mean AVRD between the two methods for each corresponding stratigraphic unit also shows slight differences between the three projects (table 3). The difference may be attributed to slight variations in the structure of the rocks between the three projects.

The mean AVRD for each stratigraphic unit, in all three projects, shows that the Grabner Milled method produces a consistently higher density than the Driekop method (table 3). The rocks that make up the MR and UG2, including their hangingwall and footwall rocks are made up of closely interlocking minerals typical of

cumulates. There are generally no visible pores on the core samples. It is unlikely that any water would have penetrated into the core sample during the immersion step in the Driekop method, unless the sample was highly altered or fractured. Therefore, pores (open and closed) within the core sample are included in the volume calculation. The comminution of the core sample, in the Grabner method, into a fine milled powder breaks up the rock and minerals within it. This comminution step is the initial step in the metallurgical process conducted at the laboratory to determine grade of the sample. The sample is now made up of a collection of very fine particles. All previously existing pores and mineral relationships within the rock are broken down and eliminated. In the Grabner Milled method, a very small quantity of this powder or pulp is placed into the sample cup and measured. The powder is allowed to settle naturally within the sample cup. There may be minute inter-particle pores within the powder, but considering the particle size, this will have little influence on the volume calculation.

The Driekop method measures a density that is close to or equal to the bulk or envelope density of the solid core sample inclusive of open and closed pores. The Grabner method measures a density close to or equal to the skeletal or true density of the powdered sample excluding all pore spaces. One may argue that through the comminution process, variables such as pores, structure, mineral assemblage and mineral relationships that make up the composition of the sample are changed, and therefore the density measured is not representative of the rock in its natural state.

The AVRD histograms for the MR sampling cuts all show similar, relatively normal histogram profiles for all three projects (figures 28 – 30). The projects show a peak AVRD for each stratigraphic unit that ranges between 4 to 6 % (figures 28 – 30). The similarities of each histogram may be attributed to similarities in rock composition between the MRHW, MR and MRFW, the main constituent of which is plagioclase pyroxenite.

The AVRD histograms of the UG2HW and UG2FW (figures 31 – 33) are similar to those of the MR sampling cut. This may be because the main constituent of the UG2HW and UG2FW is also plagioclase pyroxenite. The projects show a peak AVRD for UG2HW and UG2FW of between 4 to 6 % (figures 31 – 33). The UG2 AVRD histograms have a much broader distribution and show more variation then those of the other stratigraphic units (figures 31 – 33). The AVRD variation observed

in the UG2 chromitite layer may indicate variations in pore volume within the assemblage of chromite cumulate grains that make up the main constituent of the UG2. The peak AVRD range for the UG2 is higher than the other stratigraphic units, between 5 to 8 % (figures 31 – 33).

5.3.2. Quality control

The quality control checks on the remaining halved cores, confirmed that the results comparing the Grabner Milled method and the Driekop method were repeatable. The Driekop original values corresponded very well with the Driekop check values (mean AVRD = 0.33 %), despite slight variations in composition, which is expected between the two halved core samples (figure 34). The mean AVRD between the Grabner Milled and Driekop original results were slightly higher than the mean AVRD between the Grabner Milled and Driekop check results, 5.18 %, and 4.85 %, respectively (figure 35 and 36). The AVRD histogram of the Driekop original and Driekop check values show a peak AVRD at only 1 % (figure 37). Both the Grabner Milled/Driekop check and Grabner Milled/Driekop original AVRD histograms have peak AVRDs at 5 %, and their histogram profiles are almost identical (figure 37).

The fact that the Driekop measurements were repeatable is very important for this fairly robust method of determining density. With the correct setup, the use of calibration weights, which ensures the scale is measuring correctly, and the use of standard reference material, which ensures accuracy and precision of the density results obtained over time, this method is a good means of density determination. The Grabner Milled method uses a modern gas pycnometer that has a high degree of accuracy and precision. Being conducted in a laboratory environment, the Grabner Milled method has much more control over external variables such as temperature. The Driekop method is conducted at a field exploration camp, where a control over external variables such as temperature is more limited.

6. PART TWO: DENSITY EXPERIMENT - HOW LOCALITY, SAMPLE PREPARATION AND METHOD USED, INFLUENCES THE DENSITY RESULT OBTAINED.

6.1. PART TWO: RESEARCH METHODOLOGY

The second part of the study was set up to compare the density results obtained when measuring the same sample as a solid, using the hydrostatic immersion and gas pycnometer methods, and as a milled powder, using a gas pycnometer.

A total of 82 randomly selected core samples were used for the experiment. Each sample was first measured as a solid and then as a milled powder. The hydrostatic method and gas pycnometer method described in Part one (Chapter 5.1.1 and 5.1.2) was used for this experiment. The experiment was set up to see how locality, sample preparation and method influences the density result obtained.

Each sample was first cut to fit the sample cup of the Grabner Minidens.

The density of each solid sample was then firstly determined using the hydrostatic method and then the Grabner Minidens air gas pycnometer.

The hydrostatic method was conducted at Driekop, 30 km North of Burgersfort, referred to as "Driekop" in the results section. The same hydrostatic method was then conducted on the samples at the laboratory based in Germiston, Johannesburg, referred to as "Lab water solid" in the results section. This was to test whether external factors such as temperature and altitude have any influence on the results.

The gas pycnometer method was only conducted at the laboratory. The samples were first measured as a solid, referred to as "Grabner Solid" in the results section. The samples were then milled to 40 µm and re-measured in the Grabner Minidens, referred to as "Grabner Milled" in the results section.

Scatter plots comparing the results of each method were produced and discussed. Due to the small number of samples available no outliers were removed and the samples were not split up into their sampling cut or stratigraphic units. The mean AVRD between each method was determined and compared. The descriptive statistics of the original dataset (table C1); the list of the data used in the comparison (table C2); and the AVRD frequency data (table C3) are tabulated in Appendix C.

6.2. PART TWO: RESULTS

Scatter plots comparing the four different methods used in the experiment are given in figures 38 to 43 below. The methods used in this experiment are the two water immersion methods, the Lab water solid and the Driekop methods, as well as the Grabner solid and Grabner Milled methods. In each scatter plot there is a black and a red diagonal line. The black line represents the one-to-one linear trend line. Data points falling along this line have exactly the same value for the two results being plotted and compared. The red line represents the linear trend line of the dataset.
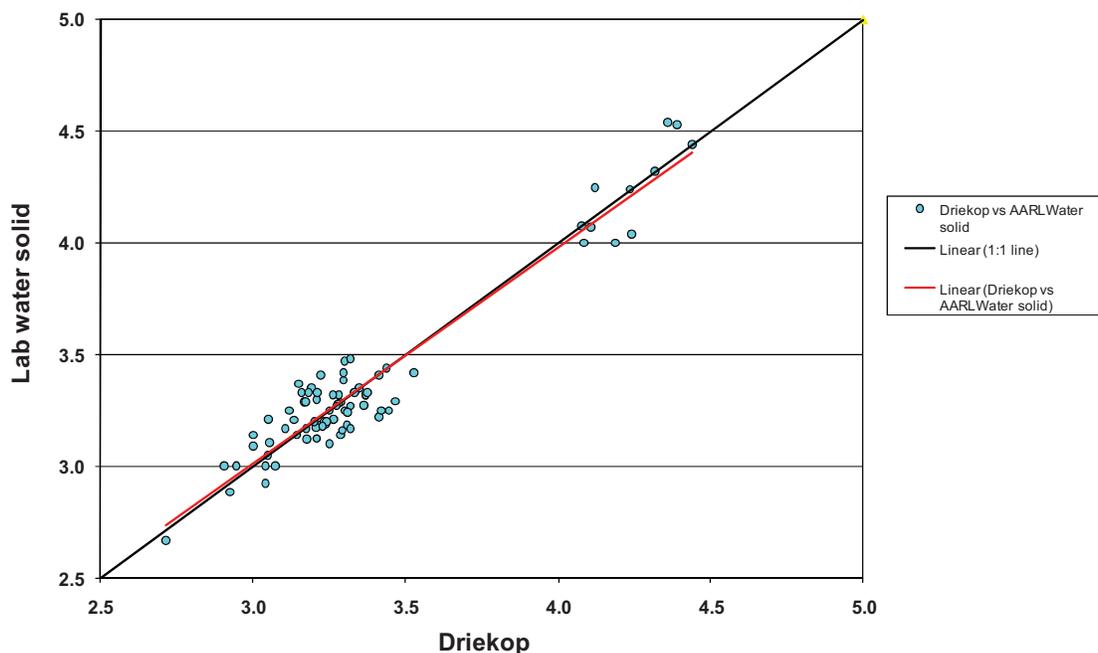
Figure 38. Scatter plot of the Lab water values over the Driekop values.

> **Notes** The mean AVRD indicates that the Driekop results are only 0.01 % higher than the Lab water solid results.

The scatter plot of the Lab water solid values and the Driekop values show good correlation (figure 38). A number of the data points fall along the one-to-one line. Approximately 24 % of the data points have an AVRD of between one and minus one percent (Appendix C). The red linear dataset trend line is very close to the

65

black linear one-to-one trend line. The mean AVRD is only 0.01 %. This indicates that the results of the two water immersion methods conducted at different localities are generally comparable.
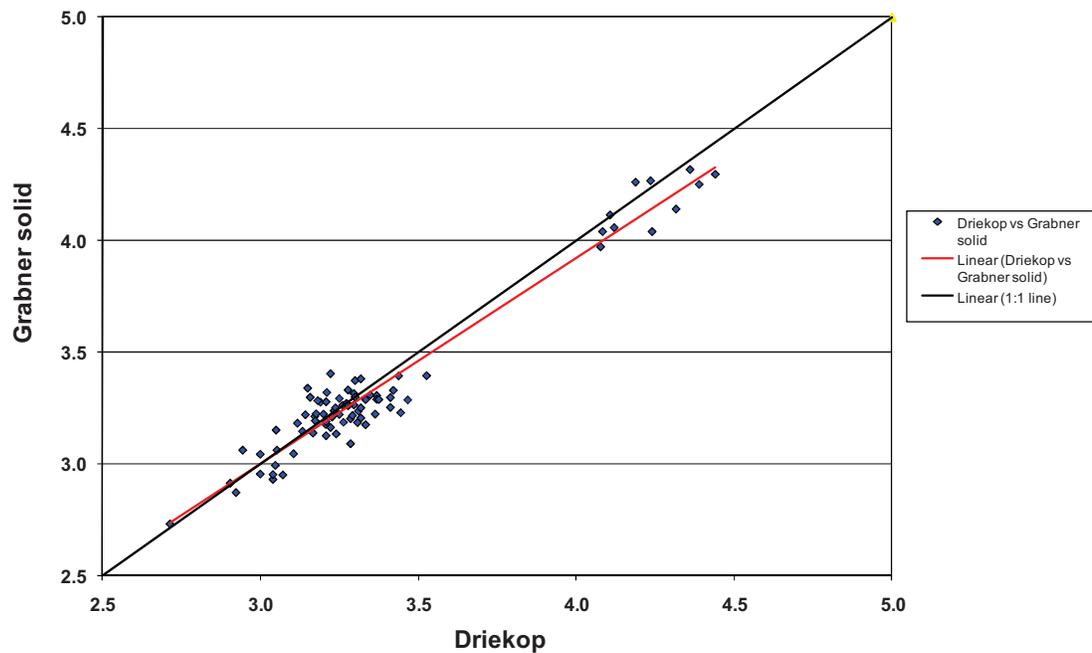
Figure 39. Scatter plot of the Grabner solid values over the Driekop values.

> **Notes** The mean AVRD indicates that the Driekop results are 0.86 % higher than the Grabner solid results.

The scatter plot of the Grabner solid values and the Driekop values also shows relatively good correlation (figure 39). Approximately 28 % of the data points have an AVRD of between one and minus one percent (Appendix C). The red linear dataset trend line is similar to the black linear one-to-one trend line at values between 2.8 to 3.5 g/cc. However, points falling between 4.0 to 4.5 g/cc have a higher density value for the Driekop method, indicated by the skewed dataset trend line at these values. The mean AVRD is only 0.86 %. This indicates that there is a good comparison between the results from the Grabner solid method and the Driekop method.
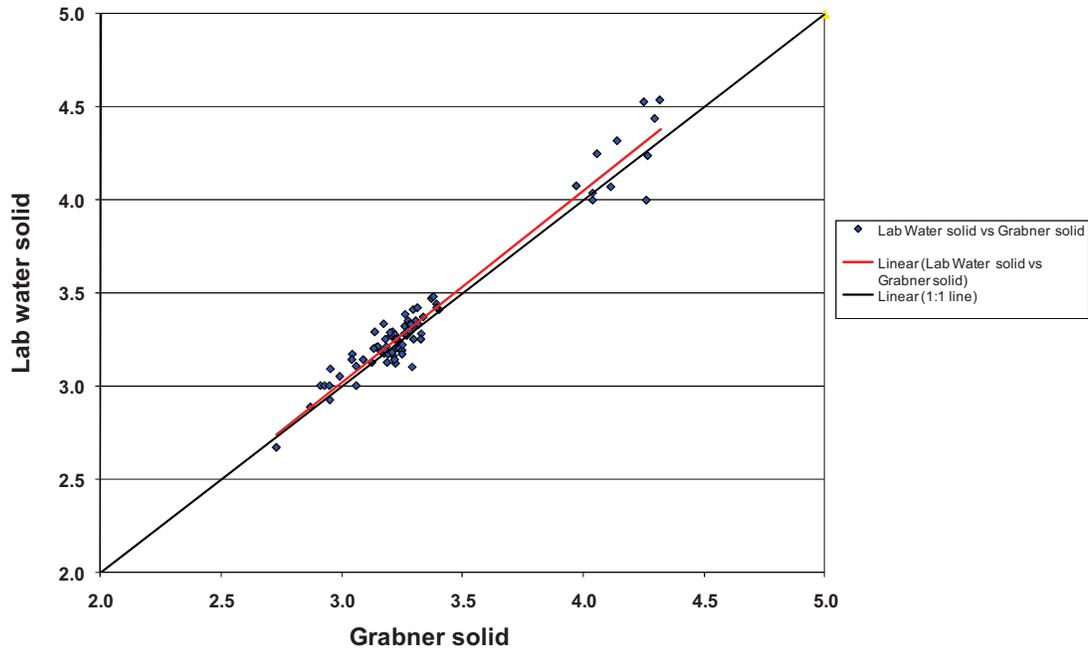
Figure 40. Scatter plot of the Lab water solid values over the Grabner solid values.

> **Notes** The mean AVRD indicates that the Lab water solid results are 0.85 % higher than the Grabner Solid results.

The scatter plot of the Lab water solid values and the Grabner solid values also shows relatively good correlation (figure 40). The red linear trend line lies just above the black linear one-to-one trend line; with slightly higher values for the Lab water solid values at densities of between 4.0 to 4.5 g/cc. Approximately 33 % of the data points have an AVRD of between one and minus one percent (Appendix C). The mean AVRD is only 0.85 %, indicating a generally good correlation. This mean AVRD is almost the same as the mean AVRD between the Grabner Solid values and Driekop values (0.86 %). This indicates that the results of all three solid methods conducted in the experiment are relatively analogous.
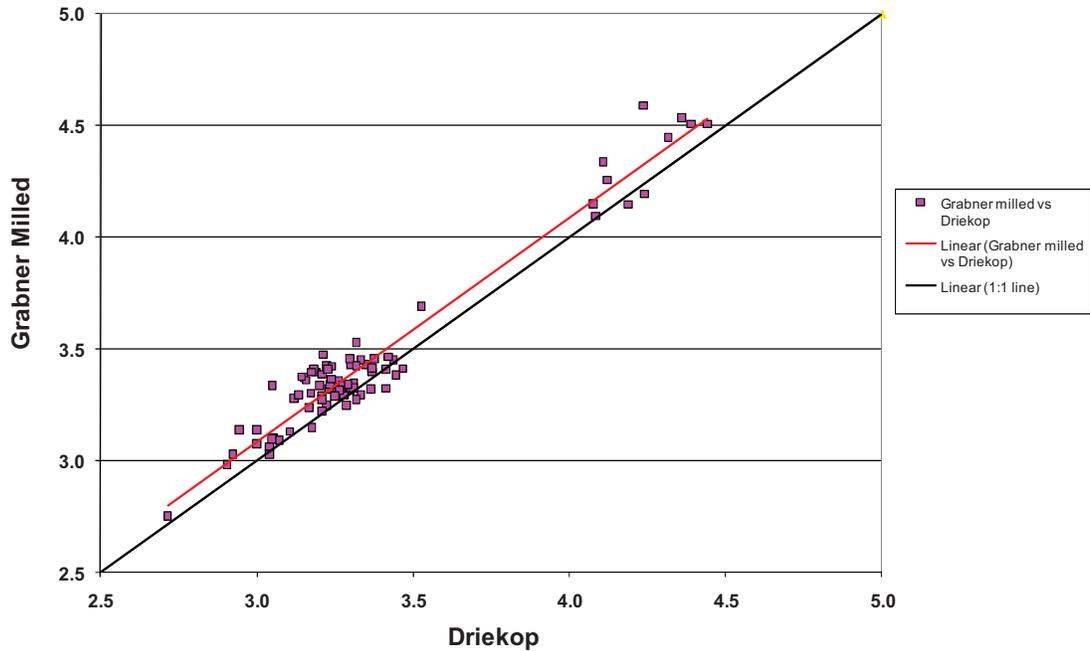
Figure 41. Scatter plot of the Grabner Milled values over the Driekop values.

> **Notes** The mean AVRD indicates that the Grabner Milled results are 2.56 % higher than the Driekop results.

In contrast the scatter plot of the Grabner Milled values and the Driekop values show that Grabner Milled values are generally higher (figure 41). The majority of the data points lie above the black one-to-one trend line, as does the red dataset trend line. The mean AVRD of the dataset is 2.56 %, indicating that the Grabner Milled values are generally higher than the Driekop values.
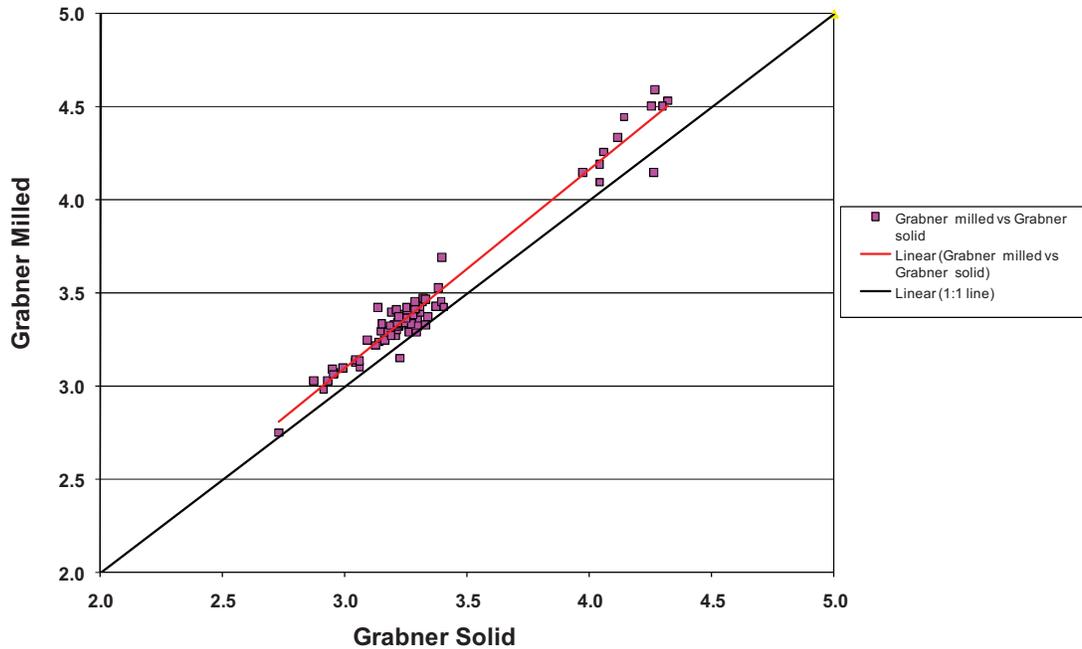
Figure 42. Scatter plot of the Grabner Milled values over the Grabner solid values.

Notes The mean AVRD indicates that the Grabner Milled results are 3.42 % higher than the Grabner Solid results.

The scatter plot of the Grabner Milled values and the Grabner solid values show similar results (figure 42). The Grabner Milled values are higher than the Grabner solid values. The majority of the data points, together with the red dataset trend line, lie above the black one-to-one trend line. The mean AVRD of the dataset is 3.42 %, indicating that the Grabner Milled values are generally higher than the Grabner solid values.
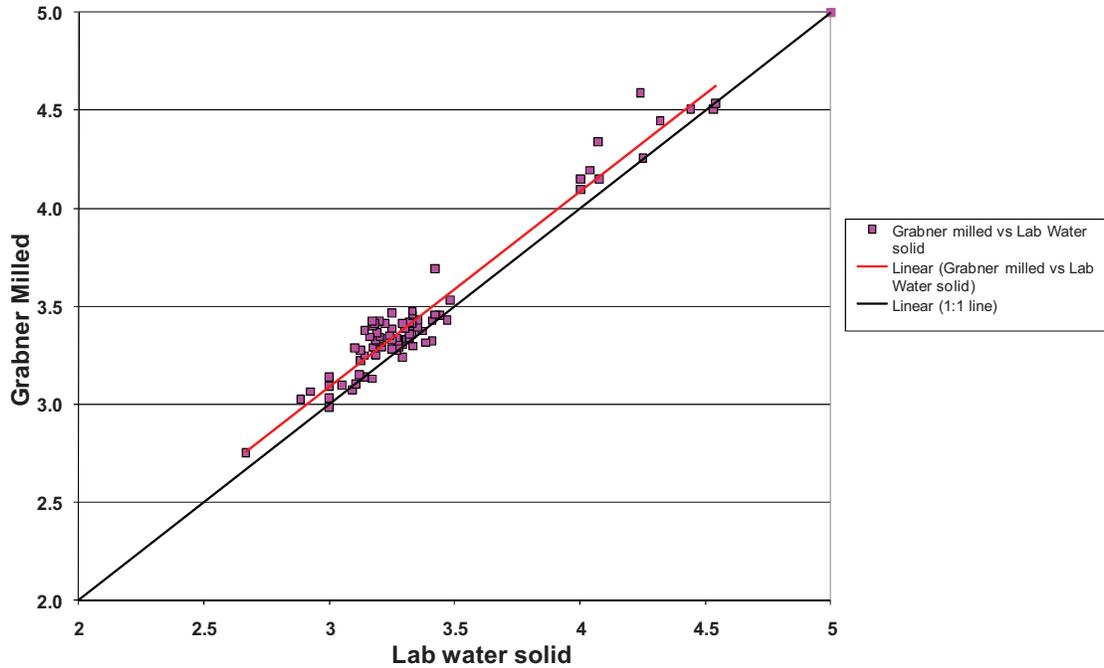
Figure 43. Scatter plot of the Grabner Milled values over the Lab water solid values.

> **Notes** The mean AVRD indicates that the Grabner Milled results are 2.57 % higher than the Lab water solid results.

Similarly the scatter plot of the Grabner Milled values over the Lab water solid values shows that the Grabner Milled values are generally higher (figure 43). The majority of the data points, together with the red dataset trend line, lie above the black one-to-one trend line. The mean AVRD indicates that the Grabner Milled results are 2.57 % higher than the Lab water solid results.

6.3. PART TWO: DISCUSSION

The density experiment on the four methods shows that the milled core samples have a higher average density than those of the solid samples. The AVRDs between the four methods are summarized in table 5 below.

Table 5. Mean AVRD between the four methods conducted in the density experiment.

	Mean AVRD (%)
AVRD of Driekop & Grabner Solid	0.86
AVRD of Lab water solid & Grabner Solid	0.85
AVRD of Driekop & Lab water solid	0.01
AVRD of Grabner Milled & Lab water solid	2.57
AVRD of Grabner Milled & Driekop	2.56
AVRD of Grabner Milled & Grabner Solid	3.42

The lowest mean AVRD was found between the two water immersion methods. Even though these methods were conducted in very different locations with different temperatures and atmospheric pressures, they showed very little difference in results. This shows that small changes in temperature and atmospheric pressure will have minimal impact on the density result determined using hydrostatic water immersion. Webb (2001), indicates that if the temperature of the water is assumed to be at room temperature an error margin of about 0.33 % is introduced. For more accurate results the temperature of the water can be monitored and measured. Using a table of water density at different temperatures (table 1), the true density of the water can be used in the density equation. Note that the density of water is approximately 1 g/cc at a temperature of 4 ℃. Both increases and decreases in temperature will reduce the density of water. Multiplying the relative density of the sample with the true density of the water will therefore reduce the density of the sample slightly.

The mean AVRD between the two hydrostatic water immersion methods and the Grabner Solid method are similar, with a mean AVRD of only 0.85 − 0.86 %. The Driekop and Lab water solid density results are marginally higher than the Grabner Solid results. This may be partially indicative of the error margin introduced in the hydrostatic water immersion method by not using the true density of water. Another reason that the Grabner Minidens produced lower results may be because the air

was able to penetrate microscopic pores within the solid cores' structure, giving slightly lower volumes.

The largest AVRD was found between the Grabner Milled and the Grabner Solid results. This proves that, by milling the sample, any pores within the sample are eliminated and only the volume of the solid particles are calculated, therefore the higher density results. The AVRD between the Grabner Milled and both solid hydrostatic water immersion methods showed similar results, although the mean AVRD was slightly less. The AVRD histogram of the Grabner Solid and the Grabner Milled results is shown in figure 44 below; 30 % of the data has an AVRD of 4 %.
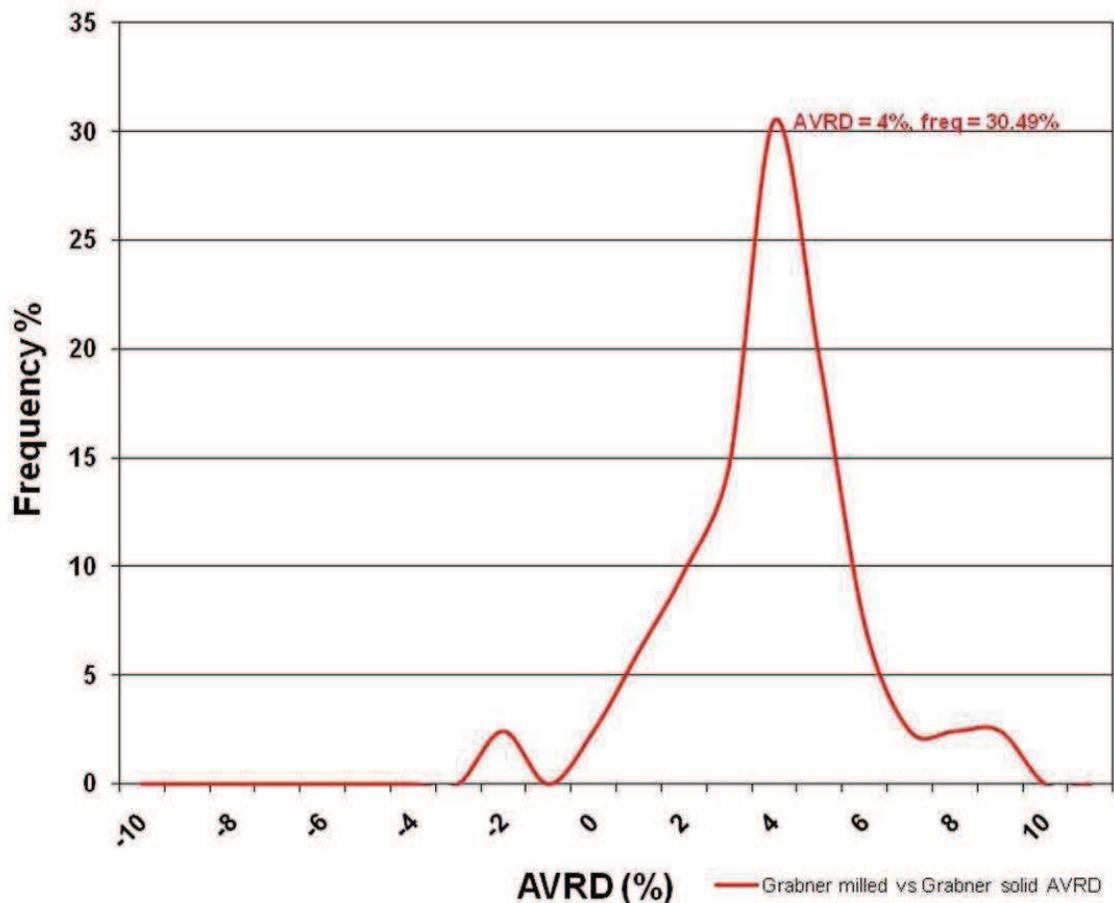
Figure 44. AVRD frequency histogram of the Grabner Milled and Grabner solid values.

7. DISCUSSION

7.1. EFFECT OF DENSITY ON RESOURCE PLANNING

The 2009 LPM resource model parameters were used to determine the effect of density on resource planning (Anglo Platinum annual report (AP), 2009 and Stevenson, 2009a and 2009b).

The weighted average density and AVRD of the MR and UG2 mining cut for each method was determined using the relative proportions of hangingwall, reef and footwall to the thickness of the optimal mining cut (table 6). For the Grabner Milled method, the density of the MR mining cut is 3.37 g/cc; and the density of the UG2 mining cut is 3.92 g/cc (table 7). For the Driekop method, the density of the MR mining cut is 3.20 g/cc; and the density of the UG2 mining cut is 3.70 g/cc (table 7). The weighted AVRD between the two methods for the MR is 5.34 % and the weighted AVRD for the UG2 is 5.52 % (table 7). The resource for the MR and UG2 was determined using the densities calculated for each method (table 8). The percentage difference in tonnage and ounces between the two methods was then determined (table 8).

The dip area was calculated using the "measured resource" area of the LPM project (Stevenson, 2009a and 2009b), and an average dip over the project of 19.5° (Langwieder, 2005). The thickness of the MR and UG2 mining cut is 1m. The percentage geological loss for the area is 20 % (Stevenson, 2009a and 2009b). The average 4E grade, which is comprised of the four elements Pt; Pd, Rh and Au was used. For the MR a grade of 5.92 g/t was used and for the UG2 a grade of 6.75 g/t was used (table 8); (AP, 2009).

The percentage difference in tonnage and 4E ounces between the two methods is shown in the last two columns of table 8. The percentage difference is 5.14 % for the MR and 5.55 % for the UG2. The percentage difference in tonnage and 4E ounces between the two methods for the MR and UG2 is very similar to the weighted AVRD between the two methods for the respective reefs, which is 5.34 % for the MR and 5.52 % for the UG2. This shows that a percentage change in density will result in the same percentage change in tonnage and 4E ounces. To further

illustrate the point, table 9 shows the resource calculation for the Grabner Method, relative to a 1 % decrease in density from the Grabner method. The last two columns in table 9 show that the percentage decrease in tonnage and 4E ounces is the same as the percentage decrease in density (1 %).

Table 6. Weighted average density and AVRD of each stratigraphic unit that make up the optimal mining cut.

	LPM							
Stratigraphic unit	Grabner Milled (g/cc)	Driekop (g/cc)	Thickness (m)	AVRD (%)	Percentage thickness	Weighted average Grabner Milled (g/cc)	Weighted average Driekop (g/cc)	Weighted average AVRD (%)
MRHW	3.28	3.12	0.10	5.18	10	0.33	0.31	0.52
MR	3.42	3.24	0.65	5.44	65	2.22	2.11	3.54
MRFW	3.27	3.11	0.25	5.16	25	0.82	0.78	1.29
UG2HW	3.42	3.25	0.15	5.09	15	0.51	0.49	0.76
UG2	4.19	3.95	0.65	5.70	65	2.72	2.57	3.71
UG2FW	3.40	3.22	0.20	5.24	20	0.68	0.64	1.05

Note: Both the Grabner Milled and Driekop methods are shown for comparison. Weighted average density and AVRD is based on the relative thickness of hangingwall, reef and footwall that make up the mining cut.

Table 7. The weighted average grade, density, AVRD and thickness for the optimal mining cut.

	LPM				
Mining Cut	Grade (g/t)	Grabner Milled (g/cc)	Driekop (g/cc)	AVRD (%)	Thickness (m)
MR	5.92	3.37	3.20	5.34	1
UG2	6.75	3.92	3.70	5.52	1

Note: Both the Grabner Milled and Driekop methods are shown for comparison.

Table 8. Resource calculation for the LPM area, based on the optimal mining cut.

										LPM	
Method	**Mining cut**	**Dip (°)**	**Dip area (m2)**	**Thickness (m)**	**Density (g/cc)**	**Tonnage after geo loss (tons)**	**Grade (g/t)**	**Content 4E (Oz)**	**% difference Content 4E (Oz)**	**% difference Tonnage after geo loss (tons)**	
Grabner Milled	MR	19.5	17,879,544	1	3.37	48,181,795	5.92	9,170,557	5.14	5.14	
Driekop	MR	19.5	17,879,544	1	3.20	45,707,266	5.92	8,699,574			
Grabner Milled	UG2	19.5	40,997,559	1	3.92	136,481,898	6.75	29,618,963	5.55	5.55	
Driekop	UG2	19.5	40,997,559	1	3.70	128,902,475	6.75	27,974,095			

Note: Both the Grabner Milled and Driekop methods are shown for comparison.

Table 9. Resource calculation for the LPM area, showing the affect of a 1 % drop in density relative to the Grabner Milled mining cut density.

										LPM Grabner Milled minus 1% comparison	
Method	**Mining cut**	**Dip (°)**	**Dip area (m2)**	**Thickness (m)**	**Density (g/cc)**	**Geological loss (%)**	**Tonnage after geo loss (tons)**	**Grade (g/t)**	**Content 4E (Oz)**	**% difference Content 4E (Oz)**	**% difference Tonnage after geo loss (tons)**
Grabner Milled	MR	19.5	17,879,544	1	3.37	20	48,181,795	5.92	9,170,557	1.00	1.00
1% reduction	MR	19.5	17,879,544	1	3.33	20	47,699,977	5.92	9,078,851		
Grabner Milled	UG2	19.5	40,997,559	1	3.92	15	136,481,898	6.75	29,618,963	1.00	1.00
1% reduction	UG2	19.5	40,997,559	1	3.88	15	135,117,079	6.75	29,322,773		

Note: The Grabner Milled density is 3.37 g/cc; a 1 % reduction of the Grabner Milled density is 3.33 g/cc.

Dilution or overbreak is another factor that needs to be considered as it will influence the density and grade of the mining cut, and therefore the tonnage and 4E ounces. Three scenarios were considered: the hangingwall and footwall thicknesses were increased equally by 5 cm; then by 10 cm; and then by 15 cm. The effect on the original resource calculation density, grade, tonnage and 4E ounces was then compared.

The weighted average density and grade of the MR and UG2 mining cut plus additional dilution for each method, was determined using the relative proportions of hangingwall (5 cm ; 10 cm; and 15 cm), reef (original mining cut) and footwall (5 cm; 10 cm; and 15 cm) thicknesses. Grade in the hangingwall and footwall was considered to be zero. The weighted average grade, density and thickness of the mining cut plus dilution (10 cm; 20 cm; and 30 cm) is given in tables 10 to 12. The difference in density, grade, tonnage and 4E ounces from the original resource calculation is given in tables 13 to 15.

The weighted average density, grade and thickness of the hangingwall, reef and footwall stratigraphic units that make up the mining cut plus dilution are given in Appendix D, tables D1 to D3. The resource calculations for the mining cut plus dilution are also given in Appendix D, tables D4 to D6.

Table 10. The weighted average grade, density and thickness for the optimal mining cut plus 10 cm dilution.

LPM 10cm dilution				
Mining Cut	Grade (g/t)	Grabner Milled (g/cc)	Driekop (g/cc)	Thickness (m)
MR	5.38	3.36	3.19	1.1
UG2	6.14	3.87	3.66	1.1

Table 11. The weighted average grade, density and thickness for the optimal mining cut plus 20 cm dilution.

LPM 20cm dilution				
Mining Cut	Grade (g/t)	Grabner Milled (g/cc)	Driekop (g/cc)	Thickness (m)
MR	4.93	3.35	3.18	1.2
UG2	5.63	3.83	3.62	1.2

Table 12. The weighted average grade, density and thickness for the optimal mining cut plus 30 cm dilution.

LPM 30cm dilution				
Mining Cut	Grade (g/t)	Grabner Milled (g/cc)	Driekop (g/cc)	Thickness (m)
MR	4.55	3.35	3.18	1.3
UG2	5.19	3.80	3.59	1.3

Table 13. Change in density, grade, tonnage and metal content for the optimal mining cut plus 10 cm.

LPM 10cm dilution									
Method	Mining cut	Decrease in density (g/cc)	Decrease in grade (g/t)	% decrease in density	% decrease in grade	Increase in tonnage	Decrease in Ounces	% increase in tonnage	% decrease in Ounces
Grabner Milled	MR	0.01	0.54	0.25	9	4,684,441	23,141	9.72	0.25
Driekop	MR	0.01	0.54	0.23	9	4,455,582	19,923	9.75	0.23
Grabner Milled	UG2	0.05	0.61	1.18	9	11,883,142	348,224	8.71	1.18
Driekop	UG2	0.04	0.61	1.14	9	11,273,304	319,005	8.75	1.14

Table 14. Change in density, grade, tonnage and metal content for the optimal mining cut plus 20 cm.

LPM 20cm dilution									
Method	Mining cut	Decrease in density (g/cc)	Decrease in grade (g/t)	% decrease in density	% decrease in grade	Increase in tonnage	Decrease in Ounces	% increase in tonnage	% decrease in Ounces
Grabner Milled	MR	0.02	0.99	0.46	17	9,368,881	42,425	19.44	0.46
Driekop	MR	0.01	0.99	0.42	17	8,911,165	36,526	19.50	0.42
Grabner Milled	UG2	0.08	1.13	2.16	17	23,766,285	638,410	17.41	2.16
Driekop	UG2	0.08	1.13	2.09	17	22,546,607	584,842	17.49	2.09

Table 15. Change in density, grade, tonnage and metal content for the optimal mining cut plus 30 cm.

		LPM 30cm dilution							
Method	Mining cut	Decrease in density (g/cc)	Decrease in grade (g/t)	% decrease in density	% decrease in grade	Increase in tonnage	Decrease in Ounces	% increase in tonnage	% decrease in Ounces
Grabner Milled	MR	0.02	1.37	0.64	23	14,053,322	58,742	29.17	0.64
Driekop	MR	0.02	1.37	0.58	23	13,366,747	50,575	29.24	0.58
Grabner Milled	UG2	0.12	1.56	2.98	23	35,649,427	883,953	26.12	2.98
Driekop	UG2	0.11	1.56	2.89	23	33,819,911	809,781	26.24	2.89

An increase in hangingwall and footwall thickness above the optimal mining cut has a much greater effect on the UG2 density than on the MR density. A 10 to 20 cm increase in overbreak causes the MR mining cut density to decrease by only 0.25 to 0.64 % for the Grabner Milled method and 0.23 to 0.58 % for the Driekop method, whereas the UG2 density decreases by 1.18 to 2.98 % for the Grabner Milled method and 1.14 to 2.89 % for the Driekop method (tables 13 to 15). The UG2 mining cut density is much more sensitive to overbreak because of the huge difference in composition and density between the reef and the hangingwall and footwall rocks. The UG2 is a chromitite layer, whereas the UG2HW and UG2FW are both made up of plagioclase pyroxenite. On the other hand, the MR mining cut density is less sensitive to overbreak because the MRHW, MR and MRFW are all made up of plagioclase pyroxenite. There are only slight differences in density between mineralized pyroxenite and un-mineralized pyroxenite.

The percentage decrease in grade associated with increases in hangingwall and footwall thickness, above the optimal mining cut, will obviously depend on the actual grade of the hangingwall and footwall at those thicknesses. Because the additional overbreak in the hangingwall and footwall was taken at a grade of 0 g/t, the grade of the mining cut will decrease in proportion with the increase in overbreak, i.e. the percentage dilution equals the percentage decrease in grade.

Because tonnage is associated with density, and grade is associated with 4E ounces, increases in overbreak will cause the tonnage to increase and the 4E ounces to decrease.

Although the UG2 mining cut density is more sensitive to dilution than the MR mining cut, the percentage change in tonnage is similar (tables 13 to 15). For every 10 cm of dilution, the MR tonnage increases by 9.72 % for the Grabner Milled method and 9.75 % for the Driekop method. For every 10cm of dilution, the UG2 tonnage increases by 8.71 % for the Grabner Milled method and 8.75 % for the Driekop method.

Grade in the hangingwall and footwall is taken as 0 g/t, therefore increases in dilution causes the total ounces to drop. The relationship between the tonnage and ounces is obviously more complicated, as it has huge cost and logistical implications. If there were sufficient grade in the hangingwall and footwall, the total available ounces may actually increase because of the increase in tonnage, but the additional

cost of extraction may render the project unfeasible. The optimal mining cut already takes all these interlinked elements into consideration. This example does however, show that for the same amount of dilution, the UG2 shows a greater drop in ounces compared to MR. From 10 to 30 cm dilution, the MR shows a drop in ounces from 0.25 to 0.64 % for the Grabner Milled method and from 0.23 to 0.58 % for the Driekop method. From 10 to 30 cm dilution, the UG2 shows a drop in ounces from 1.18 to 2.98 % for the Grabner Milled method and from 1.14 to 2.89 % for the Driekop method.

The effect of dilution on density, as well as grade has been highlighted. Compositional differences between the UG2 and the UG2HW and UG2FW means that the overall density of the UG2 mining cut is much more sensitive to dilution then the MR mining cut, which is made up of similar lithologies. Weighted average densities based on the proportions of hangingwall, reef and footwall must be taken into consideration during mining as well. Emphasis is commonly placed on the effect of dilution on grade; however the effect on density is as important.

7.2. SUMMARY OF FINDINGS BASED ON QUESTIONS POSED IN THE RESEARCH PROBLEM

Question: Is there a significant difference in results obtained when using a hydrostatic immersion or gas pycnometer method to determine rock density?

Answer: Yes there is. Part one: the comparison between the Driekop method and Grabner Milled method showed a mean AVRD of approximately 5 % for all stratigraphic units. Part two: the comparison between the four methods also showed that there was a significant difference between the solid methods and the Grabner Milled method. The most significant being between the Grabner Milled and Grabner solid method (AVRD = 3.42 %).

Question: What are the differences between the two methods?

Answer: The Driekop method calculates the bulk density for the solid core samples and the Grabner Milled method calculates the true density for the milled/powdered core samples. Applied correctly with the proper quality controls, they are both reliable methods of density determination. However, care must taken to decide what type of density is required.

Question: Are these differences significant and what are the implications thereof?

Answer: Not only is there a significant difference in results between the two methods, the type of density measured is completely different. However, the method does work as a quality control measure to check the laboratory results. Results falling outside an expected density range or AVRD for particular rock type and stratigraphic unit can be picked up. The method used will have a significant impact on resource planning, depending on which method is used in the resource calculation. A percentage change in the density of the mining cut will result in an equal percentage change in tonnage and metal content.

8. CONCLUSION

The study shows that density measurements conducted on milled core and solid core produces different results. The milled core produces a density result 3 to 5 % higher than the solid core. Milling the core sample into a fine powder changes the natural state of the rock, altering its mineral assemblage and structure, and in the process eliminating any pore spaces.

Subtle differences in the composition and structure of the rock affects the mass, and the solid volume versus the pore volume of the sample. For example, the slight difference in density between mineralized pyroxenite and un-mineralized pyroxenite.

The study highlights the need for the correct application of quality control in taking density measurements. Apart from the correct setup, calibration and use of standard reference material to ensure accuracy and precision, particular attention needs to be paid to the type of rock measured and the type of density required. Does the rock contain open and/or closed pores? Is a bulk density or a true density of the rock required? In this case, the Driekop method, using a hydrostatic immersion method on the halved core sample, calculated a bulk density for the solid core samples. The Grabner Milled method, using a gas pycnometer method, on only a portion of the milled core sample, calculated a true density for the milled core samples. Although the Grabner milled method produces different density results to the Driekop method, by comparing the results of the two methods, samples falling outside an expected density range or AVRD, for that particular type of rock and stratigraphic unit, are easily picked up. Therefore the two methods can be used for quality control.

The effect of temperature and atmospheric pressure on the hydrostatic immersion method was shown to be minimal. However, for more accurate results the temperature of the water should be monitored. The hydrostatic method of density determination is a very practical way of determining rock density at a remote exploration site. A range of different rock sizes and shapes can be used with this method. On the other hand, modern gas pycnometers need to be operated in a

laboratory controlled environment, and are only capable of measuring a small amount of sample.

For platinum deposits on the North Eastern limb, the type of method used will have a significant impact on resource planning. Furthermore, changes in density results in equal changes in tonnage and metal content. The AVRD between the two methods, for the mining cut density, was approximately 5 %, and the difference in tonnage and 4E ounces between the two methods was also approximately 5 %. The total resources are dependent on which method is used in the resource calculation.

Increases in dilution or overbreak above the optimal mining cut showed increases in tonnage and decreases in metal content (4E ounces). In terms of density, due to the similarity in rock composition between the MRHW, MR and MRFW, the MR mining cut was found to be less sensitive to dilution. On the other hand, because of the marked difference in composition between the UG2, and the UG2HW and UG2FW, dilution caused a greater change in density for the UG2 mining cut.

9. REFERENCES

Agnew, J.M., Leonard, J.J., Feddes, J. and Feng, Y. (2003). A modified air pycnometer for compost air volume and density determination. *Canadian Biosystems Engineering*, **45**, 6.27-6.35.

Anglo Platinum Limited. (2009). *2009 Annual Report, Platinum: A precious metal for a precious planet.* Anglo Platinum Ltd, 276 pp.

[ASTM] American Society for Testing and Materials. (1991). 8th edition. Compilation of ASTM Standard Definitions. Available from American Society for Testing and Materials US. Philadelphia.

[ASTM] American Society for Testing and Materials. (1997). D 2638 – 06 Standard Test Method for Real Density of Calcined Petroleum Coke by Helium Pycnometer. Available from http://www.astm.org

Barnes, S. and Maier, W.D. (2002). Platinum-group Elements and Microstructures of Normal Merensky Reef from Impala Platinum Mines, Bushveld Complex. *Journal of Petrology*, **43(1)**, 103-128.

Britt, D.T., Yeomans, D., Housen, K. and Consolmagno, G. (2002). Asteroid Density, Porosity, and Structure. *In Asteroids III* (Eds. W.F. Bottke, A. Cellino. P. Paolicchi, and R.P. Binzel), University of Arizona Press, Tuscon, 485-500.

Britt, D.T. and Consolmagno, G.T. (1998). The density and porosity of meteorites from the Vatican collection. *Meteoritics and Planetary Science,* **33**, 1231-1241.

Brown, R. (2004a). *Mafic and Ultramafic rocks of the Bushveld Complex: A note on their classification and nomenclature* (Unpublished), 2nd Edition, Anglo Platinum Exploration Geology Internal Report, 77 pp.

Brown, R. (2004b). *Some aspects of potholes and replacement pegmatites* (Unpublished)*,* Anglo Platinum Exploration Geology Internal Report, 13 pp.

Brown, R. (2005a). *The Eastern Bushveld Complex* (Unpublished)*,* Anglo Platinum Exploration Geology Internal Report, 25 pp.

Brown, R. (2005b). *The PGE reefs of the Bushveld Complex and Great Dyke* (Unpublished)*,* Anglo Platinum Exploration Geology Internal Report, 52 pp.

Brown, R.T. and Lee, C.A. (1987). *The nature and characteristics of Merensky reef potholes at Atok Platinum Mine*. (Unpublished), Internal JCI Report No. 221, 53 pp.

[BSI] British Standards Institute. (1991). Glossary of Terms Relating to Particle Technology. Available from British Standards Institute, London; British Standard BS 2955.

Cameron, E.N. (1982). The Upper Critical Zone of the Eastern Bushveld Complex-Precursor of the Merensky reef. *Economic Geology*, **77**, 1307-1327.

Capano, D. (2000). *The ways and means of density* (Internet). InTech Online, The Instrumentation, Systems, and Automation Society (ISA), 4 pp.
Available from http://www.isa.org/journals/intech/feature/1,1162,467,00.html

Cawthorn, R.G., Lee, C.A., Schouwstra, R.P. and Mellowship, P. (2002). Relationship between PGE and PGM in the Bushveld Complex. *The Canadian Mineralogist*, **40**, 311-328.

Cawthorn, R.G. and Walraven, F. (1998). Emplacement and Crystallization Time for the Bushveld Complex. *Journal of Petrology*, **39(9)**, 1669-1687.

Cawthorn, R.G. and Webb, S.J. (2001). Connectivity between the western and eastern limbs of the Bushveld Complex. *Tectonophysics*, **330**, 195-209.

Chang, C.S. (1988). Measuring Density and Porosity of Grain Kernels Using a Gas Pycnometer. *American Association of Cereal Chemists*, **65(1)**, 13-15.

Chunnett, G., Rutherford, T. and Jones, B. (2006). *Anglo Platinum Group procedure for the determination of density for QA/QC purposes* (Unpublished)*, Version* 3.0. Anglo Platinum Exploration Geology Internal Report, 14 pp.

Clarke, B.M., Uken, R., Watkeys, K. and Reinhardt, J. (2005). Folding of the Rustenburg layered suite adjacent to the Steelpoort pericline: implications for syn-Bushveld tectonism in the eastern Bushveld Complex. *South African Journal of Geology*, **108**, 397-412.

Eales, H.V. (2001). A first introduction to the Bushveld Complex and those aspects of South African Geology that relate to it. Popular Geoscience Series 2, The Council for Geoscience. 84 pp.

Gain, S.B. (1985). The geological setting of the platiniferous UG-2 chromitite layer on the farm Maandagshoek, eastern Bushveld Complex. *Economic Geology*, **80**, 925-943.

Geddis, A.M., Guzman, A.G. and Bassett, R.L. (1996). *Rapid Estimate of Solid Volume in Large Tuff Cores Using a Gas Pycnometer*. United States Nuclear Regulatory Commission, NUREG/CR-6457. 85 pp.

Goldman, R.F. and Buskirk, E.R. (1959). *Body volume measurement by underwater weighing: Description of a method*. National Academy of Sciences – National Research Council, Washington, D.C. Proceedings of a Conference Quartermaster Research and Engineering Centre, Natrick, Massachusetts, January 22-23, 1959, 78-79.

Grabner Instruments. (2008). *Minidens operating manual*. Grabner Instruments, Messtechnik, 31pp. Available from http://Grabner-instruments.com

Kinloch, E.D and Schouwstra, R.P. (2000). A short review of the Bushveld Complex, *Platinum Metals Review*, **44**, 33-39.

Langwieder, G. (2005*). Middling relationships between the UG2 and Merensky Reef in the Northeastern limb of the Bushveld Complex.* (Unpublished), Internal Anglo Platinum Report. 3 pp.

Lee, C.A. and Butcher, A.R. (1990). Cyclicity in the Sr isotope stratigraphy through the Merensky and Bastard units, Atok Section, Eastern Bushveld Complex. *Economic Geology*, **85**, 877-883.

Mabuza, M. (2006). *Two Rivers Platinum Mine: the orebody, the mining method; a perfect match*. The South African Institute of Mining and Metallurgy. International Platinum Conference 'Platinum surges ahead', 2006, 151-158.

Mathez, E.A., Hunter, R.H. and Kinzler, R. (1997). Petrological evolution of partially molten cumulate: the Atok section of the Bushveld Complex. *Contributions to Mineralogy and Petrology*, **129**, 20-24.

Mitchell, A. A. and Scoon, R. N. (2007). The Merensky Reef at Winnaarshoek, Eastern Bushveld Complex: A Primary Magmatic Hypothesis Based on a Wide Reef Facies. *Economic Geology*, **102(5)**, 971-1009.

Mondal, S.K. and Mathez, E.A. (2007). Origin of the UG2 chromitite layer, Bushveld Complex. *Journal of Petrology*, **48(3)**, 495-510.

Naldrett, A.J., Wilson, A., Kinnaird, J. and Chunnett, G. (2009). PGE tenor and metal ratios within and below the Merensky Reef, Bushveld Complex: Implications for its genesis. *Journal of Petrology*, first published online April 20, 2009. Available from http://www.petrology.oxfordjournals.org/content/early/2009/04/20/petrology.egp015.full

Orr, C., Camp, R.W. and Gibson, K.H. (1991). *Gas Comparison Pycnometer*. United States Patent 5,074,146. 24 pp.

Regimand, A. (2001). *Methods and apparatus for sealing a porous material sample for density determination using water displacement methods and associated surface conformal resilient compressible bags*. United States Patent US 6,321,589 B1. 36 pp.

SACS (South African Committee for Stratigraphy); (1980) Stratigraphy of South Africa. Part 1 (Compiler L.E. Kent). Lithostratigraphy of the Republic of South Africa, South West Africa / Namibia, and the Republics of Bophuthatswana, Transkei and Venda: *Handbook of the Geological Survey of South Africa*, 8, 690 pp.

SAMREC (The South African Mineral Resource Committee working group); (2007). The South African Code for the reporting of exploration results, mineral resources and mineral reserves (THE SAMREC CODE).

Schwellnus, J.S.I., Hiemstra, S.A. and Gasparrini, E. (1976). The Merensky reef at the Atok platinum mine and its environs. *Economic Geology*, **71**, 249-260.

Scoates, J.S. and Friedman, R.M. (2008). Precise age of the platiniferous Merensky Reef, Bushveld Complex, South Africa, by the U-Pb zircon chemical abrasion ID-TIMS technique. *Economic Geology*, **103**, 465-471.

Seabrook, C.L. (2005). *The Upper Critical and Lower Main Zones of the eastern Bushveld Complex.* PhD thesis (Unpublished), University of the Witwatersrand, Johannesburg, South Africa, 260pp.

Snelling, C. (Compiler). (Last modified 2010). *Density of Water at Temperatures from 0℃ (liquid state) to 30.9℃ by 0.1 increments* (Internet). Roger Walker 2008-2011.1p. Available from: http://www.simetric.co.uk/si_water.htm

Snowrex Precision Scales (2008). *Model NV/NHV Operating manual*. Snowrex International CO., LTD, 7pp.

Available from http://www.snowrex.com.tw/products_WeighingScale.htm

Stevenson, P.C.A. (2009a). *Lebowa Merensky Reef Geological Resource Modelling 2009.* (Unpublished)*,* Anglo Platinum Exploration Geology Internal Report, 352 pp.

Stevenson, P.C.A. (2009b). *Lebowa UG2 Geological Resource Modelling 2009.* (Unpublished)*,* Anglo Platinum Exploration Geology Internal Report, 372 pp.

Turner, P.L., Gilkey, R.W. and Lagus, P.L. (1978). *Gas Comparison Pycnometer*. US Patent 4,083,228. 11 pp.

Von Gruenewaldt, G., Sharpe, M.R. and Hatton, C.J. (1985). The Bushveld Complex: Introduction and Review. *Economic Geology*, **80**, 803-812.

Van der Neut, M. (2008). *QAQC investigation of assay data: Lebowa Mine, Limpopo Province* (Unpublished), Anglo Platinum Geology Internal Report. 15 pp.

Webb, P.A. (2001). *Volume and Density determinations for particle technologists* (Unpublished), Micromeritics Instrument Corp. 2/16/01. 16 pp.

Available from http://www.micromeritics.com

Webb, S.J., Cawthorn, R.G., Nguuri, T. and James, D. (2004). Gravity modelling of Bushveld Complex connectivity supported by Southern African Seismic Experiment results. *South African Journal of Geology*, **107**, 207-218.

Weindorf, D.C. and Wittie, R. (2003). Determining Particle density in Dairy Manure Compost. *The Texas Journal of Agricultural and Natural Resource*, **16**, 60-63.